PROCESS SIMULATION OF GASIFICATION OF VARIOUS FEEDSTOCKS

Bonginkosi P. Ndwandwe

Student number: 208505324

BSc Eng. (UKZN)

This dissertation is submitted in the fulfilment of the academic requirements of Master of Science in Chemical Engineering.

School of Engineering

College of Agriculture, Engineering and Science

University of KwaZulu-Natal

Durban, South Africa

November 2021

Supervisor: Prof Amir H. Mohammadi

PREFACE

The candidate investigated the contained material in this dissertation while established at the Discipline of Chemical Engineering in the School of Engineering. It is under the College of Agriculture, Engineering and Science at the University of KwaZulu-Natal based in Howard College Campus, South Africa. Prof. Amir H. Mohammadi provided financial support for the study.

_____

Signed: Prof. Amir H. Mohammadi

Date: 13/11/2021

DECLARATION: PLAGIARISM

I, **Bonginkosi Praise-God Ndwandwe**, declare that:

1. The research reported in this dissertation, except where otherwise indicated or acknowledged, is my original work;

2. This dissertation has not been submitted in full or in part for any degree or examination to any other university;

3. This dissertation does not contain other persons' data, pictures, graphs or other information unless specifically acknowledged as being sourced from other persons;

4. This dissertation does not contain other persons' writing unless specifically acknowledged as being sourced from other researchers. Where other written sources have been quoted, then:
    a. Their words have been re-written but the general information attributed to them has been referenced;
    b. Where their exact words have been used, their writing has been placed inside quotation marks, and referenced;

5. Where I have used material for which publications followed, I have indicated in detail my role in the work;

6. This dissertation is primarily a collection of material, prepared by myself, published as journal articles or presented as a poster and oral presentations at conferences. In some cases, additional material has been included;

7. This dissertation does not contain text, graphics or tables copied and pasted from the internet, unless specifically acknowledged, and the source being detailed in the dissertation and in the references sections.

_____

Signed: Bonginkosi P. Ndwandwe

Date: 13/11/2021

ABSTRACT

Gasification is the reduction waste to energy method, which converts organic waste types into syngas fuel, which then can be used for energy and in chemical production. In this work, ASPEN Plus software was used for modelling and simulation of the gasification processes. The investigation was carried out for three waste feedstock: palm kernel shell, meat and bone meal, and wood pellets to forecast the produced syngas using air gasification. These fuels were characterized based on their ultimate and proximate analysis. A fluidized bed gasifier was selected based on its ability to accept different types and sizes of feedstock, making them possible for commercial uses on a large scale. The circulating fluidized bed gasifier was simulated to reproduce its actual behaviour using a non-stoichiometric equilibrium model. It employed the use of minimization of Gibbs free energy to estimate the chief syngas composition (CO, H_2, CO_2 and CH_4). The operational parameters studied were the gasification temperature, gasifier pressure and equivalence ratio. The sensitivity analysis on ASPEN Plus was carried out to understand the influence of operating parameters on syngas composition, yield and lower heating value and gasifier performance parameters. Other selected parameters were carbon conversion efficiency and cold gas efficiency.

The equilibrium model was able to estimate the gasifier performance and examine the operational parameters' behaviour in the gasification process. The results from the sensitivity analysis pointed out that gasification temperature and equivalence ratio influence the gasifier performance more than gasifier pressure. An increase in equivalence ratio or gasification temperature increased the syngas yield and carbon conversion efficiency. When increasing gasifier pressure, it was found to decrease the syngas yield, increases the syngas lower heating value, cold gas efficiency and carbon conversion efficiency. Increasing equivalence ratio reduce lower heating value and cold gas efficiency. An increase in temperature increases the cold gas efficiency.

This study found that the optimal equivalence ratio is controlled from 0.2 to 0.4. The gasification temperature is controlled between 800 and 950°C and gasifier pressure is controlled between 0.1 and 2 MPa. Meat and bone meal gasification is the promising feedstock that provides higher hydrogen to carbon monoxide ratio of close to 2.0, which can be used for chemical and energy production.

ACKNOWLEDGEMENTS

I would like to send my gratitude to the following people for their supports in course of this dissertation:

Prof Amir H. Mohammadi for the support to this work through finance and guidance in research work.

Prof. Anne Stark and Prof. Michael Daramola seminars on how to compile a dissertation and article writing in research.

To my colleagues, Sthembele Myeza and Sandile Mtolo, this has been a journey people thanks for your efforts in pushing me to contribute to the body of knowledge.

To Siphamandla Biyela, Hector Vilakazi and Mendy Shozi for editing and formatting this dissertation.

I am thankful to my mother for her patience and her undying support through hard times in the course of this work.

I thank myself for showing a strong enthusiasm in completing this dissertation and God who makes everything possible for me.

TABLE OF CONTENTS **Page**

PREFACE i

DECLARATION: PLAGIARISM ii

ABSTRACT iii

ACKNOWLEDGEMENTS iv

LIST OF FIGURES ix

LIST OF TABLES xi

LIST OF ABBREVIATIONS xiii

NOMENCLATURE xiv

CHAPTER 1 : Introduction 1

1.1 Aims 4

1.2 Objectives 4

1.3 Outline of the dissertation structure 5

CHAPTER 2 : Gasification 6

2.1 Introduction 6

2.2 Feedstock 6

2.2.1 Feedstock characterization 7

2.2.2 Thermodynamic properties of the feedstock 9

2.3 Fundamentals of gasification processes 10

2.3.1 Shrinking core model 11

2.4 Types of gasifiers 13

2.4.1 Fixed bed gasifier 13

2.4.2 Fluidized bed gasifier 14

2.5 Gasification performance. 16

2.5.1 Effect of gasifier design 16

2.5.2 Effect of the feedstock properties 16

2.5.3 Effect of the gasifying medium 17

2.5.4 Effect of the temperature 20

2.5.5 Effect of the pressure 22

2.6 Gasification products and its application 23

2.6.1 Product gases 23

2.6.2 Char 24

CHAPTER 3 : ASPEN Plus Simulation of Gasification Process 26

3.1 Introduction to ASPEN Plus 26

3.2 Simulation of gasification processes 27

3.2.1 Kinetic modelling 29

3.2.2 Equilibrium modelling 30

3.3 Summary 32

CHAPTER 4 : Materials and Methods 34

4.1 Simulation components 34

4.2 Physical properties 35

4.3 Model development 36

4.4 Model description 39

4.5 ASPEN Plus blocks specification 40

4.6 Sensitivity analyses 42

4.6.1 Determination of product gas composition. 43

4.6.2 Determination of syngas yield. 43

4.6.3 Determination of lower heating value of syngas. 44

4.6.4 Determination of the cold gas efficiency. 44

4.6.5 Determination of the carbon conversion efficiency 44

CHAPTER 5 : Results and Discussion 46

5.1 Model validation 47

5.2 Sensitivity analysis on gasification temperature 48

5.2.1 Influence of gasification temperature on the syngas composition for PKS, MBM and WP gasification. 48

5.2.2 Influence of gasifier temperature on gasification performance of PKS, MBM and WP. 52

5.2.3 Influence of gasifier temperature on syngas lower heating value of PKS, MBM and WP gasification. 53

5.2.4 Influence of gasifier temperature on cold gas efficiency of PKS, MBM and WP gasification. 54

5.2.5 Influence of gasifier temperature on the carbon conversion efficiency of PKS, MBM and WP gasification. 55

5.3 Sensitivity analysis on equivalence ratio 56

5.3.1 Influence of equivalence ratio on the syngas composition for PKS, MBM and WP gasification. 56

5.3.2 Influence of equivalence ratio on the syngas yield for PKS, MBM and WP gasification. 60

5.3.3 Influence of equivalence ratio on the syngas lower heating value for PKS, MBM and WP gasification. 60

5.3.4 Influence of equivalence ratio on the cold gas efficiency for PKS, MBM and WP gasification. 61

5.3.5 Influence of equivalence ratio on the carbon conversion efficiency for PKS, MBM and WP gasification. 62

5.4 Sensitivity analysis on gasifier pressure 63

5.4.1 Influence of pressure on syngas composition for PKS, MBM and WP gasification. 63

5.4.2 Influence of gasifier pressure on syngas yield and lower heating value for PKS, MBM and WP gasification. 67

5.4.3 Influence of gasifier pressure on cold gas efficiency for PKS, MBM and WP gasification. 69

5.4.4 Influence of gasifier pressure on carbon conversion efficiency for PKS, MBM and WP gasification. 70

CHAPTER 6 : CONCLUSIONS AND RECOMMENDATIONS 71

REFERENCES 73

APPENDICES 80

APPENDIX A : Calculator blocks 80

APPENDIX B : Sample calculations 82

APPENDIX C : Supplementary information 85

LIST OF FIGURES

Figure 1-1: South African general waste type and their composition (Department of Environmental Affairs, 2018) 1

Figure 1-2: Pathways for transforming waste to several energy forms or chemicals through different conversion processes (Seo et al., 2018). 3

Figure 2-1: The potential pathways of the gasification process (Pradana and Budiman, 2015). 10

Figure 2-2: The diagram of shrinking core model showing gas-solid systems occuring in microscopic level (Fogler, 2010). 11

Figure 2-3: The classification of gasification technologies based on their design (La Villetta et al., 2017). 13

Figure 2-4: The graphic illustration of different gasifiers based on the feed and product gas positions: (A) entrained-flow, (B) fixed-bed and (C) fluidized bed gasifiers (Lian et al., 2021). 14

Figure 2-5: Several applications of syngas in industries based on H_2/CO ratio (Hernández et al., 2017). 24

Figure 2-6: Various applications of char in industries (The Peepal Leaf, 2019) 25

Figure 4-1: A process flowsheet showing a circulating fluidized bed gasifier for different feedstock. 38

Figure 5-1: Syngas composition (H_2, CO, CO_2 and CH_4) as function of gasification temperature of PKS, MBM and WP at ER = 0.3 and P =105 kPa. 51

Figure 5-2: The syngas yield as a function of gasification temperature of PKS, MBM and WP at ER=0.3 and pressure of 105 kPa. 53

Figure 5-3: Lower heating value as function of gasification temperature of PKS, MBM and WP at ER=0.3 and P=105 kPa. 54

Figure 5-4: Cold gas efficiency as a function of gasification temperature for PKS, MBM and WP at ER=0.3 and P = 105 kPa. 55

Figure 5-5: Carbon conversion efficiency as a function of PKS, MBM and WP gasification temperature at ER=0.3 and P = 105 kPa. 56

Figure 5-6: The syngas composition (H_2, CO, CO_2 and CH_4) as a function of ER for PKS, MBM and WP gasification at T = 800 °C and P = 105 kPa. 58

Figure 5-7: Syngas yield (G_Y) as a function of ER for PKS, MBM and WP gasification at ER = 0.3 and T = 800 °C. 60

Figure 5-8: Syngas lower heating value as a function of ER for PKS , MBM and WP gasification at T = 800 °C and P = 105 kPa. 61

Figure 5-9: Cold gas efficiency as a function of ER for PKS, MBM and WP gasification at T = 800 °C and P = 105 kPa. 62

Figure 5-10: The carbon conversion efficiency as function of ER for PKS, MBM and WP gasification at T = 800 °C and P = 105 kPa. 63

Figure 5-11: The syngas composition (H_2, CO, CO_2 and CH_4) as a function of a gasifier pressure for PKS, MBM and WP gasification using air at ER = 0.3 and T = 800 °C. 65

Figure 5-12: Syngas yield as a function of gasifier pressure for PKS, MBM and WP gasification using air at ER = 0.3 and T =800 °C. 67

Figure 5-13: The syngas lower heating value as a function of gasifier pressure for PKS, MBM and WP gasification using air at ER = 0.3 and T = 800 °C. 68

Figure 5-14: Cold gas efficiency as a function of gasifier pressure for PKS, MBM and WP gasification using air at ER = 0.3 and T = 800 °C. 69

Figure 5-15: Carbon conversion efficiency as a function of gasifier pressure for PKS, MBM and WP gasification using air at ER = 0.3 and T = 800 °C. 70

LIST OF TABLES

Table **Page**

Table 2-1: A selected list of different feedstock based on their classes. 6

Table 2-2: The list of different waste feedstock based on proximate analysis and higher heating values. 8

Table 2-3: The list of different waste feedstock based on ultimate analysis. 8

Table 2-4: The main gas-solid and gas-phase reactions with kinetic parameters for the gasification process (Inayat et al., 2010, Corella and Sanz, 2005, Choi et al., 2001). 12

Table 2-5: The effect of gasifying medium on product gas composition and gasification performance. 19

Table 2-6: The effect of the temperature on product gas composition and gasification performance on different experimental studies. 21

Table 3-1: ASPEN Plus reactor models used in the gasification process. 27

Table 3-2: Some research studies which have been carried out in the simulation of fluidized bed gasification processes using ASPEN Plus. 28

Table 3-3: Inputs of the kinetic models represented as hydrodynamic equations (Lei and Horio, 1998, Bai and Kato, 1999) 30

Table 4-1: Components used in the modelling of the gasification process. 34

Table 4-2: Thermodynamic property specification selected in ASPEN Plus.....35

Table 4-3: The feedstock characteristics (ultimate, proximate and sulfanal analyses) of palm kernel shell (Wan Ab Karim Ghani et al., 2009), meat & bone meal (Campoy et al., 2014), wood pellets (Campoy et al., 2014) and ash for gasification.....36

Table 4-4: Selected chemical reactions occurring in gasifiers for this study. 37

Table 4-5: Feed stream specifications (components, mass flow, presssure and temperature) of gasification process for this study. 40

Table 4-6: ASPEN Plus unit operation blocks showing scheme, block identity (ID) and its function in the gasification process simulation. 41

Table 4-7: Unit operations parameters (pressure and temperature) and specification used for gasification process simulation. 42

Table 5-1: The modelled results compared against experimental hemlock wood gasification results on performance and syngas composition at ER = 0.3. 47

Table 5-2: The H_2/CO ratio and char content of PKS, MBM and WP gasification at different gasification temperatures. 51

Table 5-3: The H_2/CO ratio and char content of PKS, MBM and WP gasification at different equivalence ratios and a temperature of 850°C. 59

Table 5-4: The H_2/CO ratio and char content of PKS, MBM and WP gasification at different gasifier pressures.....66

LIST OF ABBREVIATIONS

A/F	Air to Fuel
BFB	Bubbling Fluidized Bed
CCE	Carbon Conversion Efficiency
CFB	Circulating Fluidized Bed
CGE	Cold Gas Efficiency
ER	Equivalence Ratio
FC	Fixed Carbon
HHV	Higher Heating Value
LHV	Lower Heating Value
MBM	Meat Bone Meal
MC	Moisture Content
PKS	Palm Kernel Shell
PR-BM	Peng Robinson with Boston Mathias
S/B	Steam to Biomass
S/F	Steam to Fuel
VM	Volatile Matter
WGSR	Water Gas Shift Reaction
WP	Wood Pellets

NOMENCLATURE

G_Y	Syngas yield in Nm^3/kg
LHV_{syngas}	Syngas lower heating value in MJ/Nm^3
HHV_{fuel}	Fuel higher heating value in MJ/kg
M_{fuel}	Fuel feed rate in kg/h
Q_{syngas}	Syngas flowrate in Nm^3/h
y_i	Mole ratio or volume percent of component i

CHAPTER 1 : Introduction

Globally, energy sources in particular natural gas, oil and coal remain noticeable, based on the remarkable energy conversion efficiencies they provide. Nevertheless, their usage rate has increased, which resulted in depletion much faster, and they liberate greenhouse gases that contribute to air pollution. It has led to the exploration of new technologies to sustain the energy requirement, namely renewable energy methods. Waste biomass demonstrates a great possibility of becoming an alternative energy source to fossil fuels (natural gas, oil and coal). It is extensively obtainable and has shown a zero-tolerance to carbon dioxide (CO_2) emissions than fossil fuel processing plants emit. In the South African context, 55.7 million tonnes of general waste is generated annually in 2017 (Department of Environmental Affairs, 2018). Figure 1-1 illustrate the general waste type in South Africa contributed by various waste streams.

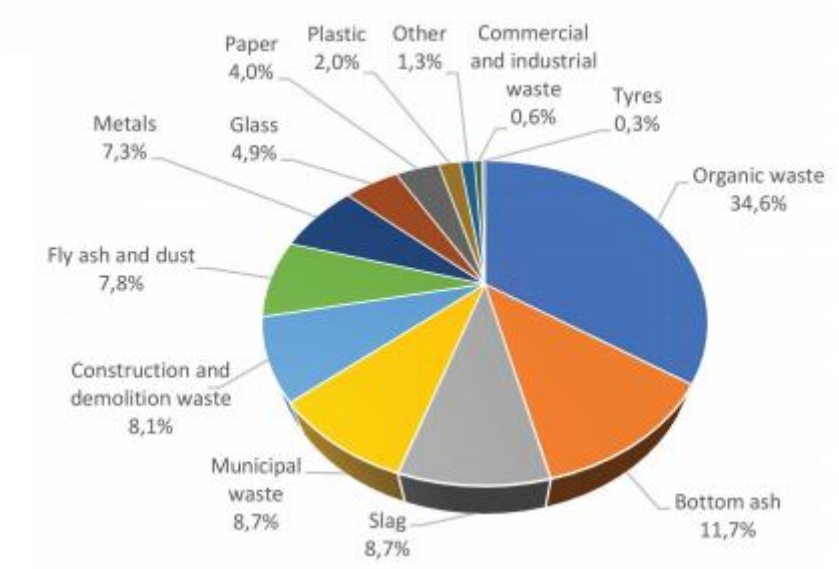

Figure 1-1: South African general waste type and their composition (Department of Environmental Affairs, 2018)

Organic waste contributes about 34.6% and it comprise of the following streams namely agricultural waste, industrial waste and pre-consumer food waste. There are several waste conversion methods such as incineration, combustion, landfilling, pyrolysis and gasification (Sikarwar et al., 2016). The Department of Environmental Affairs (2018) reported that about 50.5% of the organic waste is sent to landfills, occupying a larger volume of the land and no method is employed for waste conversion to useful products. On the other hand, incineration and combustion are prone to affect the environment as they emit toxic gases to the atmosphere, which can cause respiratory problems in humans. However, gasification has shown to be a promising method in the conversion of waste to energy method because it can take variety of waste types and produce useful products, which are not harmful to the environment

as depicted in Figure 1-2. The reduction of organic waste using gasification can reduce the pressure on energy security by employing renewable energy methods. It can also make profits for forest owners when selling their product to gasification plants as raw materials.

Gasification is a favourable energy conversion method because it is a thermochemical process that transforms organic matter to combustible gases, providing energy at high temperatures (Zhang and Zhang, 2019). The stages in gasification occurs as follows: heating and drying, devolatilization (pyrolysis), volatile organic matter reactions and char gasification (Basu, 2010). The chief product gases from gasification comprise of methane (CH_4) , hydrogen (H_2), carbon monoxide (CO), and carbon dioxide (CO_2), which are formed through a series of chemical reactions (Brown, 2011).

Gasifying mediums such as air or steam are necessary to mix with solid/liquid fuels to produce a gas called syngas. The reactor configuration and operating conditions are crucial in determining the quality of syngas. If not controlled properly, it can produce unreacted carbon (char) thus inhibiting syngas quantity and quality (Brown, 2011, Pradana and Budiman, 2015). The reactor types used comprises of fixed beds, fluidized beds and entrained-flow gasifiers. To evaluate gasifier performance, feed conditions and operating parameters need to be adjusted to determine gasifier performance and product gas compositions.

Process modelling and simulations help to apprehend the effect of operating parameters on performance of the gasifier without using more resources for developing pilot plant studies (Li et al., 2001). They can forecast the effect of different parameters on the gasification process without any hazard and at a reduced period compared to the actual pilot-scale process (Gómez-Barea and Leckner, 2010). There is limited work has been reported in the literature on simulation of gasification process which employed air fluidized bed gasifiers for various solid waste (De Andrés et al., 2019, Peng et al., 2017, Yang et al., 2016, Esfahani et al., 2012, Acevedo et al., 2018, Beheshti et al., 2015). Some scholars such as De Andrés et al. (2019) attempted to create a model for air fluidized bed gasification using sewage as a feedstock.

Campoy et al. (2014) experimented air gasification using meat and bone meal and wood pellets in fluidized bed gasifier. They studied the influence of equivalence ratio on gasifier performance parameters. In another experimental study, Wan Ab Karim Ghani et al. (2009) used air gasification system to study palm kernel shell and coconut shell in fluidized bed gasifier. However, they did not investigate the effect of temperature and gasifier pressure in their study and these studies were not compared against simulation.

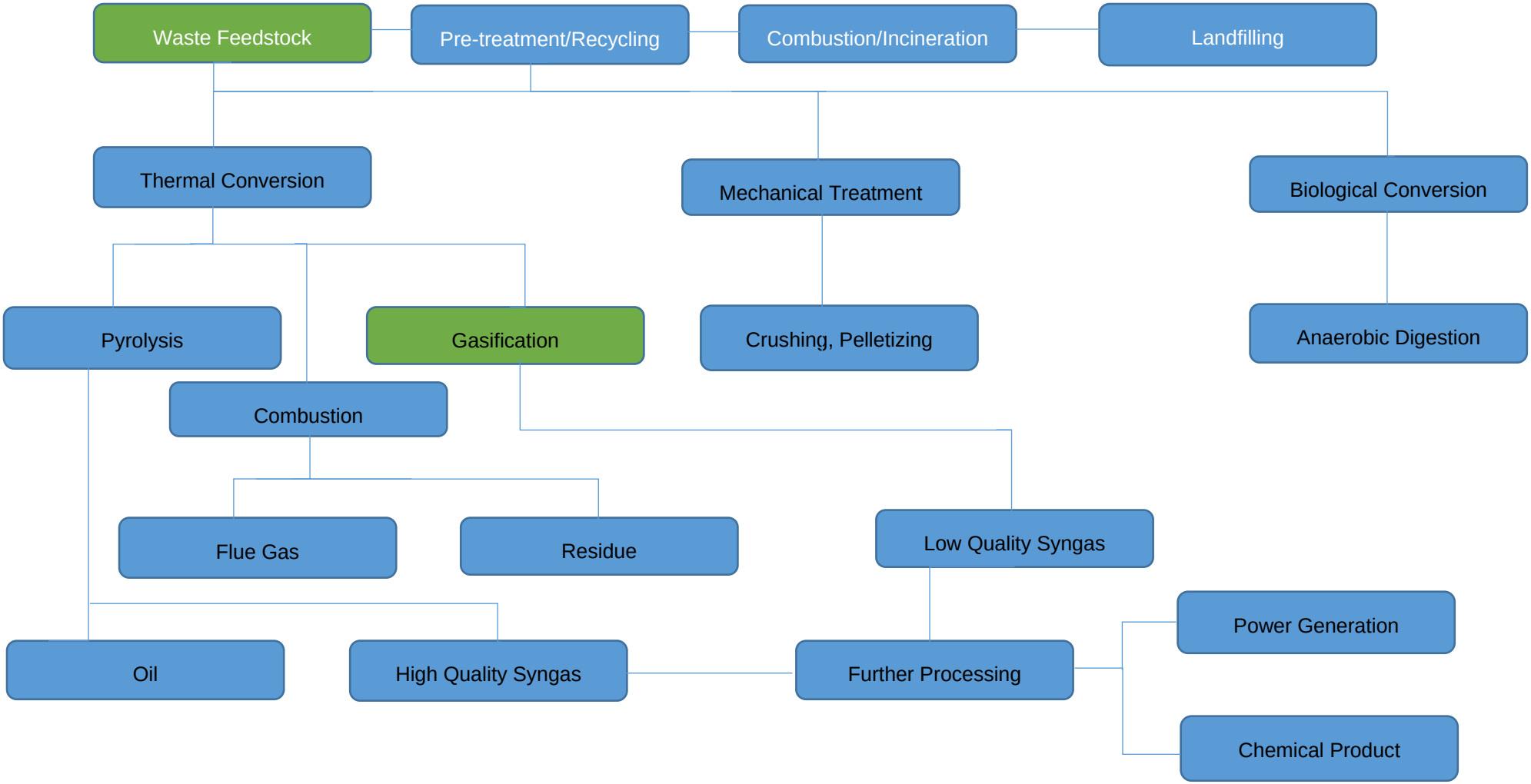

Figure 1-2: Pathways for transforming waste to several energy forms or chemicals through different conversion processes (Seo et al., 2018).

This work will fill the gap through simulating a gasification process using a non-stoichiometric model. A fluidized bed gasification simulation for palm kernel shells, meat and bone meal and wood pellets will be studied. The data obtained in this investigation will fill the gap on using these three feedstock for the designer's air fluidized bed gasifier performance. Additionally, the model will able to predict the shortcomings of operations of the fluidized bed gasifier.

1.1 Aims

This project simulates palm kernel shells, meat and bone meal, and wood pellets gasification in a fluidized bed using air. ASPEN Plus is a simulation tool, which is employed in this investigation. This study aims to achieve gaseous fuels, which can be utilized for energy and chemical production. The model's inputs to be varied are as follows: gasification temperature, gasifier pressure and equivalence ratio. It will enable to forecast the feedstock gasification performance through the analysis of syngas composition and yields, lower heating value of syngas. In addition, it will study the gasification efficiency in terms of carbon conversion and cold gas efficiency.

1.2 Objectives

The specific objectives of this project were:

(a) To select the type of gasifier, gasifying medium and gasification model suitable for various feedstock,
(b) To perform a comparative analysis of inputs on the product gas composition from gasification of various feedstock.
(c) To evaluate and compare the effect of inputs on gasification performance of the various feedstock.
(d) To perform sensitivity analysis of various feedstock in the gasification process using ASPEN Plus.
(e) To evaluate the applications of the gasification products in various industries.

1.3 Outline of the dissertation structure

Chapter One introduces and outlines the aim and objectives of the study.

In **Chapter Two,** detailed literature is reviewed on the waste feedstock and its characterization, thermodynamic properties. The fundamentals of the gasification process is discussed concerning existing gasifier technologies and the influence of the gasification performance. It then discusses the important gasification products with their applications.

Chapter Three introduces ASPEN Plus and gasification models use for the gasification process. It discusses the kinetic and equilibrium modelling methods employed in simulation of gasification processes. Thereafter, it consider the other studies, which were carried out by other scholars, and it concludes with the summary of the work reviewed when compiling this dissertation.

Chapter Four describes how the gasification model used in the study and the methodology used to achieve objectives of this study. It explains the selection of components used for the simulation, thermodynamic properties, model development and description. It then concludes with the sensitivity analysis and equations used for calculating gasification performance parameter.

Chapter Five presents the significant results of equivalence ratio, gasification temperature and gasifier pressure on gasifier performance and the subsequent discussion in relation to literature studies.

Chapter Six presents various conclusions drawn from the study and gives recommendations on the shortcomings of this study.

CHAPTER 2 : Gasification

2.1 Introduction

In the preceding chapter, the gasification process was introduced, and the aims and objectives of this dissertation. The appropriate literature will be reviewed in this chapter to understand the governing concepts of gasification. It covers waste feedstock characterization and its thermodynamic properties. Thereafter, it dwells on the fundamentals of gasification processes and how gasifier performance is affected by various input parameters. It then, scrutinizes literature studies on gasification technologies, operating and performance indicators.

2.2 Feedstock

A renewable, carbon-containing raw material that can be utilized as fuel or converted to other forms for energy production is considered a feedstock (Kataki et al., 2015). There are different feedstock options that comprise carbonaceous materials such as virgin and waste biomass, coal, waste plastics, crude oils, and waste tires. Table 2-1 shows different classes of feedstock available for energy production.

Table 2-1: A selected list of different feedstock based on their classes.

Virgin biomass	Waste biomass	Waste plastics	Other
Crops	Agricultural waste	Polyethylene	Coal
Herbaceous biomass	Forestry waste	Polypropylene	Crude oils
Woody biomass	Industrial waste	Polystyrene	Heavy oils
	Municipal waste	Polyvinylchloride	Waste tires
		Polyethylene Terephthalate	

The virgin biomass class includes crops, herbaceous and woody type biomass. Virgin biomass is converted to waste biomass during various production stages from forest products. The waste biomass considers waste from agricultural, forestry, industrial and municipal sectors. Some different waste types include polypropylene (PP), polystyrene (PS), polyvinyl chloride (PVC), polyethylene terephthalate (PET) and polyethylene (PE). Other feedstock types include coal, crude oils, heavy oils and waste tires.

Waste biomass can provide different feedstock options such as agricultural residues (meat and bone meal, palm kernel shell, coconut shell, maize, peanut husks, animal manure etc.) and forest residues (wood chips, sawdust, shrubs or coal etc.) (Basu, 2018). However, these feedstock consists of high bulk

density, heating value, moisture, and ash content (Brown, 2011). The characterization of feedstock based on its composition is discussed in the following section.

2.2.1 Feedstock characterization

The feedstock constitutes a complex organic compound that includes moisture content (MC) and Ash. According to Basu (2018), an organic compound contains the following atoms of Carbon (C), hydrogen (H), nitrogen (N), oxygen (O) and traces of sulphur (S) and occasionally chlorine (Cl). The feedstock are characterized using two methods of composition analysis, which are proximate and ultimate analysis. These methods are determined experimental following American Society for Testing Materials protocols. The proximate analysis method reports mainly moisture content (MC), fixed carbon (FC), volatile matter (VM) and Ash. Equation (2.1) determines components of the proximate analysis in as-received basis (ar).

$$FC + MC + VM + Ash = 100\% \qquad (2.1)$$

The fraction of water in the feedstock characterize the moisture content. If moisture content is removed, the components can be expressed on dry-basis (db). Furthermore, if both moisture content and ash are removed from the total components in equation (2.1) or (2.2), then remaining components are expressed as dry-ash-free basis (daf) (Basu, 2018). When the feedstock is heated at a temperature above 100 to 400 °C and at constant pressure, it liberates volatile organic compounds, representing volatile organic matter (Basu, 2018). The residual carbon, which remains in the reaction vessel after devolitization, is called fixed carbon. Ash is the remaining residual inorganic component which comprises of metal oxide compounds such as silicon dioxide, calcium oxide, iron oxide and magnesium oxide etc. (Brown, 2011). Table 2-2 shows different feedstock characterizations based on their proximate analysis and higher heating values (HHV) used for gasification processes. The elemental analysis is expressed using equation (2.2), which considers the fuel's moisture content and Ash. These corresponding elements are reported in the mass percentage (wt.%) of a representative feedstock.

$$C + H + N + S + O + Cl + MC + Ash = 100\% \qquad (2.2)$$

Table 2-3 shows different feedstock characterization based on the ultimate analysis used for gasification processes. These feedstock varies in terms of energy available to produce syngas.

Table 2-2: The list of different waste feedstock based on proximate analysis and higher heating values.

Feedstock	Proximate analysis (wt.% dry basis)				HHV**	Reference
	FC	VM	MC	Ash		
Coconut shell	26.41	30.62	4.89	42.98	16.07	(Wan Ab Karim Ghani et al., 2009)
Cork waste*	59.16	40.22	16.3	2.4	16.16	(Rodrigues et al., 2017)
Food waste*	14.6	51.1	29.3	4.9	26.33	(Naveed et al., 2009)
Meat and Bone Meal	9.1	72.1	6.9	19.1	21.3	(Campoy et al., 2014)
Mixed Plastics*	2.0	95.8	0.2	2.0	n.r	(Seo et al., 2018)
Municipal solid waste*	7.6	18.8	50.9	22.7	9.35	(Naveed et al., 2009)
Palm kernel shell	18.56	72.47	7.96	8.97	22.97	(Wan Ab Karim Ghani et al., 2009)
Pine sawdust	17.16	82.29	8	0.55	n.r	(Nikoo and Mahinpey, 2008)
Poultry waste*	8.3	40.3	7.5	43.9	9.24	(Naveed et al., 2009)
Sugarcane bagasse	11.9	82.5	6.8	5.6	n.r	(Mavukwana et al., 2013)
Wood pellets	18.3	81	6.3	0.7	19.6	(Campoy et al., 2014)

n.r = not reported , * = wt % in as received basis ****** = reported in MJ/kg of fuel

Table 2-3: The list of different waste feedstock based on ultimate analysis.

Feedstock	Ultimate analysis (%wt. dry basis)					References
	C	H	N	S	O	
Coconut shell	45.24	5.04	1.46	0.06	48.2	(Wan Ab Karim Ghani et al., 2009)
Cork waste[a]	48.1	6.3	0.5	-	26.4	(Rodrigues et al., 2017)
Food waste[a]	56.65	8.76	3.95	0.19	23.54	(Naveed et al., 2009)
Meat and Bone Meal	54.7	7.8	9.1	0.78	27.6	(Campoy et al., 2014)
Mixed Plastics[a]	60.0	7.2	-	-	22.8	(Seo et al., 2018)
Municipal solid waste[a]	36.35	4.96	1.43	0.83	10.13	(Naveed et al., 2009)
Palm kernel shell	51.63	5.52	1.89	0.05	40.91	(Wan Ab Karim Ghani et al., 2009)
Pine sawdust	50.54	7.08	0.15	0.57	41.11	(Nikoo and Mahinpey, 2008)
Poultry waste[a]	22.4	3.8	2.6	0.7	27.1	(Naveed et al., 2009)
Sugarcane bagasse	47.5	5.9	0.29	0.07	40.7	(Mavukwana et al., 2013)
Wood pellets	49.8	5.8	2.0	0.06	42.2	(Campoy et al., 2014)

[a] = expressed on as received basis. The Ash content in Table 2-2 is similar to the one above for complete representation of ultimate analysis as per equation (2.2).

2.2.2 Thermodynamic properties of the feedstock

Gasification is a thermochemical conversion process that employs thermodynamic properties in chemical reactions (Basu, 2018). There is a need to understand the thermodynamic properties such as specific heat capacity, heating value, ignition temperature and heat of reaction.

The most critical parameter in thermodynamic calculations is the specific heat capacity. It represents the specific heat of a particular material, either coal or biomass. The fraction of moisture content and operating temperature in any fuel influences the specific heat capacity (Basu, 2018). For example, the specific heat capacity of wood can be determined using the model developed by Ragland et al. (1991) shown as equation (2.3) :

$$C_{p,dry} = 0.00486\,T - 0.21293 \qquad (2.3)$$

The heat of reaction (enthalpy) is the thermodynamic property that determines whether the energy is liberated or consumed in a chemical reaction without any temperature change. It is represented by symbol ΔH_r, it can either be positive or negative. In an exothermic reaction, the heat of reaction is negative and positive in an endothermic reaction. Ignition temperature determines the lowest temperature required for any fuel to ignite for the combustion process (Brown, 2011). Furthermore, this provides sensible energy for drying and pyrolysis stages.

The heat liberated by fuel when combusted fully at standard temperature and pressure of 25°C and 101.3 kPa is the heating value (Brown, 2011). It is influenced by the liquid or gas phase of water molecules formed when the fuel is combusted. It is titled a lower heating value (LHV) when the heat is liberated and produced water is in a gas phase. On the other hand, the heating value is called higher heating value (HHV) when water vapour condenses into liquid water. The latent heat of vaporization differentiates these heating values. The higher heating values of the different feedstock are shown in Table 2-2.

The higher heating value of any fuel can be determined using the model below developed by Channiwala and Parikh (2002) for estimating solid, liquid and gaseous phase fuels:

$$HHV_{fuel} = 349.1C + 1178.3H + 100.5S - 103.4O - 15.1N - 21.1Ash \qquad (2.4)$$

The above model is only applicable when the fuel has the following weight percent ranges; Carbon is between 0 and 92 %, hydrogen is between 0.43 and 25%, oxygen is between 0 and 50%, nitrogen is between 0 and 5.6 %, Ash is between 0 and 71%, HHV is between 4.75 and 55.35 MJ/kg (Basu, 2010, Basu, 2018).

The lower heating value of fuel can be estimated using equation (2.5), where: h_g represents the latent heat of vaporization, which is 2.441 MJ/kg at 25°C (Basu, 2018).

$$LHV_{fuel} = HHV_{fuel} - h_g \left[\frac{9H}{100} - \frac{MC}{100}\right] \qquad (2.5)$$

2.3 Fundamentals of gasification processes

Gasification converts organic carbon material using air or steam to produce combustible gases at high temperatures (Zhang and Zhang, 2019). It produces a mixture of carbon monoxide, hydrogen, methane, carbon dioxide, other light hydrocarbons (ethane, propane etc.) and nitrogen gases (Pradana and Budiman, 2015). The gasification process comprises of different steps: drying, devolatilization (pyrolysis), gas-solid reactions, and char gasification reactions (Basu, 2018). Figure 2-1 shows the gasification process pathways.

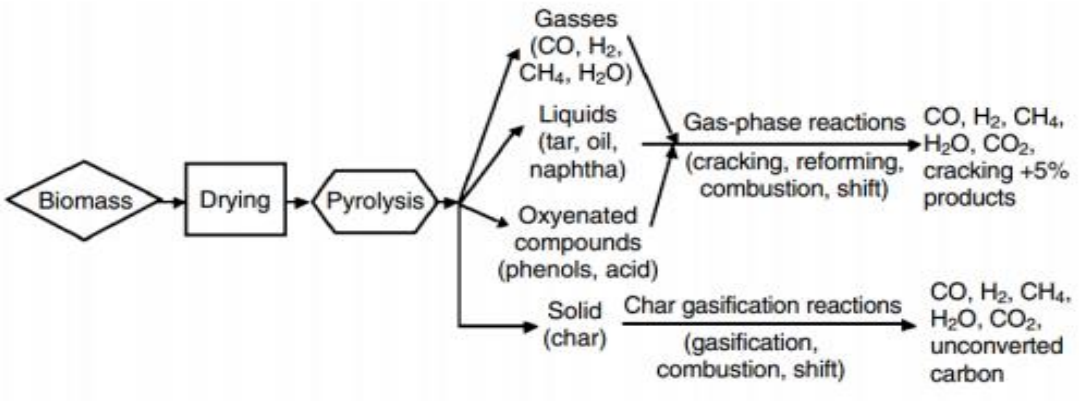

Figure 2-1: The potential pathways of the gasification process (Pradana and Budiman, 2015).

A detailed explanation of the gasification process is as follows; the feedstock (biomass, coal etc.) of desirable moisture content is evaporated through drying and heating. It then forms part of a gasifying medium, which can be either steam or air. The biomass is then disintegrated in the pyrolysis stage to liberate gases (volatile compounds), solid carbon (char), liquid mixtures such as tar (condensable hydrocarbons), oil, naphtha and large molecular hydrocarbons without oxygen (Pradana and Budiman, 2015). Contaminants such as nitrogen and sulphur containing compounds from gasification can improvise the quality of the syngas (Rezaiyan and Cheremisinoff, 2005). They need to be removed downstream as the reaction pathways proceeds char gasification commences in the presence of a gasifying medium.

The type of gasifying medium influences the syngas quality and its energy content. The char gasification employs the gas-solid reactions comprising char, oxygen, carbon dioxide and steam produced from the

pyrolysis stage. At higher temperatures, the gas-phase reactions occur where they produce hydrogen, methane, carbon monoxide and carbon dioxide. Drying and pyrolysis are endothermic processes, which requires heat to sustain the chemical reaction. The partial oxidation of char is an exothermic reaction, thus supplies heat to pyrolysis and drying.

The behaviour of chemical reactions can be explained by reaction rate. There are several rates of reaction equations for gas-solid and gas-phase reactions. These equations were developed on the simplest kinetic order model of reacting compounds (A and B) using their concentration are expressed as equation (2.6) (Fogler, 2010).

$$r_i = -kC_A C_B \qquad (2.6)$$

Where the kinetic parameter k is evaluated using equation (2.7), which consider the Arrhenius model using the frequency factor A, activation energy E_a and temperature T:

$$k_i = A \cdot e^{-\frac{Ea}{RT}} \qquad (2.7)$$

The main reactions considered for gas-solid and gas-phase reactions are shown in Table 2-4.

2.3.1 Shrinking core model

This model describes solid char, which is consumed through chemical reactions occurring on the outer surface of the solid particle. In theory, there will be unreacted core part B, which indicate the particle consumption as the solid particle shrinks to the core. The carbon content in the feedstock will be consumed by fluid medium (gas phase) as per Figure 2-2. Table 2-4 illustrates the gas-solid reactions based on shrinking core model.

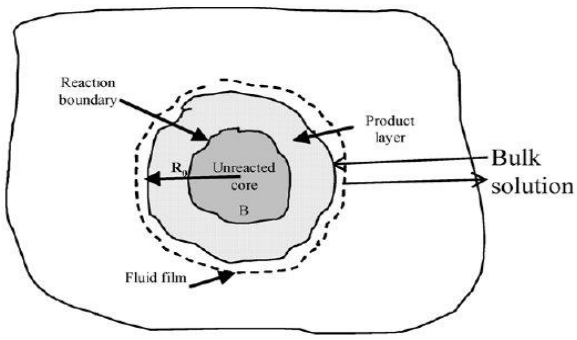

Figure 2-2: The diagram of shrinking core model showing gas-solid systems occuring in microscopic level (Fogler, 2010).

Table 2-4: The main gas-solid and gas-phase reactions with kinetic parameters for the gasification process (Inayat et al., 2010, Corella and Sanz, 2005, Choi et al., 2001).

Reaction name	**Chemical equation**	**Kinetic parameters for reactions ($mol.m^{-3}.s^{-1}$)**
Char partial oxidation	$C\ (s) + 0.5O_2(g) \leftrightarrow\ CO(g)$ $\Delta H_r =\ -110.5\ MJ/kmol$	
Char gasification	$C\ (s) + H_2O(g) \leftrightarrow\ CO(g) + H_2(g)$ $\Delta H_r = 131.3\ MJ/kmol$	$k = 2\ \times 10^5\ e^{\frac{-6000}{T}}$
Methane formation	$C\ (s) + 2H_2(g) \leftrightarrow\ CH_4(g)$ $\Delta H_r = -74.8\ MJ/kmol$	$k = 4.40\ e^{\frac{-1.62\ \times 10^8}{T}}$
Boudouard reaction	$C\ (s) + CO_2(g) \leftrightarrow\ 2CO(g)$ $\Delta H_r = 172.4\ MJ/kmol$	$k = 0.12\ e^{\frac{-17.291}{T}}$
Steam-methane reforming	$CH_4\ (g) + H_2O(g) \leftrightarrow\ CO(g) + 3H_2(g)$ $\Delta H_r = 206.1\ MJ/kmol$	$k = 3 \times 10^5\ e^{\frac{-15000}{T}}$
Water-gas shift	$CO(g) + H_2O(g) \leftrightarrow\ CO_2(g) + H_2(g)$ $\Delta H_r = -41.1\ MJ/kmol$	$k = 1 \times 10^6\ e^{\frac{-6370}{T}}$

(s) = solid phase ; (g) = gaseous phase ; ΔHr = heat of reaction ; k = kinetic parameter ; T = temperature in °K

2.4 Types of gasifiers

The reaction vessel where the gasification process occurs is called a gasifier. They differ in terms of design configuration on how this gas-solid mixing is taking place. Three various types of gasification technologies, which are fixed-bed, fluidized-bed and entrained-flow gasifiers.

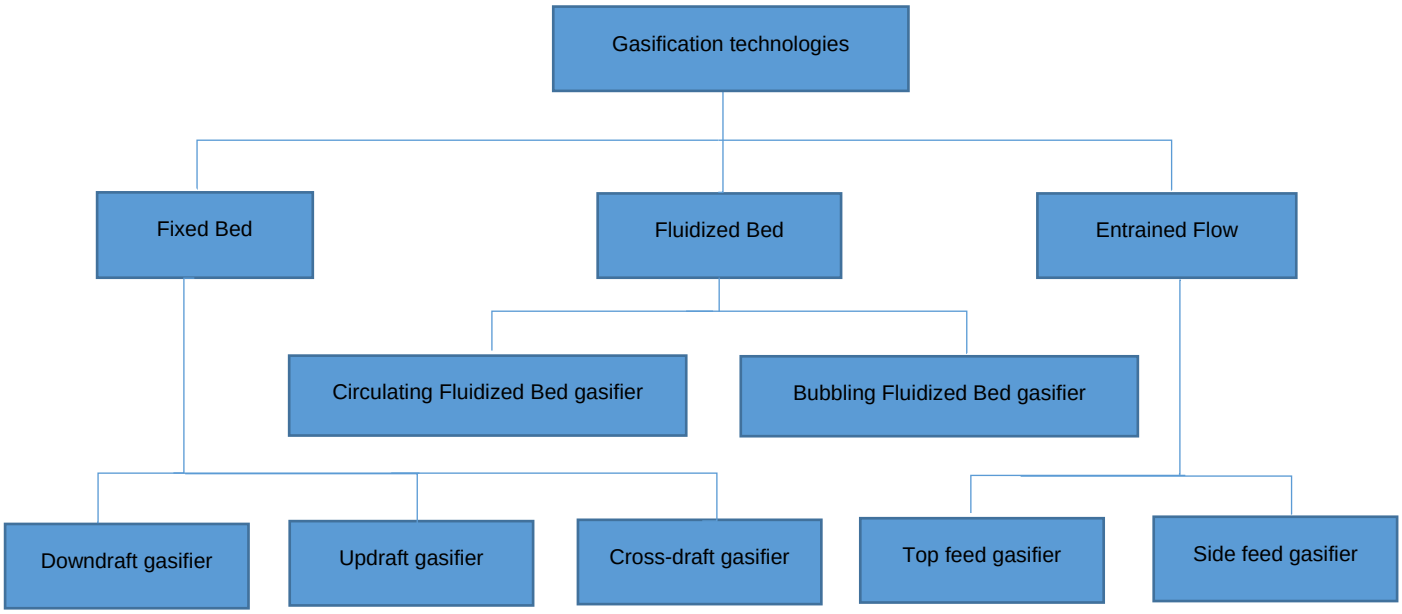

Figure 2-3: The classification of gasification technologies based on their design (La Villetta et al., 2017).

2.4.1 Fixed bed gasifier

These types of gasifiers are operated at temperatures between 300 and 1000°C on atmospheric pressure conditions (Jahromi et al., 2021). A fixed bed gasifier contains a dense bed of fuel particles held by the grate. They are modest, easy to operate, and are used for small-scale applications. These gasifiers are configured differently in terms of gasifying medium feed location and vessel design, are categorized as updraft, downdraft and cross-draft gasifiers (Yao et al., 2020, Jahromi et al., 2021).

The fuel is fed at the top, and it is counter-current flows with the gasifying medium in an updraft fixed bed gasifier. After the series of reactions inside the reactor, the product gas is extracted at the top of the gasifier. These reactions include drying, pyrolysis, reduction and oxidation (Lian et al., 2021). The gasifying medium is fed sideways in the downward fixed bed gasifier while the fuels descend to the grate and product gas is extracted at the bottom. A low product gas yield is obtained from downward gasifiers than upward gasifiers, which is a limiting factor for large-scale applications, and temperature

control is not uniform (Lian et al., 2021). According to Yao et al. (2020), the tar content makes it difficult for large-scale fixed bed gasifier applications. However, the quality of hydrogen yield is higher than the entrained-flow gasifier.

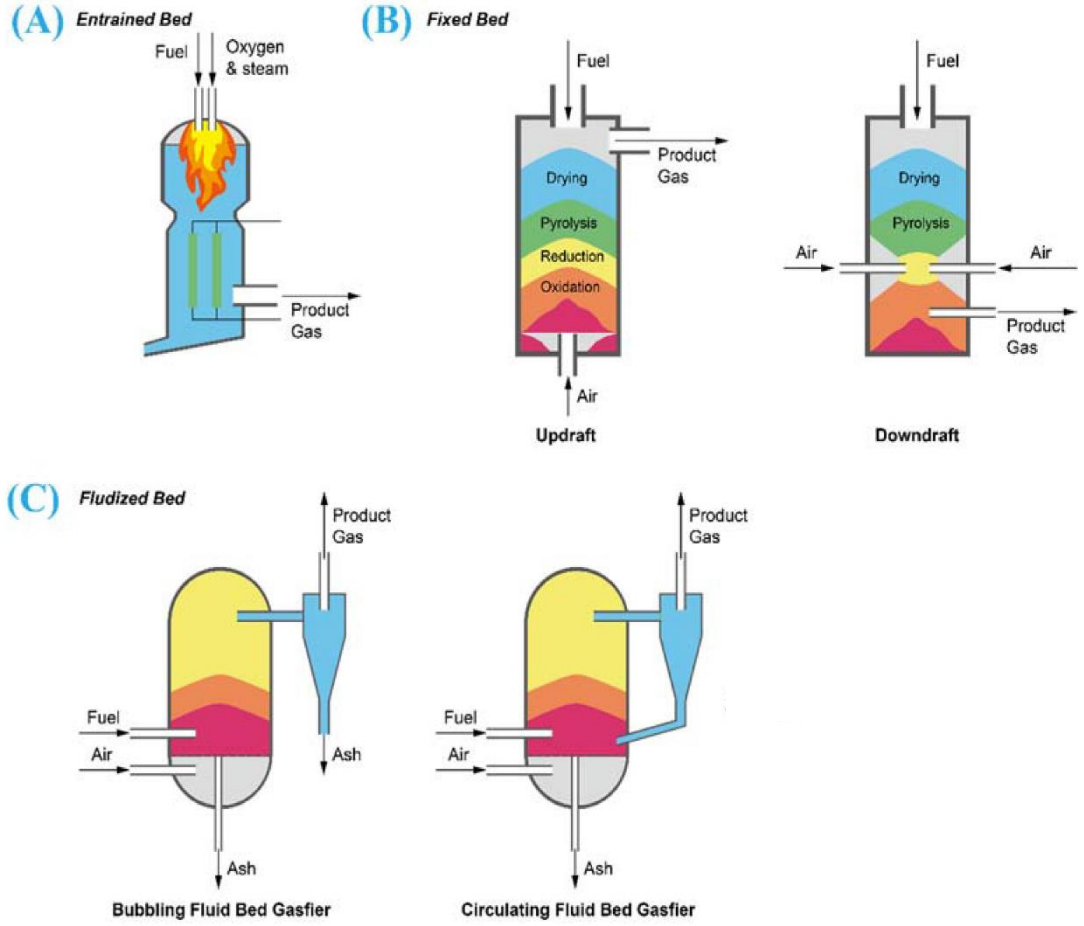

Figure 2-4: The graphic illustration of different gasifiers based on the feed and product gas positions: (A) entrained-flow, (B) fixed-bed and (C) fluidized bed gasifiers (Lian et al., 2021).

2.4.2 Fluidized bed gasifier

These gasifier types employ fluidizing the waste feedstock with a gasifying medium travelling the bed material upwards at a controlled rate. The bed material is unreactive and contains dense catalytic or inert particles such as sand, quartz or alumina for effective heat transfer. Fluidized bed gasifiers exhibit a uniform temperature due to well-mixed particles of bed, enabling them to process various fuels of different compositions. A fluidized bed gasifier's typical operating temperature ranges between 700 and 1000°C to avoid melting of ash and blockages on downstream equipment (Lian et al., 2021). However, the ash content should be less than 25 wt.% while ash melting temperature should be greater than 900 °C

(Bermudez and Fidalgo, 2016, McKendry, 2002, Basu, 2010, Basu, 2018). The fly ash melting point is also affected by impurities accumulation that comes with feedstock into the gasifier.

Two chief fluidized bed gasifiers were configured based on their fluidization medium flow rate: bubbling fluidized bed (BFB) and circulating fluidized bed (CFB) gasifiers. They can either be operated at atmospheric or pressurized conditions. In the BFB gasifier, the fuel is fed at the side of the dense bed material, and the fluidizing medium (either air or steam) is fed from the bottom. The particle size of feedstock with an acceptable range is within 0.5 to 1.0 mm for BFB gasifiers.

The moisture content of feedstock should be between 5 and 60 wt.% is required for CFB and between 10 and 55 wt.% for BFB gasifiers (Bermudez and Fidalgo, 2016, McKendry, 2002, Basu, 2010, Basu, 2018). The gasifying medium fluidizes the bed until it triggers bubble formation when air velocity (0.5 to 1.0 m/s) is greater than the minimum fluidization velocity (Bermudez and Fidalgo, 2016). The product gas exit at the top and ash is removed at the bottom of the cyclone. They produce high tar content and liberate char with product gas. The distinctive syngas ranges are : 6.0 to 35 vol.% of hydrogen, 15 to 40 vol.% of carbon monoxide, 15 to 30 vol.% of carbon dioxide, 3.0 to 8.0 vol.% of methane and 3.0 to 60 vol.% of nitrogen for fluidized bed gasifiers (Bermudez and Fidalgo, 2016, Basu, 2018). However, these ranges are greatly influenced by the gasifying medium, which can be either air or steam.

CFB gasifiers operate at higher gas velocities (3.5 to 5.5 m/s) than BFB gasifiers (Bermudez and Fidalgo, 2016). CFB gasifiers can accept small particle sizes of less than 400 μm and wide ranges of particle size distribution without feedstock losses. It has a cyclone, which separates the solids extracted with the product gas. The solids from the bottom of the cyclone and are circulated back into the fluidized bed through the riser pipe to the gasifier. This has proven to improve carbon conversion (Bermudez and Fidalgo, 2016). Both of the fluidized bed gasifiers have shown improved performance in treating fuel with high moisture content due to better mixing. However, BFB gasifiers have issues in the presence of gas channelling and bubble formation (González-Vázquez et al., 2018, Nam et al., 2020).

In comparison to all the gasifiers, fluidized bed gasifiers can accept different types and sizes of feedstock, making them possible for commercial uses on a large scale (Marcantonio et al., 2019). The temperature profile is controlled at high values and is uniform for the fluidized bed gasifiers compared to fixed bed gasifiers. It is significant to produce high efficiency of carbon conversion and tar reduction. The principle of fluidization and higher gas velocities employed in fluidized beds promotes the mixing of fuel and gasifying medium, thus resulting in higher reaction effectiveness.

2.5 Gasification performance.

The gasifier operation determines the syngas quality that is influenced by the gasifying medium (equivalence ratio), waste feedstock flow and composition, gasifier pressure and temperature. These factors influence how the gasifier performs in producing the syngas. The syngas composition and yield measure the gasifier performance, including the lower or higher heating value, cold gasification efficiency and carbon conversion efficiency. These factors are discussed below on how they influence gasification performance.

2.5.1 Effect of gasifier design

The gasifier configuration has a significant role in solid carbon and air or steam mixing inside the reactor. The gas-solid contact and mixing are essential to understand heat and mass transfer behaviour between these phases (Basu, 2018). The reaction of the gas and solids occurs at the bed surface, which can be either fixed or moving. The bed consists of different-sized particles; however, in CFB gasifiers, smaller bed particles are utilized (Pfeifer et al., 2011). According to Erakhrumen (2012), CFB gasifiers delivers higher carbon conversion efficiency compared to BFB gasifiers.

Fixed bed gasifiers have weaknesses, to mention a few, the solids product such as char and tar yield are more significant. According to Alauddin et al. (2010), irregular heat and mass transfer amongst feedstock and air or steam in the gasifier is the cause of these poor performances. On the contrary, fluidized bed gasifiers prove efficient in heat and mass transfer for the solids and gasifying agent mixing. They have improved the rate of reactions and in converting carbon to valuable products, i.e. syngas. These types of reactors employ the use of bed particles as a catalyst and for effective heat transfer. In addition, they produced an improved syngas quality. According to Alauddin et al. (2010), a fluidized bed gasifier accommodates various carbon-containing feedstock with different physical properties and heating values.

2.5.2 Effect of the feedstock properties

Campoy et al. (2014) mentioned that high volatile matter content relative to fixed carbon produces high carbon conversion efficiency. They further observed an increase in volatiles combustion, which lead to a decrease in syngas lower heating value. In their syngas composition produced, they found a higher carbon dioxide concentration. The higher the feedstock moisture content, it tends to increase the energy demand for drying. (Basu, 2018) used the carbon-hydrogen-oxygen ternary diagram to predict the formation of syngas composition from fuel.

The steam gasification is favourable to produced more H/C ratio indicating more hydrogen and methane formation. At the same time, more O/C ratio is favourable for the production of CO and CO_2 (Brown, 2011, Basu, 2018). The presence of sulphur in the feedstock produces hydrogen sulphide and ammonia, which are contaminants of the syngas (Bermudez and Fidalgo, 2016). These compounds are toxic, and they require careful separation and treatment downstream. The gasification system then needs to be integrated with gas separation and cleaning equipment that can increase the project's capital cost (Brown, 2011). After that, a careful operation of a gasifier is considered to ensure the formation of these compounds does not leave to the atmosphere, as they are dangerous to human health and the environment. On the other hand, chloride and sulphur compounds are not valuable for gasification since they are corrosive and can quickly build upon the gasifier walls (McKendry, 2002, Basu, 2018).

According to Worley and Yale (2012), the inner gasifier lining comprises refractory bricks where these compounds can stick on and remove the inner wall. Ash is considered a mineral matter that can negatively affect gasification when the operating temperature is not controlled below the ash melting point. It could results in feed blockages, slag issues, and clinkering, especially with ash containing high alkali oxides (McKendry, 2002). Seo et al. (2018) argued that low volatile containing feedstock is suitable for indirect gasification (air or oxygen). They further enlighten that high volatile matter feedstock is required for direct gasification (steam). In conclusion, the feedstock properties have a substantial effect on the gasifier performance. The feedstock requirements for different feedstock is discussed in section 2.4

2.5.3 Effect of the gasifying medium

Air and steam are popular gasifying mediums used in gasification systems. They influence the syngas composition and its yield. Air gasification of biomass produces low syngas lower heating values between 4 and 7 MJ/Nm^3 due to ~79% of nitrogen contained in air (Basu, 2010, Basu, 2018). In a study conducted by Sreejith et al. (2014), they reported optimal conditions for wood gasification using pure steam at 800°C. Their syngas composition in mole fraction was 57.7% for H_2, 4.2% for CO, 36.1 % for CO_2, and 2.1 % for CH_4. When they adjusted the steam to biomass ratio at 1.1, they obtained a syngas LHV of 9.4 MJ/Nm^3. In steam gasification, Basu (2018) reported a range of syngas LHV between 10 and 18 MJ/Nm^3.

The equivalence ratio (ER) is the ratio between the airflow rate fed into the gasifier and the stoichiometric airflow rate needed for the complete combustion of a fuel. It is a crucial operating parameter, and it's a trade-off required for operating the feed rates to the air gasification. The gasifier types have different operating ERs; for example, a fluidized bed has an optimal ER of 0.24 to 0.4 (Basu, 2010). According to De Andrés et al. (2019), higher ER increases syngas yield and carbon conversion

efficiency. Another finding was the cold gas efficiency, which was relatively constant at 40% in sludge gasification. In another study, De Andres et al. (2011) investigated sewage gasification in a fluidized bed gasifier using air. They varied ER between 0.20 and 0.40, and obtained an increase in syngas yield from 2.0 to 3.2 Nm^3/kg daf while carbon conversion was relatively between 78 and 82%. They found a cold gas efficiency of 37.25% and syngas lower heating value (LHV) of 3.33 MJ/Nm^3. In their findings, hydrogen, carbon monoxide, carbon dioxide, and methane decreased with ER increase. Wan Ab Karim Ghani et al. (2009) studied palm kernel shell gasification using air; they observe that H_2 content decreased as ER increased from 0.15 to 0.3, while CO, CO_2, and CH_4 concentration increased. The partial oxidation of carbon, boudouard and water gas shift reactions contributed to increased CO and H_2 concentration at higher temperatures (Xiao et al., 2009). In another study, Campoy et al. (2014) investigated the influence of stoichiometric ratio (similar to ER) on syngas composition and gasifier performance parameters in a fluidized bed gasifier using air. They used wood pellets (WP), meat, and bone meal (MBM) as their feedstock. For gasification of MBM, ER was increased from 0.25 to 0.42, the trends of H_2, CO and CH_4 concentration declined. While CO_2 production started rising, and ER = 0.3 was a turning point, it decreased until it reached an ER of 0.42. Wood pellets gasification, ER was varied from 0.24 to 0.36, the CO, H_2 and CH_4 concentration decline while CO_2 concentration was increased. Syngas LHV decreased from 3.8 to 1.5 MJ/Nm^3 (ER from 0.25 to 0.42) for MBM gasification. For WP gasification, the LHV drops from 5.8 to 4.7 MJ/Nm^3 when ER was varied between 0.24 and 0.36. The syngas yield (GY) was found to increase for both feedstock with an increase in ER.

Carbon conversion efficiency describes the ratio of carbon converted from biomass to syngas. The carbon conversion efficiency (CCE) for MBM was relatively at 99%, whilst wood pellets varied between 90 and 96%. Campoy and co-authors did not consider the amount of un-reacted carbon that exit with the syngas as volatiles in their study. Cold gas efficiency is the energy provided by syngas divided by fuel or biomass energy. Campoy et al. (2014) reported that cold gas efficiency (CGE) decreases from 30% to 20% for MBM gasification. While for WP gasification, it was relatively between 55% and 60%. The yield of tar decreased with an increase in ER for WP and MBM as feedstock. In another investigation, Chang et al. (2011) reported a higher hydrogen yield, improved by steam.

Table 2-5: The effect of gasifying medium on product gas composition and gasification performance.

Operating parameters	Syngas composition ranges	Gasification performance indicator	References
FS: Meat and Bone Meal **GT:** Fluidized Bed **ER :** 0.25 to 0.42 **GM:** Air Bed Temp.:808 – 857 °C Air flow : 14 Nm^3/h Fuel flow : 7.2 – 12 kg/h	**H_2 :** ~ 0.2 – 8 vol.% **CO :** ~ 5.2 – 10.3 vol.% **CO_2 :** ~ 12.1 – 14.2 vol.% **CH_4 :** ~ 2 – 4 vol.%	**GY:** ~ 0.92 to 1.03 Nm^3/kg daf **CGE :** ~ 20 to 30% **LHV :** ~ 1.5 to 3.8 MJ/Nm^3 **CCE :** ~99% **Tar content :** 18.5 to 25 g/Nm^3	(Campoy et al., 2014)
FS: Wood Pellets **GT:** Fluidized Bed **ER :** 0.24 to 0.36 **GM:** Air Bed Temp.:785 – 813 °C Air flow : 18 Nm^3/h Fuel flow : 11.9 – 17.9 kg/h	**H_2 :** ~8 – 13 vol.% **CO :** ~ 16 – 18 vol.% **CO_2 :** ~ 14.2 – 15 vol.% **CH_4 :** ~ 4.8 – 5.8 vol.%	**GY :** ~ 0.88 to 1.0 Nm^3/kg daf **CGE :** ~55 to 60% **LHV :** ~ 4.7 to 5.8 MJ/Nm^3 **CCE :** 90 to 96% **Tar content :** 15.4 to 24.6 g/Nm^3	(Campoy et al., 2014)
FS: Palm Kernel Shell **GT:** Fluidized Bed **ER :** 0.15 to 0.45 **GM:** Air	**H_2 :** 8 – 11 vol.% **CO :** 15 – 20 vol.% **CO_2 :** 16 – 30 vol.% **CH_4 :** ~ 1 vol.%	**GY :** 1.08 to 2.07 mol/kg of fuel **LHV :** 1.48 to 3.47 MJ/Nm^3	(Wan Ab Karim Ghani et al., 2009)
FS: Palm Kernel Shell **GT:** Fluidized Bed **ER :** 0.23 to 0.27 **GM:** Air **Temperature** = 900°C	**H_2 :** ~ 25 – 32 vol.% **CO :** ~ 5 – 6 vol.% **CO_2 :** ~ 4 vol.% **CH_4 :** 7 – 9 vol.%	**Hydrogen yield :** 20 to 26.4 g/kg of fuel	(Esfahani et al., 2012)
FS: Palm oil waste **GT:** Fixed Bed **ER :** 0.25 to 0.42 **GM:** Steam	**H_2 :** 47 – 58 vol.% **CO :** 14 – 33 vol.% **CO_2 :** 14 – 26 vol.% **CH_4 :** 3 – 6 vol.%	**GY :** 1.2 to 2.48 Nm^3/kg **LHV :** 8.73 to 11.98 MJ/Nm^3	(Lv et al., 2007)
FS: Sewage sludge **GT:** Fluidized bed **ER :** 0.20 to 0.40 **GM:** Air	**H_2 :** 8.5 - 15 vol.% **CO :** 7 - 11 %vol.% **CO_2 :** 12 – 14 vol.% **CH_4 :** 2.5 – 4.2 vol.%	**GY :** 2.0 to 3.2 Nm^3/kg daf **CCE :** 78 to 82%	(De Andres et al., 2011)
FS: Helmock Wood **GT:** Fluidized Bed **ER :** 0.3 **GM:** Air (At optimal conditions)	**H_2 =** 5.5 vol.% **CO =** 16.60 vol.% **CO_2** = 15.00 vol.% **CH_4** = 3.40 vol.%	**CGE** = 71.4% **HHV** = 4.82 MJ/Nm^3	(Li et al., 2004)
FS: Olive kernels **GT:** Fixed bed **GM:** Air	**H_2 :** 20 – 30 wt.% **CO :** ~15 – 20 wt.% **CO_2 :** ~ 40 – 55 wt.% **CH_4 :** ~10 – 12 wt.%	**GY :** 0.6 to 0.84 m^3/kg **LHV :** 8.8 to 10.4 MJ/Nm^3	(Skoulou et al., 2008)

A large quantity of energy for heating the gasifier is desirable when using steam. However, steam usage is not suitable for many applications due to higher energy requirements. It will increase the operational expenditure when steam availability is minimal or is an issue. The study by Li et al. (2009) suggested that the steam could produce low-quality syngas due to low gasification temperature caused by additional moisture in the reactor.

The research findings above concluded that at ER = 0.4 or greater, low syngas LHV is produced due to a lower concentration of combustible gases—however, only carbon dioxide content increases in the syngas composition. According to Skoulou et al. (2008), the two contradictory trends that can explain ER influences on gasification can be described as follows. An increase in oxygen fed in the gasifier increases ER, which stimulates syngas, which is less attractive for applications downstream. However, these oxidation reactions favour having more carbon dioxide while lowering the H_2, CO and CH_4 production. According to Mohammed et al. (2011), H_2 and CO yields decline when ER is greater than 0.40, while CO_2 content increases in the syngas. It can be explained by the CO partial combustion and water gas shift reactions promote high CO_2 content. According to Skoulou et al. (2008), an optimized syngas quality is provided at high ERs due to oxidation reactions which liberate heat to the gasifier. In another investigation, Lv et al. (2007) reported that low ER results lower the gasifier temperature, affecting how the gasifier produces syngas. Lv and co-authors regarded ER as a critical parameter in evaluating the syngas composition through feedstock gasification.

2.5.4 Effect of the temperature

The crucial parameter in the gasification process is temperature since it affects the quality of the syngas. For example, at a low gasification temperature of less than 1000°C, the product gas may produce unreacted carbon known as char. At higher gasification temperatures beyond 1000°C, the slag is formed, and ash can melt, causing blockages in the system. Wan Ab Karim Ghani et al. (2009) found an increase in temperature between 700 and 900°C to produce a syngas yield of 2.36 to 5.90 mol/kg of palm kernel shell. They obtained a syngas lower heating value of 3.71 MJ/Nm^3 at a temperature of 800°C. The syngas LHV increased from 2.78 to 4.45 MJ/Nm^3 at 700 to 850°C, and it started to decrease to 3.72 MJ/Nm^3 at 900°C. The combustible gas components H_2, CO and CH_4 declined as the temperature was increased. However, syngas LHV depends chiefly on combustible gases, which should decrease as the temperature is increased. It contradicts what other authors reported, who performed air gasification in the fluidized bed gasifier. Esfahani et al. (2012) reported a decrease in higher heating value using palm kernel shell in air gasification from 25.8 to 18.3 MJ/kg when the temperature was increased from 750 to 1100°C. In another research, Sreejith et al. (2014) used wood gasification and found a decrease in

LHV of 17.5 to 11 MJ/Nm^3 as the temperature increased from 500 to 700°C. The heating value was higher since they used steam as their gasifying medium.

Table 2-6: The effect of the temperature on product gas composition and gasification performance on different experimental studies.

Operating parameters	Syngas composition ranges	Gasification performance indicator	References
FS: Cork waste **GT:** Fluidized Bed **T :** 750 – 850°C **GM:** Air		**GY :** 2.16 to 2.54 Nm^3/kg **CGE :** ~ 34.9 to 59.9% **LHV :** ~ 4.5 MJ/Nm^3 **CCE :** 57 to 85%	(Rodrigues et al., 2017)
FS: Palm Kernel Shell **GT:** Fluidized Bed **GM:** Air **Optimal ER** = 0.26		**Hydrogen yield:** 14 to 22 g/kg of fuel **Tar yield:** 0.05 to 0.15 g/kg of fuel **Ash yield:** 0.07 to 0.22 g/kg of fuel	(Esfahani et al., 2012)
FS: Palm Kernel Shell **GT:** Fluidized Bed **ER :** 0.25 to 0.42 **GM:** Air **T:** 700 to 900°C	**H_2 :** ~ 58 to 65 vol.% **CO :** ~ 18 to 20 vol.% **CO_2 :**~ 12 to 26 vol.% **CH_4 :** ~ 2 vol.%	**GY :** 2.30 to 5.9 Mol/kg of fuel **LHV :** 2.78 to 4.45 MJ/Nm^3	(Wan Ab Karim Ghani et al., 2009)
FS: Wood **GT:** Fluidized Bed **ER :** 0.25 to 0.42 **GM:** Steam		**LHV :** 11 to 17.5 MJ/Nm^3	(Sreejith et al., 2014)
FS: Sewage sludge **GT:** Fluidized Bed **Temp :** 750 – 850°C **GM:** Air	**H_2 :** 8.0 – 12 vol.% **CO :** 7 - 11 vol.% **CO_2 :** 13 – 15 vol.% **CH_4 :** ~ 4.2 vol.%	**GY =** ~2.4 Nm^3/kg daf **CGE =** 37.25% **LHV=** 3.33 MJ/Nm^3 **CCE =** 70 to 82%	(De Andres et al., 2011)

In another investigation, Rodrigues et al. (2017) investigated the cork waste gasification in a fluidized bed gasifier. They found an increase in dry gas yield from 2.16 to 2.54 Nm^3/kg of cork waste when the temperature was increased from 780 to 850°C. Rodrigues and co-authors studied the temperature influence on cork wastes gasification using air in a semi-batch fluidized bed gasifier. An increase in temperature from 780 to 900°C produced 34.9 to 59.9 % in cold gas efficiency. Carbon conversion efficiency increased by 28% from 57% when the temperature was increased from 780 to 850°C. A producer gas had a higher heating value of 4.5 MJ/Nm^3.

De Andres et al. (2011) investigated sewage gasification in a fluidized bed gasifier using air. They varied temperature between 750 and 850°C, and they found syngas yield to be approximate 2.4 Nm^3/kg daf,

and carbon conversion was relatively between 70 and 82%. They found an increase in hydrogen and carbon monoxide, while carbon dioxide and methane decreased with gasification temperature increases.

According to Skoulou et al. (2009), an increase in syngas yield is influenced by the higher temperature, which liberates volatiles from the feedstock. According to Le Chatelier's principle, in an endothermic reaction, the products are favoured by equilibrium due to increased temperature. While, in an exothermic reaction, the equilibrium shifts in the direction of the products when the temperature is lowered. The boudouard, steam-methane reforming, water gas shift are endothermic reactions; therefore, the CO and H_2 production is improved by increasing temperature. However, Lv and co-authors (2004) explained that increasing temperature lowers the CH_4 yield while increasing the H_2 and CO yields on the steam methane reforming reaction. In char partial combustion reaction, which is an exothermic resulted in a decrease in CO yield, was explained by higher temperature. However, an increase in the temperature favours an increase in carbon conversion efficiency since char and H_2O are favoured in endothermic reactions such as water gas shift and boudouard reactions. According to Lv et al. (2004), the syngas yield is favoured at higher temperatures but did not favour the syngas heating value.

2.5.5 Effect of the pressure

Gasification process can either operated at atmospheric conditions or higher pressure (pressurized conditions). According to Ruiz et al. (2013) pointed out the pressurized gasification is more efficient although it requires high investment cost. Brown (2011) argued that high-pressure gasification has some advantages against atmospheric pressure systems. The gas volume produced is small, requiring smaller reaction units and pipes to construct the gasifier. The product gases are relatively close to equilibrium conditions when the pressure is increased. It is significant for the direct use of pressurized syngas in the internal gas combustion reactor and reduces the cost of syngas compressors. A reduced yield of char and tar is obtained when the gasifier pressure is increased (Ruiz et al., 2013) .According to Wang et al. (2008), a pressurized gasification system produces syngas suitable for turbines or engines. Furthermore, Kirkels and Verbong (2011) expanded on suggesting these systems are to be used in large plants due to intensive cost they require at low scale.

Sreejith et al. (2014) observed H_2 and CO contents decrease while CO_2 and CH_4 contents increase as the gasifier pressure increases from 0.1 to 0.8 MPa. They investigated wood gasification using steam. Lower heating value and syngas yield decrease with an increase in pressure. The syngas composition production can be explained using Le Chateliar's principle on equilibrium since lower moles of gases favours higher pressure. In steam methane reforming, a decrease in hydrogen and carbon monoxide production is expected due to the equilibrium shift to favour the reverse reaction. Thus, an increase in methane formation, which can be explained by the methanation reaction. Carbon dioxide formation is

expected to increase when pressure is increased in the boudouard reaction as it has low gas moles than carbon monoxide. Mayerhofer et al. (2012) performed a steam gasification in a fluidized bed gasifier using wood pellets. They studied the effect of pressure, steam to biomass ratio (0.80 to 1.20) and temperature (750 to 840°C) on the influence of tar yield and syngas composition. They varied pressure between 0.10 and 0.25 MPa and found that CO_2 and CH_4 concentration increases while CO concentration decreases, which increased the tar yield. They used olivine as a bed material while the biomass particle size was less than 25 mm were used.

2.6 Gasification products and its application

The gasifier design and operation is responsible for producing product gas or syngas, oils and char. However, for this investigation, only syngas and char are reported. In literature, char is reported as unreacted carbon and Ash (Nikoo and Mahinpey, 2008), while others reported char as only unreacted carbon (Doherty et al., 2009) from the product stream. Dry syngas is free from steam produced, which can be used for sufficient heat energy for the gasifier operation. The producer gas and char uses are explained in detail below.

2.6.1 Product gases

The syngas is produced from gasification varies based on the feedstock and the gasifying medium used. The H_2/CO ratio is the critical factor in producing desirable products from synthesis of syngas. Hydrogen and carbon monoxide can produce valuable chemicals such as ethanol, methanol, gasoline and naphtha (Basu, 2018) . Furthermore, H_2/CO ratio plays a crucial role; for example, the ratio must be greater than 2.15 for the Fischer-Tropsch (FT) synthesis, which produces wax, diesel, gasoline and naphtha (de Carvalho Miranda et al., 2020, Bermudez and Fidalgo, 2016). The synthesis of components (FT products, ammonia, hydrogen, alcohols etc.) is attributed through the steam methane reforming reactions.

Hydrogen production employs the water-gas-shift reaction (Hannula, 2009) in Table 2-4 from syngas (Bermudez and Fidalgo, 2016, Higman and Van der Burgt, 2008). The production of fertilizer is significant through the production of ammonia from the Haber-Bosch process, which utilizes nitrogen and hydrogen (Higman and Van der Burgt, 2008). The operating pressure should be between 1.0 and 2.0 MPa and the temperature should be greater than 450°C (Brown, 2011, Basu, 2018). Methanol (CH_3OH) is an essential compound used for the chemical industries (Lücking, 2017), and H_2/CO ratio should be close to 2.0, as seen in Figure 2-5.

It can be produced using the following equations (2.8) and (2.9).

$$CO + 2H_2 \rightarrow CH_3OH \quad (2.8)$$

$$CO_2 + 3H_2 \rightarrow CH_3OH + H_2O \quad (2.9)$$

It is a significant chemical since it can be applied to various industries and producing variety of chemicals (Bermudez and Fidalgo, 2016). The ethanol production require a H_2/CO ratio of 1.0 (Higman and Van der Burgt, 2008), and for power generation a steam methane reforming reaction is to be employed to achieved a H_2/CO ratio greater than 50 (Bermudez and Fidalgo, 2016).

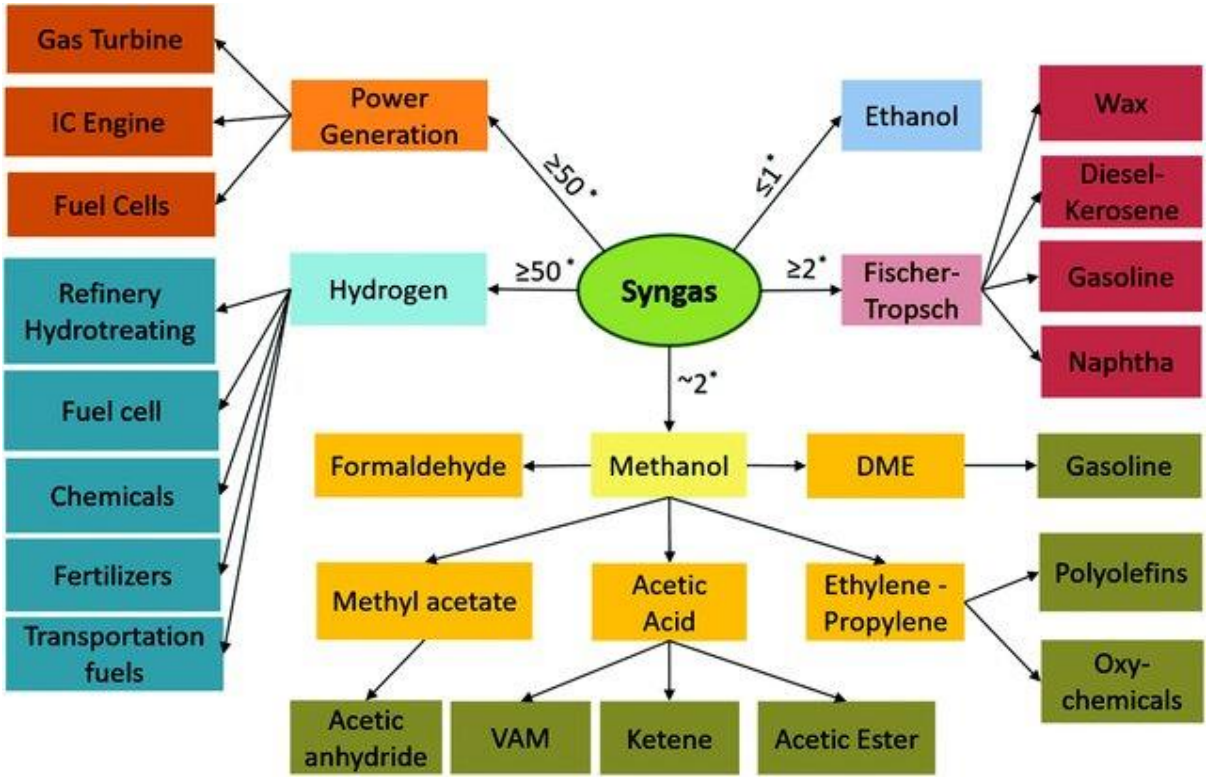

Figure 2-5: Several applications of syngas in industries based on H_2/CO ratio (Hernández et al., 2017).

2.6.2 Char

A solid-by product is called char, and it is produced at the low-temperature gasification method, which is less than 1000°C. It consists of a variety of carbon content depending on the feedstock used; for example, activated carbon is produced from coal gasification. It is applied in industries chiefly for the adsorption of contaminants such as volatile organic compounds and residues from pesticides. Char content is expressed as mass of carbon that was not converted to useful products per syngas volume. There are several studies reported char content in CFB gasifiers to be between 1.7 and 13.1 g/Nm^3 (Van

der Drift et al., 2001), while in BFB gasifiers is within a range of 1.04 to 43.61 g/Nm^3 (Meehan, 2009, Brown, 2011). The maximum permissible particulates of 50 mg/Nm^3 in the syngas is acceptable in internal combustion engine for power generation (Brown, 2011, Bermudez and Fidalgo, 2016). Activated char is applied in the following industries to mention a few: drinking water industry, wastewater treatment, pharmaceutical industry, gas storage and electric energy, chemical and smelting industry, atmospheric pollution control, catalyst and catalyst carrier and indoor air contamination.

Figure 2-6: Various applications of char in industries (The Peepal Leaf, 2019) .

Although char is a by-product, it can be sold to other industries for process economics of the plant. However, there is still a shortage of supply in activated carbon due to the low production of char. When the gasifier is operated at a high temperature, the solid by-product produced is called slag. It is formed as a molten product due to the high gasifier temperature than the ash content (Basu, 2010). When cooled, the slag appears to be a glass type of material as it comprises not vaporized inorganic material from the feedstock. However, this solid by-product is classified as a non-hazardous material; it is widely used in sandblasting and road construction material. Ash can be in cement industry due to the presence of silicon dioxide, which is a binding agent.

CHAPTER 3 : ASPEN Plus Simulation of Gasification Process

3.1 Introduction to ASPEN Plus

ASPEN Plus is a software tool, which has been commercialized since the 1980s by an organization called AspenTech (Aspen Plus, 2018). A user (chemist, engineers or industrial experts) creates process models of industries, simulates them to understand its performance, and compares it to an actual plant. It does not perform engineering calculations using manual methods that consumes a lot of time. It is widely used for chemical engineering applications because it can perform complex engineering calculations by simulating unit operations such as separators, heat exchangers, reactors and distillation columns, etc. For example, in reaction engineering, reactor models can be used to understand their performance based on reaction kinetics, conversion rates, design equations, and reaction dynamics.

ASPEN Plus can also be used for process optimization, economic valuation and sensitivity analysis. It consists of databanks for physical properties, chemical unit operations, and cutting-edge computation techniques. A user utilizes these functions to perform effective and quicker representation of the actual plant through simulation. With a tool like ASPEN Plus, industry experts can provide the plant's performance and precisely foresee challenges in productivity, thus reducing pilot costs.

There are ASPEN Plus blocks which are used as reactor models (RSTOIC, RYIELD, RGIBBS, REQUIL and RCSTR etc.), separators (SEP, SEP2, CYCLONE etc.), mixers (MIXER), heat exchangers (HEATER). The ASPEN Plus built-in models are used to simulate reactors are explained below since the gasification process consider reactions engineering. Some of the reactor models require reaction kinetics or/ and stoichiometric ratio or neither of the two.

In RCSTR reactor model, it requires both reaction kinetics and stoichiometry for numerical simulations. RSTOIC reactor model only requires stoichiometry for simulations. Meanwhile, the RYIELD reactor is used when stoichiometry and kinetics are unknown, and it uses the computation of mass yield to predict product formation. REQUIL or RGIBBS can either be used for single-phase equilibria or both phase and chemical equilibria calculations. RGIBBS reactor model is used to estimate the products based on minimization of Gibbs free energy. Whereas, REQUIL reactor model is based on calculating the stoichiometric phase and chemical equilibrium. The number of feed streams to each reactor can have more than one which are mixed inside the reactor. Only the RCSTR reactor model is rigorous, indicating it can integrate the Langmuir model such as Langmuir Hinshelwood Hougen and Watson (LHHW) or power-law or user-defined kinetics. MS Excel or FORTRAN subroutines are used for user-defined kinetics. Table 3-1 shows the ASPEN Plus reactor models used in the gasification process.

Table 3-1: ASPEN Plus reactor models used in the gasification process.

Reactor Model	Feed streams	Rigorous	Stoichiometric	Kinetics
RCSTR	Multiple	Yes	Required	Required
REQUIL	Multiple	No	Not Required	Not Required
RGIBBS	Multiple	No	Not Required	Not Required
RSTOIC	Multiple	No	Required	Not Required
RYIELD	Multiple	No	Not Required	Not Required

3.2 Simulation of gasification processes

Process modelling or simulation has shown to reduce the costs associated with equipment's used for larger scales in experimental work and shorten the period. According to Gómez-Barea and Leckner (2010), simulation can provide insights for creating and optimizing the actual experiments. De Andrés et al. (2019) researched fluidized bed gasifier simulation using sewage sludge as a feedstock in ASPEN Plus. (Doherty et al., 2009) created a simulation model for circulating fluidized bed gasification systems in ASPEN Plus using hemlock wood. In their study, they categorized feedstock as unconventional component due it complexity as it requires ultimate and proximate analysis. In ASPEN Plus, any feedstock (i.e. coal and biomass etc.) are characterized by ULTANAL (represents ultimate analysis), PROXANAL (represents proximate analysis) and SULFANAL (represents sulphur content in the feedstock). The fuel physical properties are forecasted by enthalpy and density models are called HCOALGEN and DCOALIGT correspondingly (Adeniyi et al., 2019, Peng et al., 2017). However, due to complexity in process modelling of gasification, it then requires some simplifications, which are listed below:

- The devolitization of feedstock occurs instantaneously due to high temperatures (Yang et al., 2016, Nikoo and Mahinpey, 2008).
- Hydrogen and nitrogen react to produce ammonia, while sulphur presence produces hydrogen sulphide (Yang et al., 2016).
- The gasification process occurs at a steady state and isothermal conditions (Doherty et al., 2009).
- The solid particles of biomass do not change their spherical shapes based on the shrinking core model (Nikoo and Mahinpey, 2008).
- The char contents consist of carbon and Ash only (Nikoo and Mahinpey, 2008, Doherty et al., 2008).

- The cyclone used for removing particulates from a product gas had an efficiency of 85% (Doherty et al., 2009).

According to Tinaut et al. (2008), biomass gasification modelling is significant to evaluate the effect of biomass's feed conditions and gasifier operating parameters. Four models have been studied in the simulation of gasification: kinetic models, equilibrium models, computational fluid dynamics, and artificial neural networks. For this study, kinetic and equilibrium modelling will be discussed in this section.

Table 3-2: Some research studies which have been carried out in the simulation of fluidized bed gasification processes using ASPEN Plus.

Reference	Model	Investigated parameters	Gasifier operating conditions
(De Andrés et al., 2019)	Equilibrium	**Inputs:** ER, S/B and temperature **Outputs:** syngas composition and yield, CCE, CGE	FS : Sewage sludge T = 750 to 850 °C **GM**: Air and steam
(Doherty et al., 2008)	Equilibrium	**Inputs:** ER , air and gasification temperature **Outputs:** product gas composition, CGE, LHV	**FS**: Hemlock wood **T** = 717.85 °C **P** = 105 kPa **GM**: Air
(Hussain et al., 2018)	Equilibrium	**Inputs:** Temperature and S/B **Outputs:** LHV ,HHV and syngas composition	**FS** : Palm kernel shell **T** = 500 to 700 °C **P** = 101.3 kPa **GM**: steam
(Yang et al., 2016)	Kinetic	**Inputs:** S/F, gasification temperature **Outputs:** Hydrogen yield	**FS**: Heavy oils **T** = 600 to 800 °C **P** = 18.75 atm (1.9 MPa) **GM** :steam
(Nikoo and Mahinpey, 2008)	Kinetic	**Inputs**: S/B , ER and Temperature **Outputs**: CCE ; product gas composition	**FS**: Pine sawdust **T** = 700 to 900 °C **P** = 105 kPa **GM**:Air and steam
(Peng et al., 2017)	Kinetic	**Inputs:** S/F ,gasification temperature **Outputs:** hydrogen and tar yield, char conversion	**FS** : crude oils **T** = 700 to 850° C **P** = 18.75 atm (1.9 MPa) **GM** : steam
(Beheshti et al., 2015)	Kinetic	**Inputs:** biomass particle size, ER, S/B and T **Outputs:** product gas composition, hydrogen yield, tar concentration, LHV, CGE and CCE	**FS** : wood pellets **T** = 700 to 900 °C **P** = 105 kPa **GM** : Air and steam

FS = Feedstock , T = gasification temperature , P = gasifier pressure and GM = gasifying medium , CGE = cold gas efficiency, CCE =carbon conversion efficiency, ER = Equivalence ratio, S/B = steam to biomass ratio , S/F = steam to fuel ratio, LHV = lower heating value and HHV = higher heating value.

Other simulation studies which were carried out using steam gasification carried out for palm kernel shell (Shahbaz et al., 2017, Acevedo et al., 2018, Hussain et al., 2018), meat and bone meal (Califano et al., 2017, Soni et al., 2008) and wood pellets (Hannula, 2009, Robinson et al., 2016).

3.2.1 Kinetic modelling

These types of models seek to understand the product gas distribution at any location inside the reactor. It considers the reactor geometry and hydrodynamics, and it is significant in the design of the reactor. Nikoo and Mahinpey (2008) developed a kinetic model to simulate fluidized bed gasification using steam. They used four ASPEN Plus reactors to simulate the process stages: feed decomposition, volatile matter reactions, carbon (char) gasification, and solid separation from product gas. They decomposed the feed using the ASPEN Plus reactor unit called RYIELD. It employs calculation of mass yield to produce elemental species composition of C, H, N, O, S and Ash based on ultimate and proximate analysis of the biomass. The conversion of volatile matter to product gas was carried out in a RGIBBS unit using the Gibbs energy equilibrium rule for estimating the product gases. The char was then fed in two continuous stirred tank reactors, RCSTR, which converts char to useful products using reaction kinetics and bed hydrodynamic equations (Pérez-Fortes et al., 2008). They used Peng-Robinson equations of state to estimate the thermodynamic properties of gases.

In another research, Beheshti et al. (2015) developed a kinetic model for simulating fluidized bed gasification using wood pellets. They expanded on kinetic modelling by clarifying the two RCSTRs, indicating the reactors used for the bed and freeboard section in the bubbling fluidized bed gasifier models. Air and steam were used as the gasifying medium. They used the model to study biomass particle size, equivalence ratio, steam to biomass ratio and gasification temperature on gasifier performance parameters. Beheshti and co-authors were interested in the following parameters: syngas composition, hydrogen yield, tar concentration, lower heating value, carbon conversion efficiency and cold gas efficiency.

Hussain et al. (2018) studied the kinetic model on the circulating fluidized bed gasifier simulation using palm kernel shell as a feedstock. However, they used different ASPEN Plus blocks compared to Nikoo and Mahinpey (2008) when simulating char gasification. They used ASPEN Plus block on solids FLUID BED reactor, which required kinetics for char conversion to product gases. They simplified their model by only considering methane as a hydrocarbon and not considering tar cracking. The gasification temperature range was between 500 and 700 °C. The Peng Robinson with Boston Mathias alpha function equation of state was employed for predicting the physical properties of components used in the simulation. The original Peng-Robinson was modified by the alpha function which is a function of temperature, it enhances the forecasting the vapour pressure of pure components at elevated temperatures (Adeniyi et al., 2019) .

Yang et al. (2016) developed a kinetic model to study the steam gasification in a fluidized bed gasifier using heavy oils. Yang and co-authors used reaction kinetics and hydrodynamics in modelling the

gasification process. ASPEN Plus block, RCSTR was used for char gasification modelling. They studied the effect of gasification temperature (600 to 800 °C) on hydrogen and tar yield.

In another study, Begum et al. (2014) used ASPEN Plus to simulate gasification in a fluidized bed gasifier using wood as feedstock. They used two RCSTR blocks for char gasification modelling by inputting reaction kinetics and hydrodynamics. They employed FORTRAN subroutines and MS Excel as their inputs for modelling in ASPEN Plus. The used IDEAL property method to predict the thermodynamic properties of the gasification components. In another study, Peng et al. (2017) developed a kinetic model for steam gasification in a fluidized bed gasifier using different crude oils. They used ASPEN Plus to create a model, which considers reaction kinetics and bed hydrodynamics. Altafini et al. (2003) pointed out the kinetic modelling to be suitable for low operating temperatures, less than 800°C. Table 3-3 shows the bed hydrodynamics employed in kinetic modelling.

Table 3-3: Inputs of the kinetic models represented as hydrodynamic equations (Lei and Horio, 1998, Bai and Kato, 1999)

Bai and Kato, 1999	$\Delta P = \rho_s g (\varepsilon_z z_d + \int_{z_d}^{z} \varepsilon_s dz)$
Liu et al., 2011	$\frac{\varepsilon_s - \varepsilon_{s\infty}}{\varepsilon_y - \varepsilon_{s\infty}} = e^{-a(y-y_d)}$
Lei and Horio, 1998	$a D_r = 0.019 [\frac{U_g}{\sqrt{gD_r}}]^{-0.32} [\frac{\psi_s}{\rho_g U_g}]^{-0.22} [\frac{\rho_s - \rho_g}{\rho_g}]^{0.41}$
Bai and Kato, 1999	$\frac{\varepsilon_y}{\varepsilon_s^*} = 1 + 0.00614 [\frac{U_g \rho_s}{\psi_s}]^{-0.23} [\frac{U_g}{\sqrt{gD_r}}]^{-0.383} [\frac{\rho_s - \rho_g}{\rho_g}]^{1.21}$
Liu et al., 2011	$\varepsilon_{s\infty} = 4.04 \varepsilon_s^{*\,1.214}$
Bai and Kato, 1999	$\varepsilon_s^* = \frac{\psi_s}{[\rho_s (U_g - U_t)]}$
Bai and Kato, 1999	$U_{mf} = \frac{\mu}{\rho_g d_r} [(33.2^2 + 0.0651 \mathrm{Ar})^{0.8} - 33.7]$
Lei and Horio, 1998	$\mathrm{Ar} = [\frac{g d_r^3 (\rho_p - \rho_g) \rho_g}{\mu^2}]$

3.2.2 Equilibrium modelling

These models are primarily used to understand the achievable product gas yields. Equilibrium models help to simulate experiments that can exhibit hazards or are costly to run to understand better the gasification system's potential behaviour (Li et al., 2004). The model does not consider the geometry and its concern with the reaction. It is significant in estimating product gas yields, potential biomass conversion and gasification efficiencies. In that way, it cannot be used for estimating reactor design and analysis. These equilibrium models are categorized as stoichiometric and non-stoichiometric (Basu, 2010).

According to Puig-Arnavat et al. (2016), stoichiometric equilibrium models involve well-known chemical compounds and reaction mechanisms. However, it is not applicable when the chemical reaction or reacting species are not clearly defined. On the other hand, non-stoichiometric models are applied in reactions where the chemical formula of reacting species are unknown. It employs ultimate analysis, which considers the elemental species in numerical simulation (Puig-Arnavat et al., 2016). It performs computation using the Gibbs free energy by lowering the energy close to zero to estimate the equilibrium concentrations of products. The minimization of Gibbs free energy is computed using the equation (3.1) to estimate product concentrations:

$$G_{total} = \sum_{i=1}^{N} n_i \Delta G^0{}_{f,i} + \sum_{i=1}^{N} n_i RTIn\left(\frac{n_i}{\sum n_i}\right) \qquad (3.1)$$

De Andries et al (2019) developed an equilibrium model to evaluate the performance of sewage gasification in a fluidized bed gasifier. In their model, they separated the drying and devolatilization stages of biomass. They used two RYIELD reactor blocks for these stages in the gasification process. ASPEN Plus reactor block, RSTOIC reactor block was used for the formation of ammonia and hydrogen sulphide. Another RSTOIC block was used to produce tar from residual char content. They used two RGIBBS blocks to simulate char gasification and separated Ash after the first reactor. The second RGIBBS reactor was mainly used to restrict the chemical equilibrium, and this model is called non-stoichiometric.

De Andries et al. (2019) investigated the effect of gasification temperature and equivalence ratio on syngas composition and gasifier performance parameters. In another investigation, Sreejith et al. (2014) established a non-stoichiometric model to simulate wood gasification. They used the RSTOIC reactor block to simulate wood drying, and the evaporated moisture was removed using a separator SEP block from the process. The RYIELD reactor block was used to devolitized woody biomass, and unreacted char was removed using separator SEP2 block. The volatiles were then gasified using steam in a RGIBBS reactor, which employs minimization of Gibbs free energy.

Sreejith et al. (2014) studied the influence of pressure, temperature and steam to biomass ratio on gasifier performance. They used Redlich-Kwong coupled with Boston-Mathias equations of state for estimating the thermodynamic physical properties. Begum et al. (2013) developed a non-stoichiometric model in a fixed bed gasification system. They used ASPEN Plus to simulate gasification using woody biomass as a feedstock. It employed external FORTRAN codes for drying and pyrolysis; these processes were model using RSTOIC and RYIELD, respectively. Two RGIBBS reactors were used for volatile reactions and the combustion of char. Air was used as the gasifying medium in a fixed bed gasifier.

Begum et al. (2013) separated the product gas from by-products using separation SEP block. The Redlich-Kwong-Soave equations of state were used to predict the thermodynamic properties. They studied the influence of air to biomass ratio and gasification temperature on syngas composition. Doherty et al. (2009) created an equilibrium model to simulate circulating fluidized bed gasification using wood as a feedstock. They used ASPEN Plus and employed RGIBBS reactor block for estimating the equilibrium concentration of product gases. It minimizes Gibbs free energy and can be restricted chemical equilibrium if not reached in some systems. They used wood as feedstock while air was gasifying agent to improve fluidization in the gasifier. They made assumptions on the cyclone efficiency to be 85%. However, they employed ASPEN Plus block, CYCLONE, for separating solids from product gas. Doherty (2008) studied the influence of equivalence ratio, air and gasification temperature on syngas composition and gasifier performance parameters.

Acevedo et al. (2018) developed a stoichiometric model to simulate palm kernel shell gasification using ASPEN Plus. They used the RYIELD reactor block to simulate drying and pyrolysis. Steam was used as a gasifying medium for volatiles reactions and char gasification in a REQUIL reactor block. This block was used to compute products based on stoichiometric chemical reactions, and it did not involve reaction kinetics. Peng-Robinson equations of state were used to estimate the thermodynamic properties of reacting components. Acavedo et al. (2018) investigated the influence of steam to biomass ratio and temperature on product gas composition.

3.3 Summary

This section summarizes chapter 2 and 3 on how it actually fits in the aim of this study. The feedstock selected for this investigation represents agricultural waste (represented as palm kernel shell), farm abattoir waste (represented as meat and bone meal) and forestry waste (represented as wood pellets). A literature data on heating value of feedstock (fuel), ultimate and proximate analysis were collected and represented as Table 2-2 and Table 2-3.

Table 2-3The importance of understanding these characteristic of feedstock makes a clear picture on the energy available, which can be provided by feedstock and its applicability for further processing downstream. Utilizing these fuels can reduce an environmental impact,which is associated with landfilling and combustion since that contribute to global warming thus negatively affecting the environment. The conversion of waste, which has received attention, is gasification, which process organic carbon to methane, hydrogen, carbon monoxide in sustainable method. It employs air or steam to convert the feedstock to produce syngas (combustible gas) which can reduce the negative environmental impacts. The unit operations, which are employed for conversion of feedstock to combustible gases, are fluidized bed, fixed bed and entrained flow gasifiers (section 2.4). Amongst these

gasifiers, fluidized bed gasifier has shown a capability to accommodate more than one feedstock as compared to other gasifiers. They prove to be efficient in heat and mass transfer for the solids and gasifying medium mixing. They have improved the rate of reactions and in converting carbon to valuable products, i.e. syngas. These types of reactors employ the use of bed particles as a catalyst and for effective heat transfer. A fluidized bed gasifier's typical operating temperature ranges between 700 and 1000°C to avoid melting ash and blockages on downstream equipment (Lian et al., 2021). However, the ash content should be less than 25 wt.% while ash melting temperature should be greater than 900 °C (Bermudez and Fidalgo, 2016, McKendry, 2002, Basu, 2010, Basu, 2018). The influence of gasification performance is studied on feedstock properties, gasifier design, gasifying medium, gasifier pressure and temperature. A syngas with a lower heating value between 4 and 7 MJ/Nm^3 is produced when using air gasification (Basu, 2018), it is suitable for application in energy production (Rezaiyan and Cheremisinoff, 2005). An optimal equivalence ratio recommended by other scholars is between 0.2 and 0.4 for fluidized bed gasifiers (Bermudez and Fidalgo, 2016, Basu, 2018). The typical ranges of syngas yield and lower heating value, cold gas efficiency and carbon conversion efficiency were compared in Table 2-5 and Table 2-6.

The reactor models employed in ASPEN Plus include RCSTR, RPLUG, RYIELD, REQUIL and RSTOIC. These reactor models either consider reaction kinetics or stoichiometric ratios, rigorous models like LHHW, custom sub-routine FORTRAN codes. Several scholars in literature, which has a similar manner as argued in section 3.2, use ASPEN Plus as a simulation tool. Palm kernel shell (PKS), meat and bone meal (MBM) and wood pellets (WP) are to be fed in ASPEN Plus gasification model using ULTANAL, PROXANAL and SULFANAL which represents feedstock characterization. The physical properties will be estimated using HCOALGEN and DCOALIGT models. The kinetic and equilibrium modelling is discussed as available methods used for simulating gasification process. In order to meet the objective of this study, an equilibrium modelling was used which does not require reaction kinetics and it is suitable for predicting the product gas composition achieved by the gasifier. It consider the Gibbs free energy minimization to predict the syngas composition. Air was selected as a gasifying medium based on analysis from Table 3-2 since most studies considered steam and it is a cheap reagent. This study will expand on the simulation which was carried by (Doherty et al., 2009). The author of this dissertation felt like this investigation will fill new information on using palm kernel, meat and bone meal and wood pellets gasification using a circulating fluidized bed gasifier. The investigated parameters are to be gasifier pressure, temperature and equivalence ratio. These inputs were to be evaluated on syngas composition, syngas yield and lower heating value, cold gas efficiency and carbon conversion efficiency.

CHAPTER 4 : Materials and Methods

4.1 Simulation components

Table 4-1 shows all components used for this gasification simulation study. ASH and FDSTOCK are defined as non-conventional solid components since their exact chemical formulae are not known. The FDSTOCK variable simulates a feedstock (i.e. palm kernel shells, meat and bone meal, wood pellets). These feedstock can be analysed using a proximate and ultimate method more similar to coal materials. ASPEN Plus have embedded enthalpy and density models for estimating coal properties. It was used for calculating the properties of ASH and FDSTOCK.

Table 4-1: Components used in the modelling of the gasification process.

Component ID	Stream Class	Name of component	Chemical Formula
FDSTOCK	NC		
ASH	NC		
C	CI	CARBON-GRAPHITE	C
H2	MIX	HYDROGEN	H2
N2	MIX	NITROGEN	N2
H2O	MIX	WATER	H2O
CO2	MIX	CARBON-DIOXIDE	CO2
CO	MIX	CARBON-MONOXIDE	CO
CH4	MIX	METHANE	CH4
S	MIX	SULFUR	S
H2S	MIX	HYDROGEN-SULFIDE	H2S
CL2	MIX	CHLORINE	CL2
HCL	MIX	HYDROGEN-CHLORIDE	HCL
NH3	MIX	AMMONIA	H3N
O2	MIX	OXYGEN	O2

The components used in this simulation includes a mixture of both conventional and non-conventional solid components with no particle size distribution, as seen in Table 4-1. The stream class selected was MIXCINC, which contains substreams, MIX stands for MIXED substream (which represent conventional components), CI represents CISOLID (conventional solids), and NC represents Non-conventional components substreams.

4.2 Physical properties

Thermodynamic property is crucial for estimating the physical properties of the components available for chemical reactions. The Peng Robinson equations of state coupled with the Boston Mathias (PR-BM) alpha function is used for the gasification model. This property method is appropriate for chemical industries specializing in a refinery, gas processing, petrochemicals and coal gasification. It is widely used to estimate thermodynamic properties for light gases and hydrocarbons, as it is appropriate for mixtures that are non-polarity or showed mild polarity.

The property method is significant in models specification, which is used to calculate the properties of non-conventional components. Enthalpy and density models that are selected were HCOALGEN and DCOALIGT, respectively. However, these models were used to calculate the enthalpy and density of the feedstock and ash only. HCOMB is the heat of combustion of coal, and it is user-defined on ASPEN Plus. This property was obtained from the literature for the feedstock selected. It was termed HHV in this study, and it was reported on a dry basis.

Table 4-2: Thermodynamic property specification selected in ASPEN Plus

Property method	Model name
Thermodynamic property base method	PR-BM
Enthalpy model	HCOALGEN
Density model	DCOALIGT

In ASPEN Plus, non-conventional components (feedstock and ash) required specification of proximate (PROXANAL: ASPEN Plus user defined function), ultimate (ULTANAL: ASPEN PLUS user define) and sulfanal analyses. These attributes were specified after entering the enthalpy and density models. In practice, the sulfanal analysis is not specified, however in this study, the content of sulphur was specified as organic for all the feedstock due to low content. The PROXANAL and ULTANAL, each amount up to 100%. The conversion from dry basis to as received basis was done to ensure the ASPEN Plus simulation is carried out without any errors. SULFANAL was used to specify the quantity of sulphur in the feedstock. Only organic component was chosen for this study, and it was set to be equal to the sulphur content in the feedstock.

Table 4-3: The feedstock characteristics (ultimate, proximate and sulfanal analyses) of palm kernel shell (Wan Ab Karim Ghani et al., 2009), meat & bone meal (Campoy et al., 2014), wood pellets (Campoy et al., 2014) and ash for gasification.

	Palm kernel shell	Meat & bone meal	Wood pellets	Ash
Proximate Analysis (dry basis, wt.%)				
MC	7.96	6.9	6.3	0
FC	18.56	9.1	18.4	0
VM	72.47	72.1	81	0
Ash	8.97	19.1	0.7	100
Ultimate Analysis (dry basis, wt. %)				
Carbon	51.63	54.7	49.8	0
Hydrogen	5.52	7.8	5.8	0
Oxygen	40.91	27.6	42.2	0
Nitrogen	1.89	9.1	2.0	0
Sulfur	0.05	0.78	0.06	0
Chlorine	-	-	-	0
Ash	8.97	19.1	0.7	100
HHV_{fuel}	22.97	21.3	19.6	
Sulfunal Analysis				
Pyritic	-	-	-	0
Sulfate	-	-	-	0
Organic	0.05	0.78	0.06	0

FC = Fixed Carbon ,MC = Moisture Content, VM = Volatile Matter and HHV = Higher Heating Value in MJ/kg.

4.3 Model development

ASPEN Plus flowsheet is used to develop the gasification model, which consist of the reaction blocks: ASPEN Plus blocks used are RYIELD, HEATER, MIXER, SEP and RGIBBS. The feedstock is characterised as obtained from literature studies.

The model development takes into consideration the following steps to be done.

- Use ASPEN Plus data banks and select METSOLID as a global unit set.
- Select input mode to steady state and stream class to MIXCINC. Choose flow basis as mass since using solids as fuels.

- Choose a thermodynamic property method to Peng Robinson equation of state coupled with Boston Mathius (PR-BM) for simulations of palm kernel shell, meat and bone meal and wood pellets. Select components to be used for the gasification modelling as seen in Table 4-3.
- FDSTOCK and ASH were selected to be the non-conventional components.
- Specify the mass flow rate of the feedstock, compositions, temperatures, pressures, and thermodynamic states of the unit feed streams (solid, liquid or gas) and of the oxidant stream.
- Define operating units such as temperature and pressure based on the fluidized bed unit's operation in the RGIBBS reactor. Use FORTRAN code (from Appendix A) to determine the mass yield of the elemental species (C, H, N, S, Cl and O)
- Name the ASPEN Plus simulation blocks and define operating parameters and use calculation blocks to perform desired calculations.

Table 4-4: Selected chemical reactions occurring in gasifiers for this study.

Chemical reaction	**Name of the reaction**	**Reaction type**	**Equation No.**
$C + 0.5O_2 \leftrightarrow CO$	Char partial oxidation	Exothermic	$(\mathbf{4}.1)$
$C + CO_2 \leftrightarrow 2CO$	Boudouard reaction	Endothermic	$(\mathbf{4}.2)$
$C + H_2O \leftrightarrow CO + H_2$	Carbon-water reaction	Endothermic	$(\mathbf{4}.3)$
$C + 2H_2 \leftrightarrow CH_4$	Methanation reaction	Exothermic	$(\mathbf{4}.4)$
$CO + 0.5O_2 \leftrightarrow CO_2$	Carbon mono-oxidation	Exothermic	$(\mathbf{4}.5)$
$H_2 + 0.5O_2 \leftrightarrow H_2O$	Hydrogen combustion	Exothermic	$(\mathbf{4}.6)$
$CO + H_2O \leftrightarrow CO_2 + H_2$	Water gas shift reaction	Exothermic	$(\mathbf{4}.7)$
$CH_4 + H_2O \leftrightarrow CO + 3H_2$	Steam-methane reforming	Endothermic	$(\mathbf{4}.8)$
$H_2 + S \rightarrow H_2S$	Hydrogen sulphide formation	Endothermic	$(\mathbf{4}.9)$
$0.5N_2 + 1.5H_2 \leftrightarrow NH_3$	Ammonia formation	Endothermic	$(\mathbf{4}.10)$

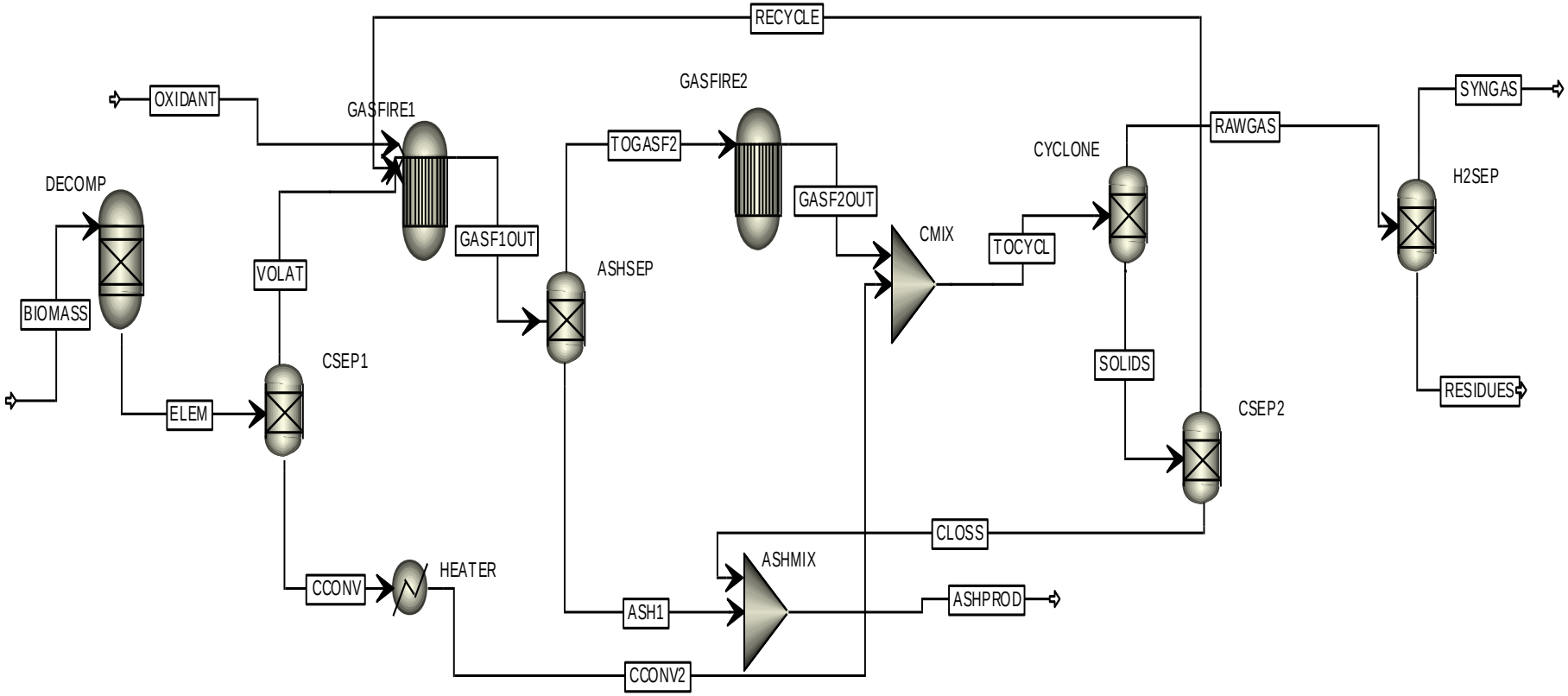

Figure 4-1: A process flowsheet showing a circulating fluidized bed gasifier for different feedstock.

4.4 Model description

In Figure 4-1, FDSTOCK is a non-conventional component in the BIOMASS stream. The FDSTOCK mass flow rate of 33.626 kg/h at 105 kPa and 25°C is fed into the pyrolysis reactor DECOMP block. The drying and pyrolysis were simulated using the RYIELD reactor block. It decomposes proximate and ultimate analysis into elemental components by estimating the mass yields. The pyrolysis unit operates at 105 kPa and 450°C. It is used to evaporate the moisture bound in the feedstock and pyrolyse it simultaneously. The decomposition is carried out using a calculator block, which converts the non-conventional components into mass flow rates of C, H_2, N_2, O_2, S and H_2O in the outlet stream as ELEM. This stream has low energy compared to the BIOMASS feed stream, and it is then compensated by adding an enthalpy stream QBREAKDWN.

The CSEP1 block separates the volatile gases from unreacted char from the pyrolysis product. The CCONV stream consists of 5% of unreacted char, which is assumed did not volatize. It is fed into the HEATER to heat up the unreacted char to the gasifier temperature. The VOLAT, OXIDANT, and RECYCLE streams are then fed into the GASIFIRE1 block (RGIBBS). In this reactor block, char partial oxidation and char gasification reactions occur. It employs the principle of minimization of Gibbs free energy to compute product gases. The OXIDANT stream comprises air, which oxidizes the char for the gasification process in the GASIFIRE1 reactor block. The user based on the desired equivalence ratio sets the OXIDANT stream flow rate.

The GASIFIRE1 reactor block is operated at a pressure of 105 kPa and temperature of 717.85°C, subsidiary operating condition was set at a zero temperature approach. The GASIF1OUT stream is fed into the ASHSEP separator block, which removed 100% of ash from the diluted product gas. The TOGASIF2 stream is introduced to the GASIFIRE2 block, where the system temperature approach was restricted at an equilibrium temperature of 305 °C. This was performed to match the syngas composition reported in the literature. The CMIX block combines un-reacted char with gaseous product from the GASIFIRE2 reactor block. The TOCYCL stream is separated using the gas-solid separator CYCLONE. Only solid char is contained in the SOLIDS stream, it is removed at the bottom of CYCLONE, and it is fed into CSEP2, which is a char separator block. The RAWGAS stream comprises all the product gases such as H_2, CO, H_2O, CO_2 and CH_4. It's only H2 SEP block, which only removes H_2O to produce dry syngas.

The char separator CSEP2 block separates the SOLIDS stream into RECYCLE stream to maintain the bed constantly in the reactor, which is transferred back into the GASIFIER1 block. The stream CLOSS

is transferred to the ASHMIX block, where it is combined with ash from ASHSEP block. ASHPROD stream contains ash, and unreacted char are fed to the ash processing plant for compliance with the environmental regulations.

Table 4-5: Feed stream specifications (components, mass flow, presssure and temperature) of gasification process for this study.

Stream	Component	Mass flow (kg/h)	Pressure (kPa)	Temperature (°C)
OXIDANT	21% vol. O_2 79% vol. N_2	85	105	450
BIOMASS	Specified as its proximate, ultimate and sulphur analysis	33.626	105	25

4.5 ASPEN Plus blocks specification

Having the feed streams, the blocks were selected for specific purposes based on design operational conditions on the gasification simulation study. Table 4-6 provides description of ASPEN Plus unit operation blocks used in the simulation. Table 4-7 outlines the parameters of unit operations of gasification modelling.

Table 4-6: ASPEN Plus unit operation blocks showing scheme, block identity (ID) and its function in the gasification process simulation.

ASPEN PLUS Name	Scheme	Block ID	Function
HEATER		C-HEATER	It increases the solid carbon stream temperature to the gasifier temperature. It calculate the energy required to heat solid carbon to gasifier temperature.
MIXER		ASHMIX CMIX	It combines ash with solid carbon to produce char. CMIX It simulates the mixing of carbon with the gas to the cyclone.
RGIBBS		GASFIRE1 GASFIRE2	It simulates the gas-solids and gas-phase reactions by using Gibbs free energy reactor and temperature approach method. GASIFIRE2 Gibbs free energy reactor – it restricts the system's chemical equilibrium to adjust the required amount of the syngas composition produced from literature.
RYIELD		DECOMP	Transforms the non-conventional components from the feed stream into mixed and solid components and it performs drying instantaneously.
SEP		ASHSEP CSEP1 CSEP2 CYCLONE	It separates the ash from the product gases. CSEP1 splits 5% of solid carbon from the volatile compounds. CSEP2 separates 2% of carbon from the feed stream and recycle the remaining carbon. They are used for the gas-solid separation process. CYCLONE simulates the cyclone by removing specified percentage of solid carbon. Used for gas-solid separation instead of a specific cyclone design which require model, calculation method and type.

Table 4-7: Unit operations parameters (pressure and temperature) and specification used for gasification process simulation.

Block ID	Pressure (kPa)	Temperature (°C)	Specification
ASHMIX	105	-	Mixes ash and char to be sent to ash processing plant
ASHSEP	105	-	Separated 100% of ash produced
C-HEATER	105	450	Heated up the char to the desired temperature for the process
CMIX	105	-	It reacts the heater char with un-purified gas.
CSEP1	105	-	5% of carbon material in the feedstock volatized with volatile matter.
CSEP2	105	-	Recycles 2% of char from cyclone residue stream to the ash processing plant.
CYCLONE	105	-	Purifies syngas by using cyclone effect on separation of 85% of unreacted carbon.
DECOMP	105	500	It decomposes the non-conventional components FDSTOCK for elemental mass balance of H_2O, C, H,O, N and S.
GASIFIRE1	105	-	Calculate the phase equilibriums concentration of gases.
GASIFIRE2	105	717.85	It restrict the chemical equilibrium with a temperature approach of 305°C to correct the yields of syngas.

4.6 Sensitivity analyses

The operating and design variables (equivalence ratio, temperature and pressure) affect the process variability; however, sensitivity analysis determines this. It is an essential tool to understand optimal conditions in a designed unit operation. Sensitivity analysis is carried out by varying one of the operating variables while others were kept constant.

In this study, the air flow rate represented as equivalence ratio is varied from 0.15 to 0.45. The gasification temperature is varied from 600 to 1000 °C. The gasifier pressure is varied between 0.1 and 2.0 MPa. To assess the gasification performance of gasification, the following parameters are evaluated: syngas composition, syngas yield, lower heating value, cold gas efficiency and carbon conversion efficiency. The gasification performance parameters are calculated using the following procedures.

4.6.1 Determination of product gas composition.

The technologies (i.e. energy or chemical production) available to use syngas rely mainly on the gas compositions. For an example, in the Fischer-Tropsch synthesis a ratio of H_2/CO of greater 2.15 is required. The Gibbs free energy minimization equations are below for the estimation of the producer gas such as CH_4, CO_2, CO, H_2 and H_2O. RGIBBS block in ASPEN Plus employs the following equations (4.11) to (4.15) to determine the components of the syngas produced.

$$\frac{\Delta G^{\circ}{}_{CH4}}{RT} + In\left(\frac{n_{CH4}}{n_{total}}\right) + \frac{1}{RT}\lambda_C + \frac{4}{RT}\lambda_H = 0 \qquad (4.11)$$

$$\frac{\Delta G^{\circ}{}_{CO2}}{RT} + In\left(\frac{n_{CO2}}{n_{total}}\right) + \frac{1}{RT}\lambda_C + \frac{2}{RT}\lambda_O = 0 \qquad (4.12)$$

$$\frac{\Delta G^{\circ}{}_{CO}}{RT} + In\left(\frac{n_{CO}}{n_{total}}\right) + \frac{1}{RT}\lambda_C + \frac{1}{RT}\lambda_O = 0 \qquad (4.13)$$

$$\frac{\Delta G^{\circ}{}_{H2}}{RT} + log\left(\frac{n_{H2}}{n_{total}}\right) + \frac{2}{RT}\lambda_H = 0 \qquad (4.14)$$

$$\frac{\Delta G^{\circ}{}_{H2O}}{RT} + In\left(\frac{n_{H2O}}{n_{total}}\right) + \frac{2}{RT}\lambda_H + \frac{1}{RT}\lambda_O = 0 \qquad (4.15)$$

where

$\Delta G^{\circ}{}_i$ is the Gibbs free energy of specified component i

R is the universal gas constant at standard temperature and pressure is 8.31 $J.mol^{-1}.K^{-1}$

T is the temperature of the reaction in °K

n_i is moles of components i (i.e. CH_4, CO_2, CO, H_2 and H_2O)

λ_i is the langrage multipliers of the elemental species such hydrogen (H) and oxygen (O)

4.6.2 Determination of syngas yield.

The amount of dry gas produced from the gasifier contains nitrogen, which does not constitute to required syngas production. The production or yield of gas produced is based on the volume of syngas produced per amount of fuel on dry ash-free basis (daf), given by the equation (4.16):

$$G_Y = \frac{Q_{syngas}}{M_{fuel} \times (1 - w_{H_2O} - w_{Ash})} \quad (4.16)$$

Q_{syngas} is the volumetric flowrate of syngas produced in Nm^3/h

M_{fuel} is mass flowrate of the solid fuel feed in kg/h

w_i is the weight fraction of water or ash in wt.%.

G_Y is the producer gas or syngas yield in Nm^3/kg daf.

4.6.3 Determination of lower heating value of syngas.

The energy content (MJ) provided by a 1 Nm^3 of syngas is important for downstream applications is referred to as lower heating value (LHV). The higher the LHV, the more favourable the syngas produced. Equation (4.17) is used to calculate the LHV of the syngas on dry basis:

$$LHV_{syngas} = 10.78\, y_{H_2} + 12.63\, y_{CO} + 35.88\, y_{CH_4} \quad (4.17)$$

Where

LHV_{syngas} is syngas lower heating value (MJ/Nm^3)

y_i is the volume fraction of combustible gases such as hydrogen, methane and carbon monoxide.

4.6.4 Determination of the cold gas efficiency.

CGE is defined as the produced energy by syngas over the energy obtainable from the fuel or feedstock (Basu, 2010). It is a measure of gasifier performance, which is also termed gasification efficiency. Equation (4.18) is employed to compute the cold gas efficiency:

$$\eta_{CGE}\ (\%) = \frac{M_{syngas} \times LHV_{syngas} \times n_v}{M_{fuel} \times LHV_{fuel}} \times 100 \quad (4.18)$$

Where

M_{syngas} is the syngas flowrate in kg/h

LHV_{fuel} is the lower heating value of the feedstock (fuel) in MJ/kg

n_v is the molar gas volume at standard temperature and pressure is 22.4 $kmol/Nm^3$

4.6.5 Determination of the carbon conversion efficiency

The converted carbon from the feedstock to syngas product is significant for determining the usefulness of the feedstock. Since it contributes to the syngas yield and heating value. The carbon conversion efficiency (CCE) is the ratio of the quantity of carbon left by the gasifier in the syngas (as CO, CO_2 and CH_4 etc.) to the carbon fed in the system with the fuel. It is computed using equation (4.19)

$$\eta_{CCE}(\%) = \frac{Amount\ of\ carbon\ in\ syngas}{Amount\ of\ carbon\ in\ fuel} \times 100 \qquad (4.19)$$

CHAPTER 5 : Results and Discussion

A simulation of the gasification process was carried out using ASPEN Plus to evaluate the fluidized bed gasifier performance of various feedstock. A non-stoichiometric equilibrium model was used to forecast the achievable syngas compositions and their yield and gain insights into syngas' lower heating value, cold gas efficiency, and carbon conversion. In order to understand the objective of this study, palm kernel shells, meat bone meal and wood pellets were the waste feedstock for the gasification process. The feedstock varied in terms of the ultimate and proximate composition and their heating value.

The air flowrate (relates to equivalence ratio), gasifier pressure and gasification temperature were input parameters. They were used to evaluate their influence on the gasification process parameters. The feed and operational conditions were studied to determine the optimal gasification conditions without affecting the process and operational stability. Chapter 2 describes the implications of equivalence ratio (ER), gasification temperature and gasifier pressure. ASPEN Plus was used for simulating and modelling the gasification process in section 3.2. The literature data of palm kernel shell, meat and bone meal and wood pellets on ultimate and proximate analysis was obtained.

A gasification model was validated before evaluating the gasification process is discussed in section 5.1. The relative error was considered to assess the actual experiments' difference that needs to be considered for the existing plant setting. A sensitivity analyses was carried out on gasification temperature, equivalence ratio and gasifier pressure. This study discovers the influence of gasification temperature on gasifier products and performance. It is of interest to the future design engineer to understand the performance of the gasifier. The results of this study were compared against experimental studies carried out by other scholars using fluidized bed gasifier. It is discussed in section 5.2.

The volume of air required in the gasification process considers the fuel flow rate and its composition. Section 5.3 offers detailed results from the effect of equivalence ratio on the gasification process using the three feedstock. It is a critical operational factor that determines the air volume required for the gasification and optimal conditions to operate the gasifier. Section 5.4 provides a summary of results for the effect of gasifier pressure. It gives insights into which pressure conditions results in attaining maximum syngas yield. It enables the prospective designer to select the correct operation settings when designing or operating a foreseeable plant.

The fuel flow rate was kept constant in all runs while varying either gasifier pressure, gasification temperature, or airflow rate based on ER.

5.1 Model validation

The validity of a model determines the accuracy, and it informs variability of the experimental results from modelled results. The variable used is called relative error (ε_r). The magnitude of the relative error is calculated using the experimental variable (X_e) and model variable (X_m). It is beneficial for determining the over and underestimations of the model, which can be either positive or negative. The equation of computing relative error is shown below:

$$\varepsilon_r = \frac{X_m - X_e}{X_e} \times 100$$

Table 5-1 outlines the model's performance against the experimental results of hemlock wood gasification in terms of relative error. The syngas composition results comprising hydrogen, nitrogen, carbon monoxide, methane, and carbon dioxide were comparable from model and experimental results. The selected parameters on the model validation showed a relative error of ± 15% based on hemlock wood gasification. The relative error of H_2, N_2 and CH_4 were close to 5 %. The model over predicted the hydrogen, nitrogen and methane, whilst under predicted carbon monoxide, carbon dioxide.

Table 5-1: The modelled results compared against experimental hemlock wood gasification results on performance and syngas composition at ER = 0.3.

Parameter	**Experimental (Li et al., 2004)**	**Model (This study)**	**Relative error (%)**
Syngas comp. (vol.%)			
H_2	5.50	5.62	-2.18
N_2	59.50	62.27	-4.66
CO	16.60	15.27	8.01
CH_4	3.40	3.58	-5.29
CO_2	15.00	13.26	11.60
HHVsyngas[MJ/Nm^3, dry]	4.82	4.07	15.56
CGE (%)	71.40	69.78	2.27

The over prediction of methane and hydrogen contributed to the model error in calculating the syngas higher heating value and cold gas efficiency. The model limitations contribute to the error since it did not consider the bed hydrodynamics (particle size, porosity, char reactivity and fluidization velocity) and reaction kinetics. De Andrés et al. (2019) reported a high methane concentration compared to the experimental value. In addition, Prins et al. (2007) and (Doherty et al., 2009) argued that more CH_4 concentration is contained in fluidized bed gasifiers as compared to the forecasted amount (Gu et al., 2019, Rupesh et al., 2016). The concentration of ammonia (NH_3) and hydrogen sulphide (H_2S) were very low (less than 90 ppm, as seen in Table C-1, Table C-2 and Table C-3 in Appendix C) and results

were not discussed in this study. The ash and char removed from the gasifier was to be sent to cement plants and water treatment industries due to their binding agent ability.

5.2 Sensitivity analysis on gasification temperature

5.2.1 Influence of gasification temperature on the syngas composition for PKS, MBM and WP gasification.

In the fluidized bed gasifier model, the temperature was varied between 600 and 1000 °C while the equivalence ratio (ER= 0.3) and gasifier pressure (P =105 kPa) were kept constant. The mass flow rate of each feedstock was 33.626 kg/h. Except for their ultimate and proximate analysis, the operating conditions for palm kernel shell, meat and bone meal, and wood pellets were similar. The moisture content of all feedstock were between 5 and 60 wt.% and their ash contents were below 25 wt.% which was also reported by (Basu, 2018, Bermudez and Fidalgo, 2016, McKendry, 2002). These are suitable feedstock properties for the circulating fluidized bed gasifier.

The steam produced was removed from raw syngas, and dry syngas is reported in this study as H_2, CO, CO_2 and CH_4 concentrations. The nitrogen concentration between 40 and 70% for all the feedstock gasification is reported in Table C- 4 and it agrees with other scholars (Basu, 2018, De Andres et al., 2011, Bermudez and Fidalgo, 2016). Methane was the only hydrocarbon used in this study to represent the hydrocarbons in the syngas. In Figure 5-1: Syngas composition (H2, CO, CO2 and CH4) as function of gasification temperature of PKS, MBM and WP at ER = 0.3 and P =105 kPa. Figure 5-1, the syngas composition produced of the three feedstock is plotted against the gasification temperature. The model predicted syngas composition, the trend of H_2 and CO concentration increases with an increase in temperature, whereas for CO and CH_4 concentration decreases. However, a decrease in CO concentration was not expected in the air gasification system.

According to Le Chateliar's principle, in an endothermic reaction, an increase in temperature shifts the equilibrium to favour products, while it favours reactants in an exothermic reaction. A decrease in CO production was due to char partial oxidation reaction (equation 4.1), which favoured reverse reactions instead of the forward reaction. As a result, higher temperatures did not favour CO production, as it decreases with an increase in temperature. An increase in temperature ensured that unreacted char is oxidized to maximize CO and H_2 produced based on the steam-methane reforming reaction (equation 4.8). The CO concentration decreases at temperatures above 600 °C while the CO_2 concentration increases due to carbon mono-oxidation reaction (equation 4.5).

Meat and bone meal gasification produced higher H_2 and CH_4 concentrations as compared to wood pellets and palm kernel shells relative to an increase in temperature. The reason may cause by the hydrogen to carbon atom ratio (H/C) in feedstock composition, which is higher for MBM (≈ 0.14) as compared to PKS (≈ 0.11) and WP (≈ 0.12). MBM contains lower fixed carbon as seen in Table 4-3, which means lower amount of char, will leave the gasifier unconverted to useful syngas components. The higher CO and CO_2 concentration for WP and PKS can be explained by oxygen to carbon atom (O/C) ratio (Basu, 2018). CH_4 concentration was higher at a low temperature below 800 °C, which can be caused by the large quantity of organic volatiles that were released from the pyrolysis stage as seen in Table C- 1, Table C-2 and Table C- 3. As the temperature is increased, there is lower volatiles produced while char concentration increases.

According to Le Chateliar's principle, since an increase in temperature favours reverse reaction in an exothermic reaction, methane formation decreased in methanation reaction (equation 4.4). Based on the steam-methane reforming reaction, carbon monoxide and hydrogen production are expected to increase since it's an endothermic reaction. When comparing the overall results on syngas composition trends, these results improved compared to (Lv et al., 2004), where they found the only hydrogen to increase thus producing low syngas. MBM gasification has been shown to have higher combustible gases concentration compared to other feedstock.

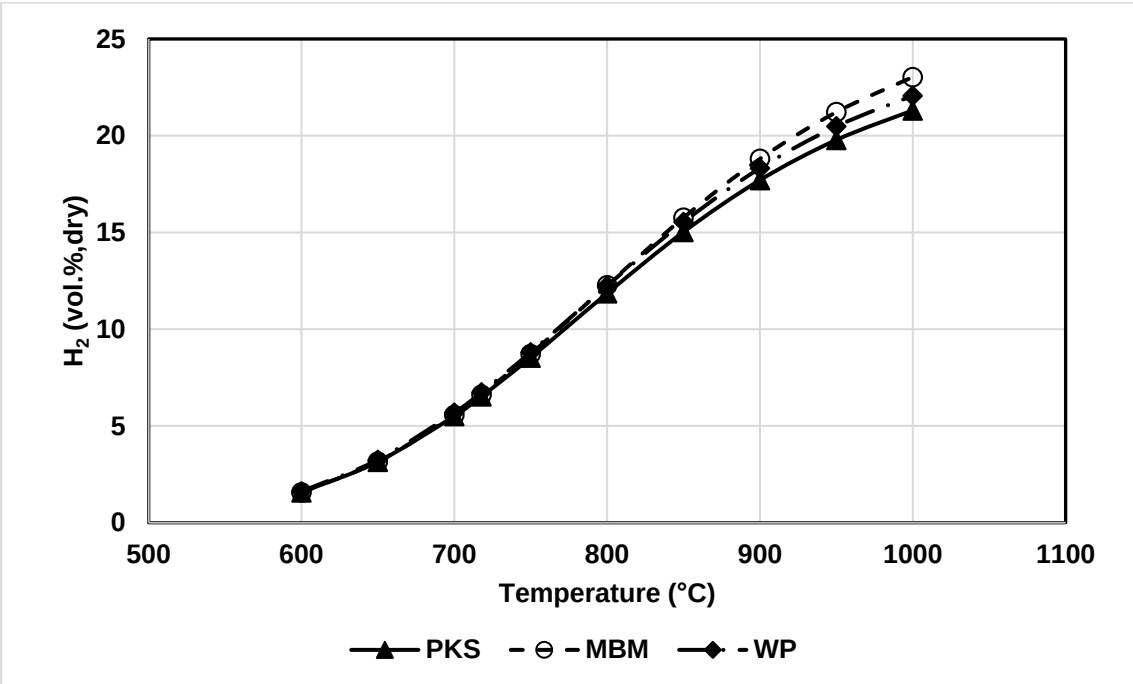

Figure 5-1 A: Hydrogen concentration as a function of gasification temperature

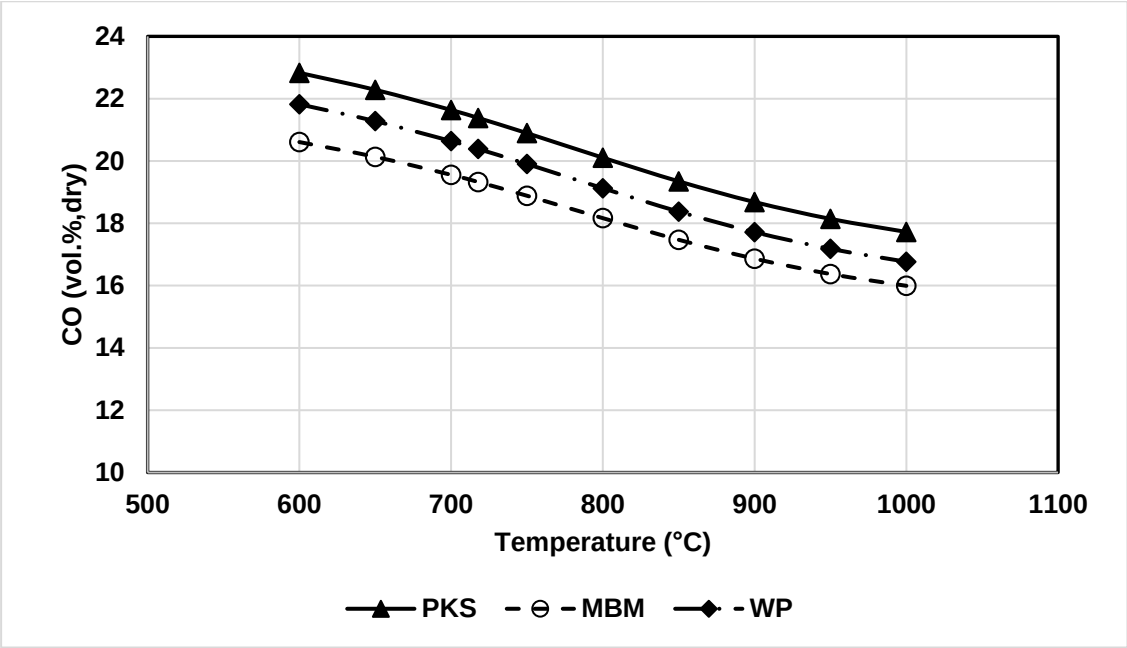

Figure 5-1 B: Carbon monoxide concentration as a function of gasification temperature

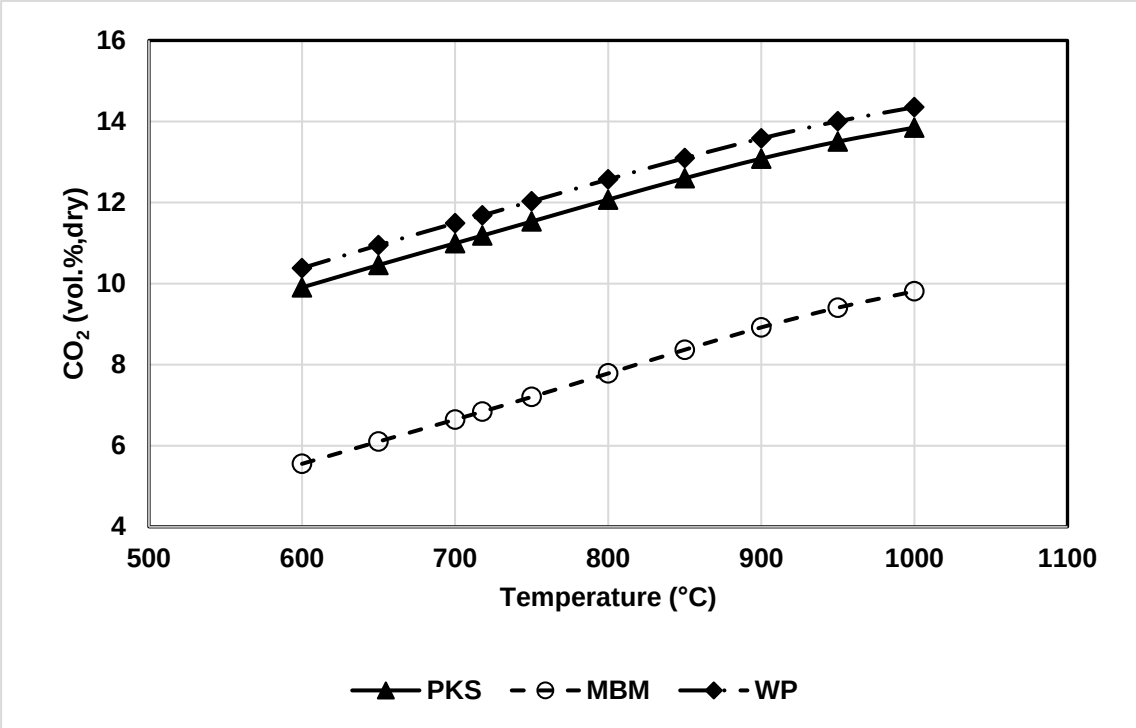

Figure 5-1 C: carbon dioxide concentration as a function of gasification temperature

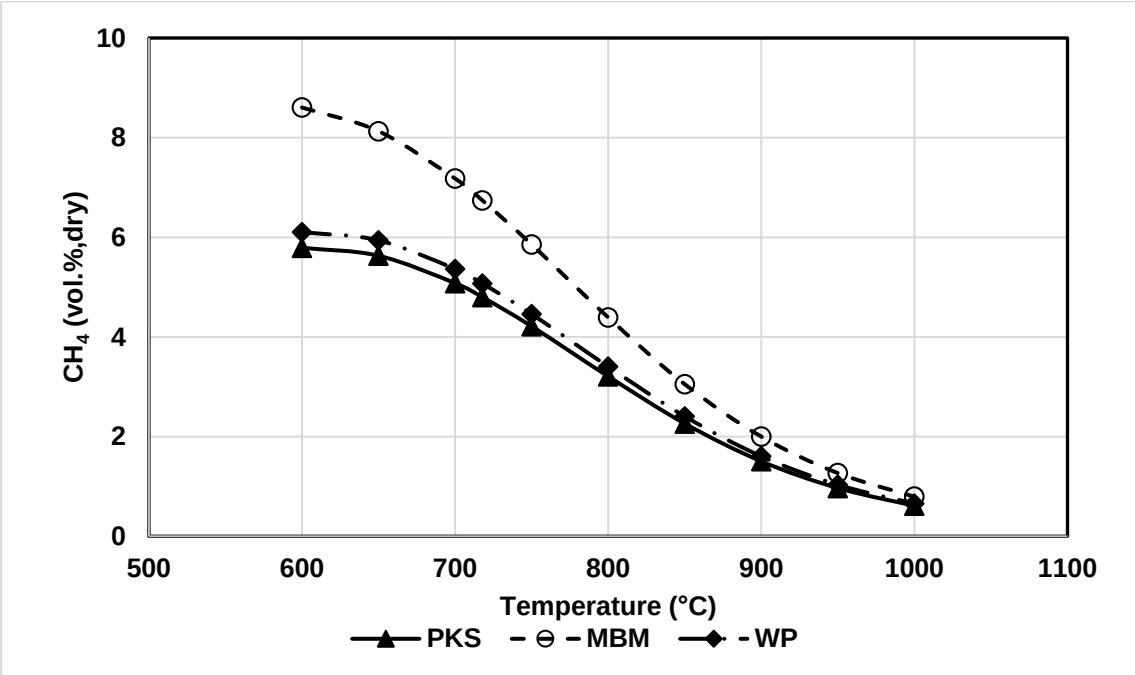

Figure 5-1: Syngas composition (H_2, CO, CO_2 and CH_4) as function of gasification temperature of PKS, MBM and WP at ER = 0.3 and P =105 kPa.

Table 5-2: The H_2/CO ratio and char content of PKS, MBM and WP gasification at different gasification temperatures.

					H_2/CO			
Temperature (°C)	**600**	**700**	**750**	**800**	**850**	**900**	**950**	**1000**
PKS	0.07	0.25	0.41	0.59	0.78	0.95	1.09	1.20
MBM	0.08	0.28	0.46	0.68	0.90	1.12	1.30	1.44
WP	0.07	0.28	0.44	0.64	0.85	1.03	1.19	1.32
					Char content (g/Nm^3)			
Temperature (°C)	**600**	**700**	**750**	**800**	**850**	**900**	**950**	**1000**
PKS	42.40	34.42	32.15	30.32	28.42	26.30	24.07	21.95
MBM	34.34	30.73	31.06	31.74	31.93	31.31	30.05	28.50
WP	47.32	41.17	40.05	39.35	38.48	37.06	35.16	33.05

Table 5-2 shows how the H_2/CO ratio and char content behave when the gasification temperature is increased. At temperatures above 900°C, the ratio is suitable to be used for various application such as ethanol production (Hernández et al., 2017, Bermudez and Fidalgo, 2016, Higman and Van der Burgt, 2008). The char content decreases, as the temperature is increases. It may explain by the char oxidation, which is converted, to carbon dioxide as it shows high concentration.

5.2.2 Influence of gasifier temperature on gasification performance of PKS, MBM and WP.

The dry syngas flow rate divided by the mass flow of feedstock on a dry ash-free basis was used to determine the syngas yield. Figure 5-2 shows the effect of gasification temperature on the syngas yield for palm kernel shell (PKS), meat and bone meal (MBM) and wood pellets (WP) gasification. The syngas yield (G_Y) is expressed as volumetric flow rate in dry-free nitrogen per dry ash-free basis (daf) of the feedstock (Nm^3/kg daf.). The study's finding is that an increase in temperature increases the syngas yield due to organic volatiles liberated and the conversion of char attained at higher temperatures. MBM gasification showed a greater syngas yield due to higher presence of ash in the feedstock.

The syngas yield for MBM gasification was higher as it ranges from 0.94 to 1.69 Nm^3/kg of feedstock. In contrast, the PKS and WP gasification syngas were 0.83 to 1.43 Nm^3/kg and 0.77 to 1.35 Nm^3/kg, respectively. MBM gasification showed a higher syngas yield which may be due to high syngas flow and greater ash content which is 19.1 wt.% in the feedstock. Rodrigues et al. (2017) also reported an increase in syngas yield from 2.16 to 2.54 Nm^3/kg of cork waste experiments using a fluidized bed gasifier. This study reported low results compared to Rodrigues et al. (2017) due to relative error in calculations of the model. Auxiliary to that, it can be due to bed material, fluidizing velocity, reactivity of char and porosity of the cork waste used in the experiment which enhance higher syngas yield for cork waste. However, the findings on PKS gasification agreed the literature trend but it was over predicted with what was reported by (Wan Ab Karim Ghani et al., 2009), which were between 2.30 mol/kg (0.10 Nm^3/kg) and 5.9 mol/kg (0.27 Nm^3/kg) of PKS in air gasification.

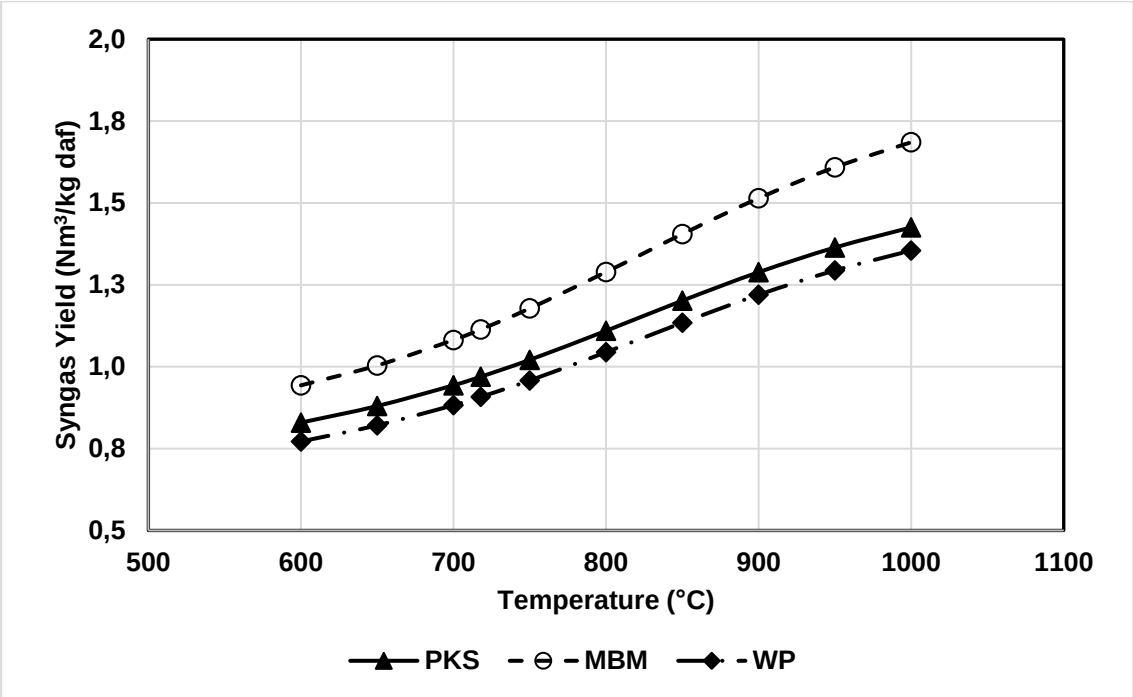

Figure 5-2: The syngas yield as a function of gasification temperature of PKS, MBM and WP at ER=0.3 and pressure of 105 kPa.

5.2.3 Influence of gasifier temperature on syngas lower heating value of PKS, MBM and WP gasification.

In Figure 5-3, syngas lower heating value is plotted against temperature for the three-feedstock gasification. The syngas lower heating value (LHV) was expressed as the specific energy produced per volume of syngas on a dry N_2 free basis. An increase in gasification temperature decreases the syngas lower heating value for three feedstock. The gasification temperature was varied between 600 and 1000 °C, the model predicted the syngas LHV for all feedstock gasification between 4.5 and 6.0 MJ/Nm^3. This agrees with what was reported by (Wan Ab Karim Ghani et al., 2009, Basu, 2010, Rodrigues et al., 2017) which was discussed in section 2.5.

MBM gasification shows high syngas lower heating value between 600 and 900 °C, this can be explained by high methane concentration. It is the main contributor of the syngas lower heating value is methane concentration, which was higher for MBM gasification, as seen in Figure 5-1. These feedstock are suitable for the energy production based on their syngas lower heating value they provide (Rezaiyan and Cheremisinoff, 2005).

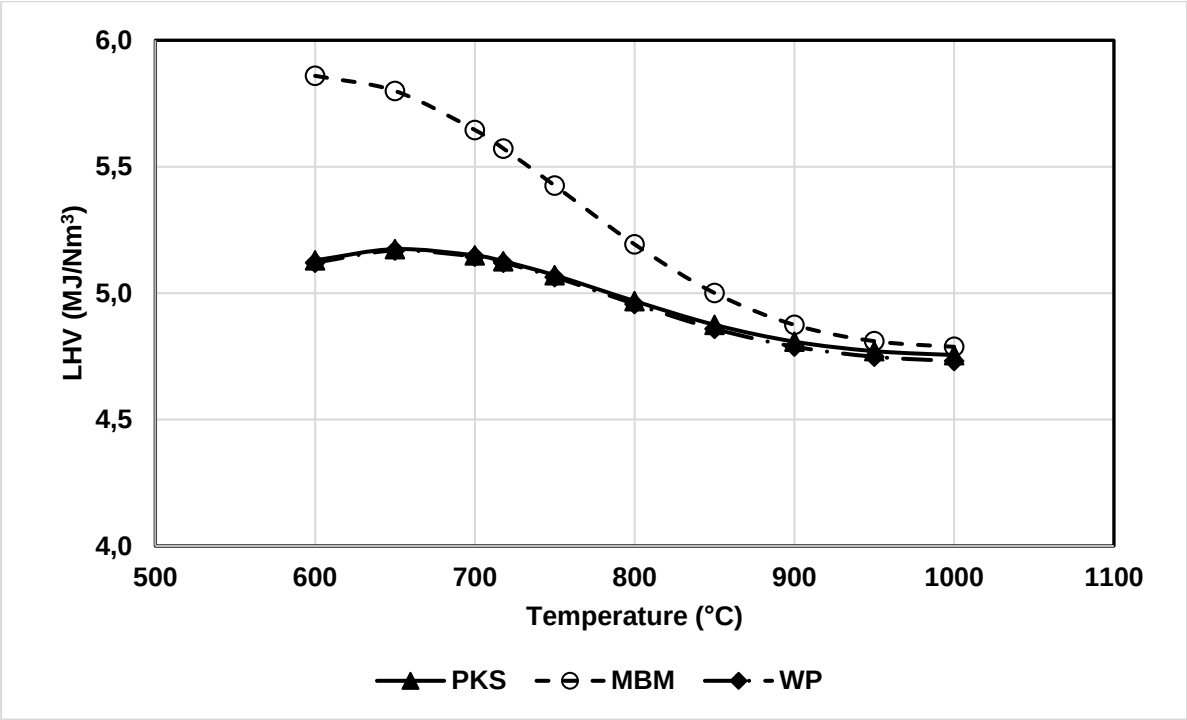

Figure 5-3: Lower heating value as function of gasification temperature of PKS, MBM and WP at ER=0.3 and P=105 kPa.

PKS and WP gasification has shown a relative similar syngas lower heating value trend, which can be explained by their feedstock composition, which is more or less equal in terms of C, H and O atoms. The carbon content in these feedstock is lower than MBM, which can explain the low carbon conversion.

5.2.4 Influence of gasifier temperature on cold gas efficiency of PKS, MBM and WP gasification.

The cold gas efficiency (CGE) evaluates the gasifier performance based on the heating values of the syngas relative to the feedstock. Figure 5-4 shows the influence of gasification temperature on cold gas efficiency for PKS, MBM and WP gasification. The CGE increased with an increase in gasification temperature from 600 to 1000 °C. It was due to more syngas production with its lower heating value decreased when temperature was increased. At 600 °C, MBM gasification shows a higher CGE due to the higher syngas LHV being greater at low temperature. However, the CGE decreases when the temperature is increased. Overall, WP gasification offers higher cold gas efficiency above 700 to 1000 °C.

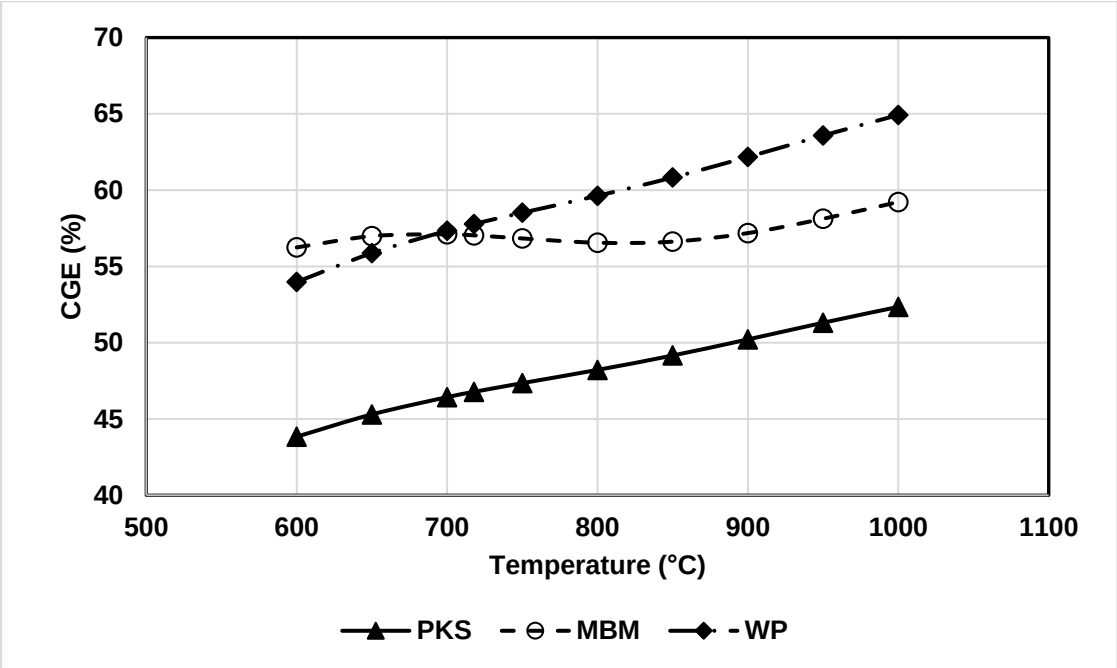

Figure 5-4: Cold gas efficiency as a function of gasification temperature for PKS, MBM and WP at ER=0.3 and P = 105 kPa.

This can be due to the high volatile organic matter present in wood pellets as it contains 81 wt.% when compared with palm kernel shell and meat and bone meal. The sensitivity analysis shows a cold gasification efficiency ranges from 43.84 to 52.34 % for PKS, 56.25 to 59.22 % for MBM and 53.98 to 64.92 % for WP. The CGE ranges from 44 to 66 % were reported by (Puig-Arnavat et al., 2010, Van der Drift et al., 2001, La Villetta et al., 2017, Mansaray et al., 1999). This study agrees with what was reported in literature, except some relative error which can be contributed by the model limitations. Rodrigues et al. (2017) also reported an increase in temperature from 780 to 900 °C produced 34.9 to 59.9 % in cold gas efficiency.

5.2.5 Influence of gasifier temperature on the carbon conversion efficiency of PKS, MBM and WP gasification.

The quantity of carbon converted from feedstock to valuable gas is called carbon conversion. Figure 5-5 shows the carbon conversion efficiency as a function of gasification temperature for the three feedstock. Wood pellets and palm kernel shell gasification produced an increase in carbon conversion efficiency with an increase in gasification temperature. For meat and bone meal gasification, carbon conversion efficiency decreases, which was not expected. This can be explained by low concentration of carbon monoxide and carbon dioxide produced through MBM gasification. De Andres et al. (2011) found an increase in carbon conversion from 70 to 82 % when gasification temperature was increased from 750

to 850 °C. In a previous study, Rodrigues et al. (2017) also found carbon conversion efficiency to increase from 57 to 85 % when the temperature was increased from 780 to 850 °C. The results predicted by the model are within this range.

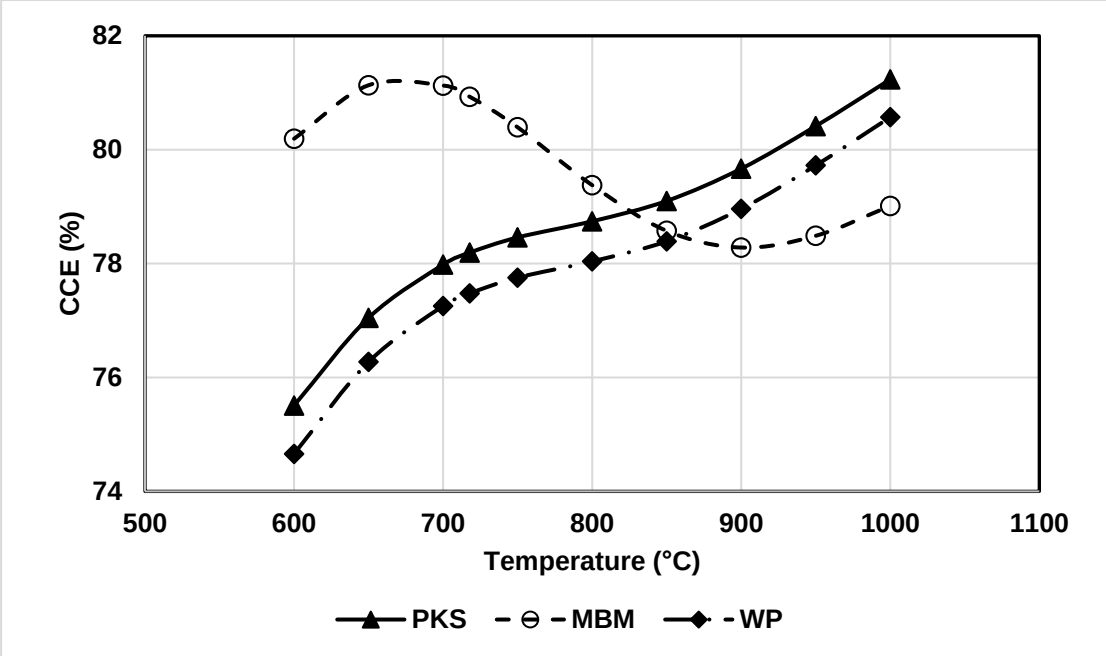

Figure 5-5: Carbon conversion efficiency as a function of PKS, MBM and WP gasification temperature at ER=0.3 and P = 105 kPa.

A decline in carbon conversion efficiency in MBM gasification can be explained by lower char content in the syngas. In the product stream, char was found with the syngas product due to incomplete carbon conversion. When gasification temperature was varied between 600 and 1000 °C, the model predicted the carbon conversion efficiency of PKS to be between 75.51 and 81.23 %. In addition, the carbon conversion efficiency of PKS was from 74.66 to 80.57 % and for MBM, it was between 78.28 and 80.19 %.

5.3 Sensitivity analysis on equivalence ratio

5.3.1 Influence of equivalence ratio on the syngas composition for PKS, MBM and WP gasification.

The equivalence ratio is the supplied air flow rate to the gasifier divided by the stoichiometric amount of air. In this study, ER is varied between 0.15 and 0.40 while gasifier pressure and gasification temperature were kept constant. The mass flow rate of each feedstock were kept at 33.626 kg/h, and gasifier pressure was 105 kPa while gasification temperature was 800 °C. In Figure 5-6, the influence

of ER on the syngas composition for PKS, MBM and WP gasification. The syngas is composed of H_2, CO, CO_2, and CH_4; they are reported on dry basis as percentage volume.

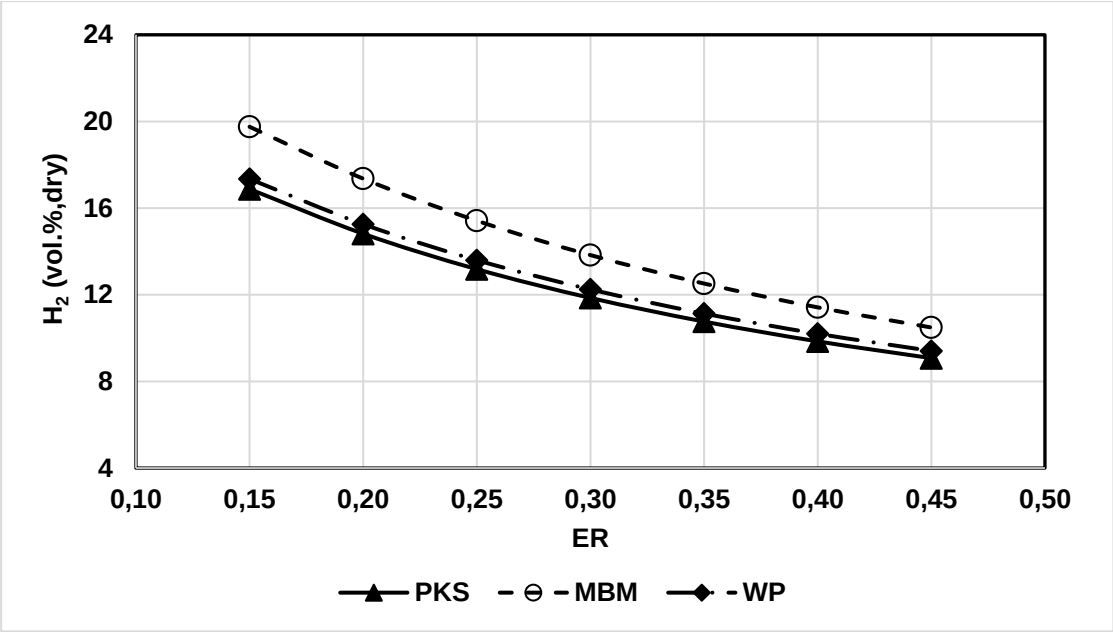

Figure 5-6 A: hydrogen concentration as a function of equivalence ratio

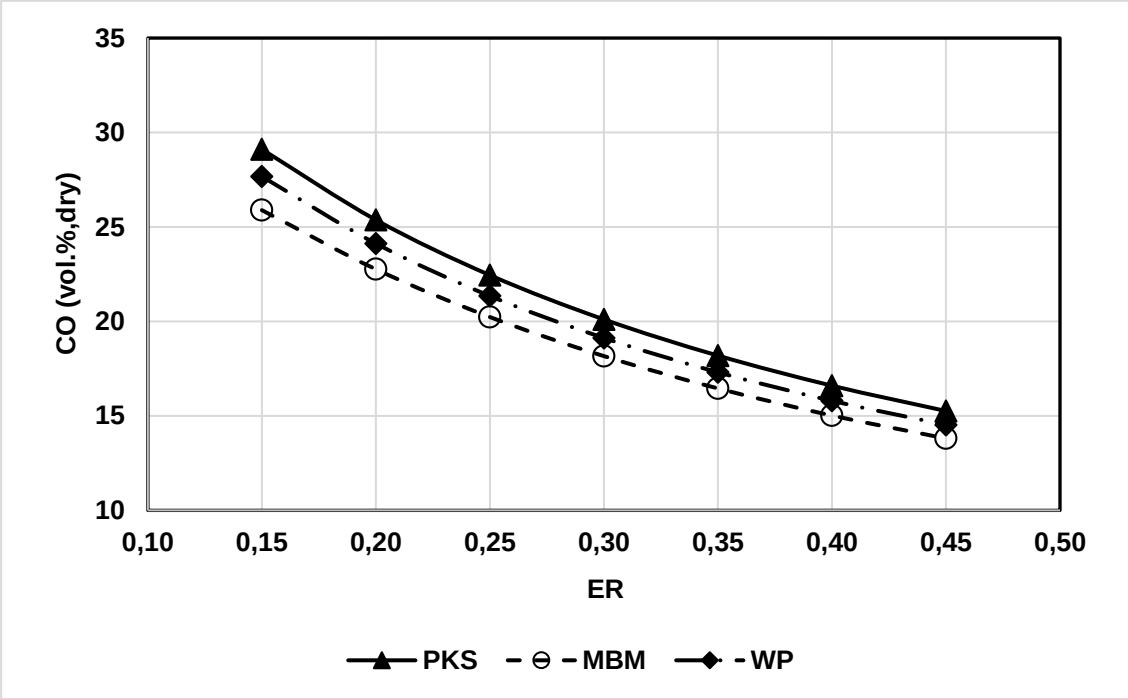

Figure 5-6 B: carbon monoxide concentration as a function of equivalence ratio

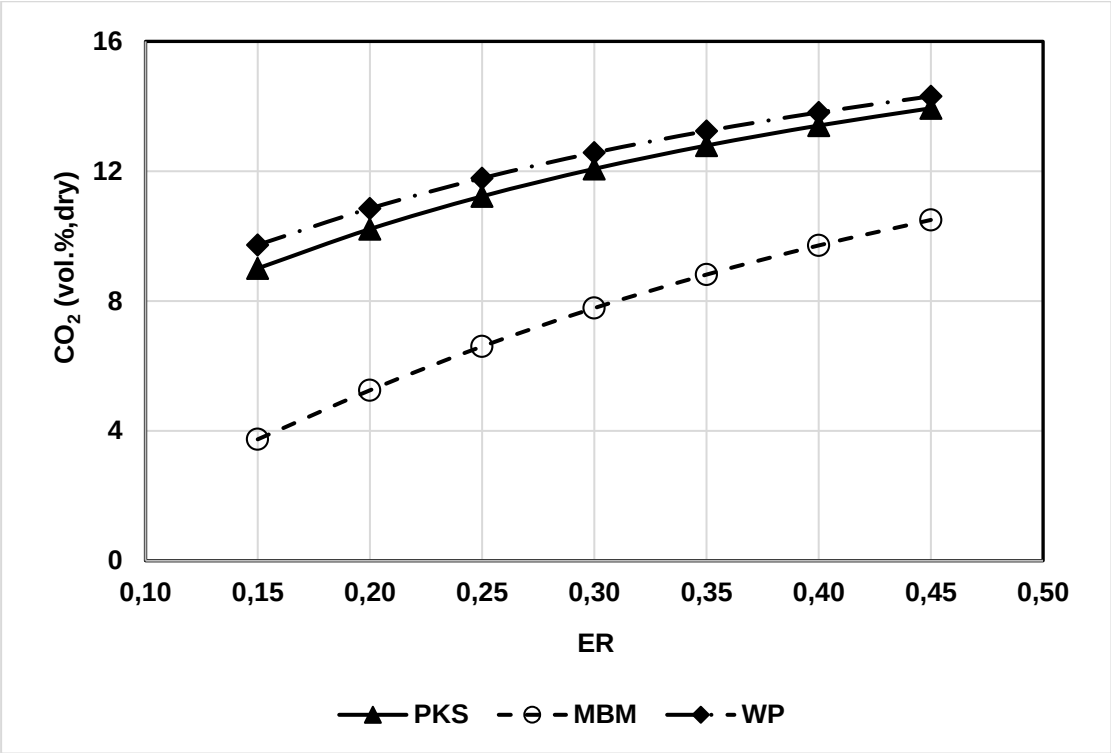

Figure 5-6 C: carbon dioxide concentration as a function of equivalence ratio

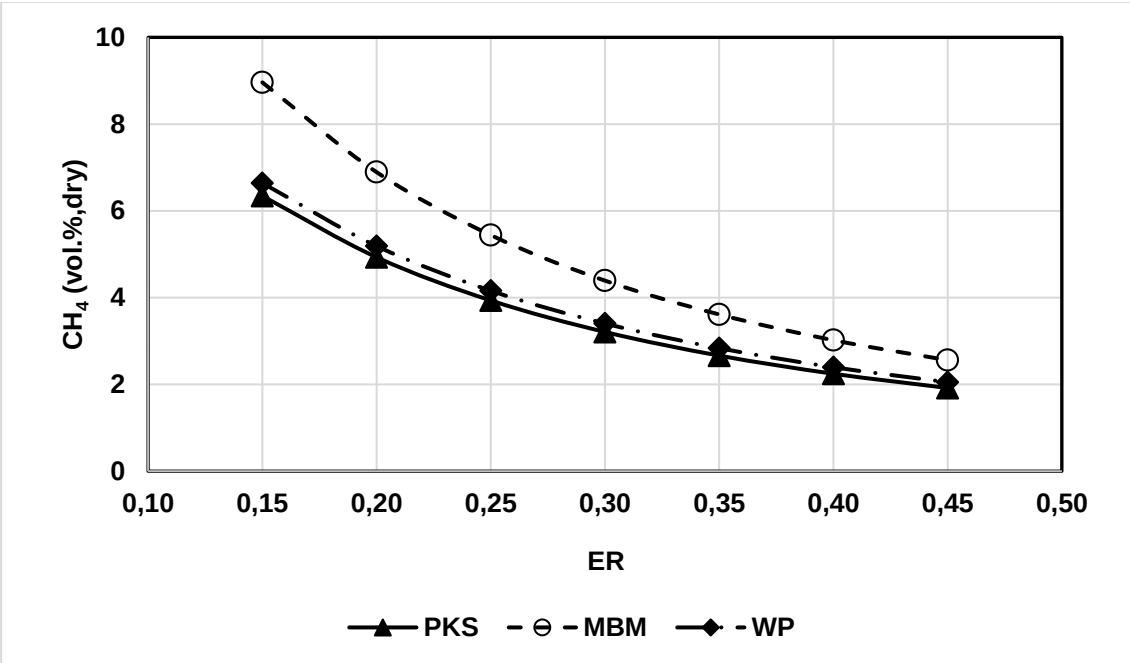

Figure 5-6: The syngas composition (H_2, CO, CO_2 and CH_4) as a function of ER for PKS, MBM and WP gasification at T = 800 °C and P = 105 kPa.

The concentrations of hydrogen, carbon monoxide and methane decreases with an increase in equivalence ratio. The oxygen quantity supplied to the gasifier increases, which indicates an increase in ER due to greater conversion of the carbon present in the fuel. However, the concentration of carbon monoxide increases with an increase in ER. A similar observation was also reported by Campoy et al. (2014) when they investigated the influence of ER on syngas composition using WP and MBM gasification in a fluidized bed gasifier using air.

As seen in Figure 5-6, more CO and CO_2 were produced since the air was used as a gasifying medium (Basu, 2018). The hydrogen to carbon (H/C) atomic ratio in the feedstock can determine whether the feedstock will produce a higher concentration of H_2 and CH_4. MBM has a higher H/C ratio (≈ 0.14) which answer the increased production of H_2 and CH_4. While the higher production of CO and CO_2 can be related to the O/C ratio. WP gasification shows a higher CO_2 due to an O/C ratio of 0.85 compared to other feedstock. PKS has a lower hydrogen content, which can result from increasing in CO concentration in syngas.

The amount of carbon monoxide and hydrogen decreases due to the complete combustion of the solid fuel. The hydrogen concentration decreases from 10.9 to 5.8 vol.% for MBM gasification. However, its H_2 concentration was found to be more significant compared to PKS and WP. An increase in oxygen supply into the gasifier oxidizes the carbon from the feedstock, thus producing more CO and CO_2 while decreasing methane production.

Table 5-3: The H_2/CO ratio and char content of PKS, MBM and WP gasification at different equivalence ratios and a temperature of 850°C.

				H_2/CO			
Equivalence ratio	**0.15**	**0.20**	**0.25**	**0.30**	**0.35**	**0.40**	**0.45**
PKS	0.77	0.77	0.77	0.78	0.78	0.78	0.78
MBM	1.01	1.00	1.00	1.00	0.99	0.99	0.99
WP	0.83	0.84	0.84	0.85	0.85	0.85	0.85
				Char content (g/Nm^3)			
Equivalence ratio	**0.15**	**0.20**	**0.25**	**0.30**	**0.35**	**0.40**	**0.45**
PKS	75.50	56.64	41.22	28.42	17.66	8.55	1.23
MBM	72.62	57.37	43.79	31.93	21.62	12.65	4.81
WP	80.40	60.99	45.17	32.06	21.04	11.67	3.60

Table 5-3 shows the H_2/CO ratio and char content in the syngas at different equivalence ratio for PKS, MBM and WP gasification. ER increases with the H_2/CO ratio due oxidation of carbon from the feedstock. The char content indicate the contamination of particulate in the syngas, ER between 0.30 and 0.40 is favourable for CFB gasifier.

5.3.2 Influence of equivalence ratio on the syngas yield for PKS, MBM and WP gasification.

The influence of ER on the syngas yield (G_Y) for the three feedstock is shown in Figure 5-7. The syngas yield considers the combined volume of H_2, CO, CO_2, and CH_4 per kg of fuel on a dry ash-free basis.

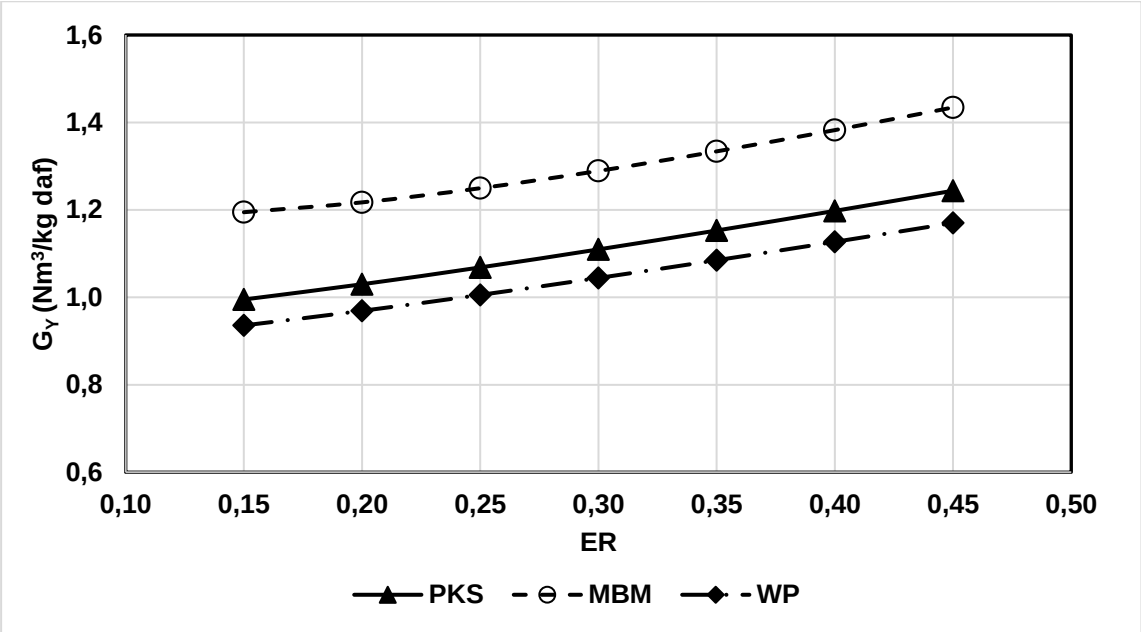

Figure 5-7: Syngas yield (G_Y) as a function of ER for PKS, MBM and WP gasification at ER = 0.3 and T = 800 °C.

The findings from this study were that syngas yield increases as the ER increases, and this was also reported by other scholars (De Andres et al., 2011, Campoy et al., 2014). This indicates that the organic volatile matter was liberated at higher temperatures and conversion of carbon from the feedstock. MBM gasification produced greater syngas yield than WP and PKS gasification, which the high ash amount can explain in MBM. The model predicted the syngas yield results of 0.97 to 1.13 Nm^3/kg for WP gasification. In addition, 1.03 to 1.20 Nm^3/kg for PKS gasification and 1.22 to 1.38 Nm^3/kg for MBM gasification when optimal ER was between 0.2 to 0.4.

5.3.3 Influence of equivalence ratio on the syngas lower heating value for PKS, MBM and WP gasification.

Figure 5-8 shows the lower heating value of the syngas as a function of ER. The influence of ER was varied between 0.15 and 0.45 for all three feedstock gasification. The syngas lower heating value decreases as the ER increases, which has been found by other researchers (Campoy et al., 2014, De Andres et al., 2011). The volume of combustible gases decreases with an increase in ER, as seen in

Figure 5-6. These gases are carbon monoxide, methane and hydrogen; they determine the syngas lower heating value. The syngas LHV was highest for MBM gasification since it produced higher methane and hydrogen concentration.

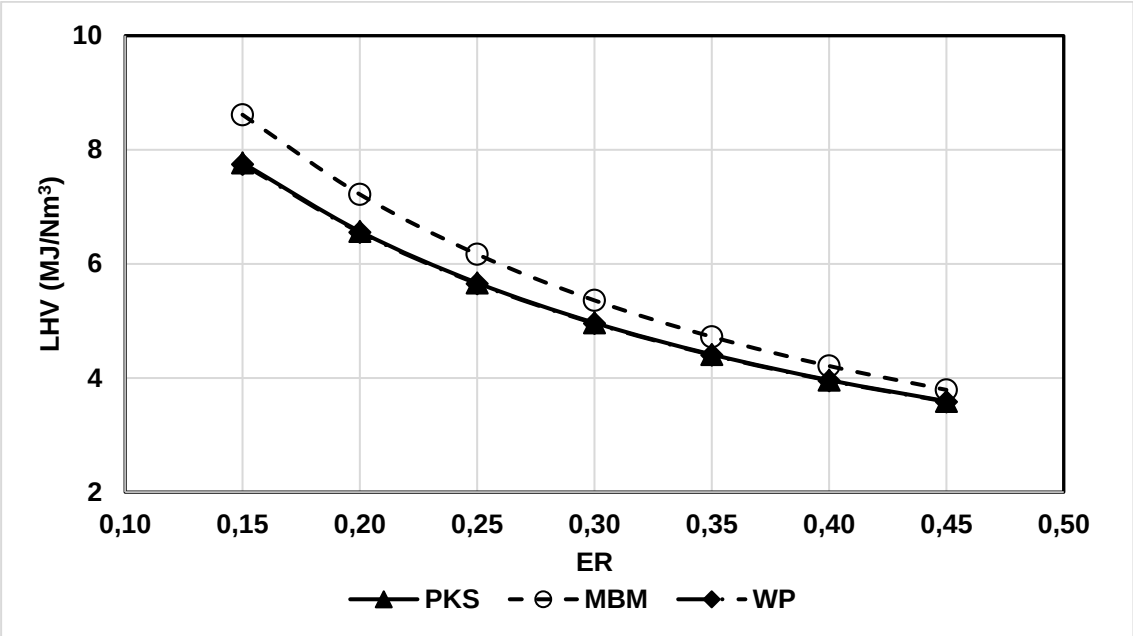

Figure 5-8: Syngas lower heating value as a function of ER for PKS , MBM and WP gasification at T = 800 °C and P = 105 kPa.

The gasification of PKS and WP were found to produce relatively close lower heating values. The possible reason is their H/C ratio of 0.12 (for WP) and 0.11 (for PKS), which determines the production of hydrogen and methane. An increase further in ER would decrease the LHV of the syngas due to combustion and partial oxidation reactions and the increasing volume of non-combustible gases (i.e. nitrogen in air). For optimal conditions, ER between 0.20 and 0.40 is considered for fluidized bed gasifiers (Basu, 2010). MBM gasification produced a syngas LHV from 4.21 to 7.22 MJ/Nm^3 ; WP gasification had syngas LHV between 3.95 and 6.55 MJ/Nm^3 and PKS gasification produced a syngas LHV between 3.96 and 6.57 MJ/Nm^3. These results indicate these feedstock can produce syngas fuels suitable for energy production (Rezaiyan and Cheremisinoff, 2005).

5.3.4 Influence of equivalence ratio on the cold gas efficiency for PKS, MBM and WP gasification.

Figure 5-9 show the influence of ER on cold gas efficiency for PKS, MBM and WP gasification. An increase in ER resulted in decreasing the cold gas efficiency. This can be explained by a decrease in combustible gases produced at higher temperatures, which decreases the lower heating value. Since cold

gas, efficiency depends mainly on syngas lower heating value. In another study, De Andres et al. (2011) reported a low CGE of 37.25 % for sludge gasification.

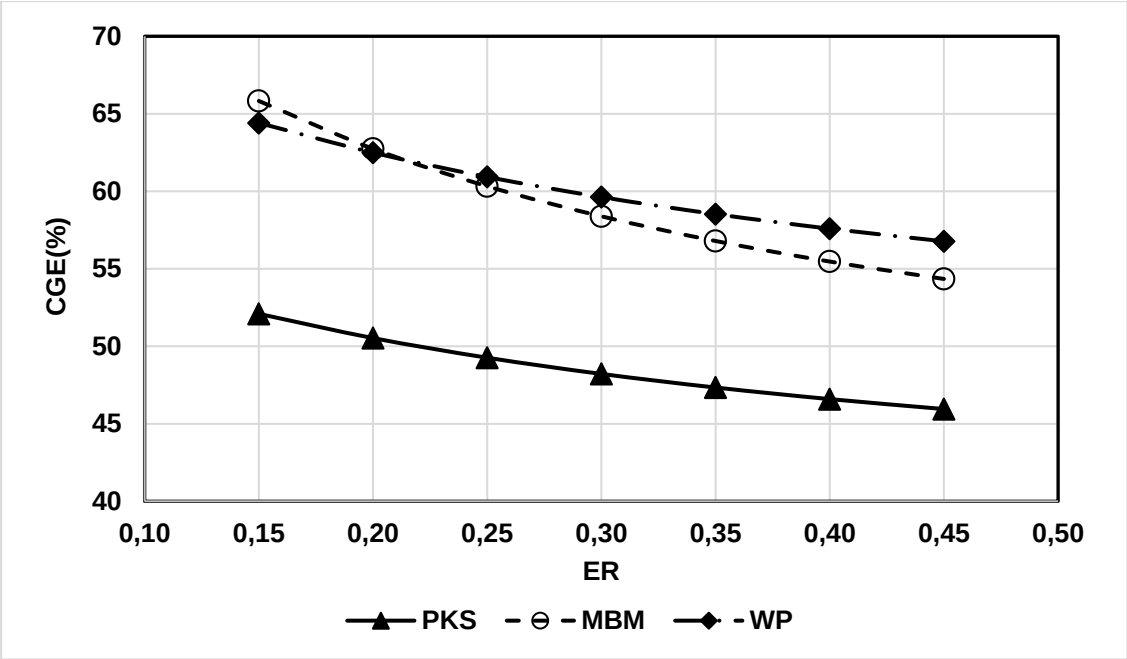

Figure 5-9: Cold gas efficiency as a function of ER for PKS, MBM and WP gasification at T = 800 °C and P = 105 kPa.

Campoy et al. (2014) reported a decrease in CGE with an ER increase when investigating the MBM gasification. In this study, MBM gasification predicted a decline in CGE from 62.74 to 55.47 % when ER was varied between 0.2 and 0.4. The model over predicted CGE due to inaccuracy in the model. PKS gasification produced a CGE from 50.53 to 46.59 %, whereas for WP gasification produced a range of CGE from 62.49 to 57.59 %. At an ER range between 0.2 and 0.4, the wood pellets gasification has the highest cold gas efficiency.

5.3.5 Influence of equivalence ratio on the carbon conversion efficiency for PKS, MBM and WP gasification.

Carbon conversion efficiency is the amount of carbon in syngas divided by the amount of carbon in the feedstock. The influence of ER on carbon conversion efficiency for PKS, MBM and WP gasification is shown in Figure 5-10. The carbon conversion increases with an increase in equivalence ratio. The reason is high carbon conversion at higher temperatures due to low methane and carbon monoxide.

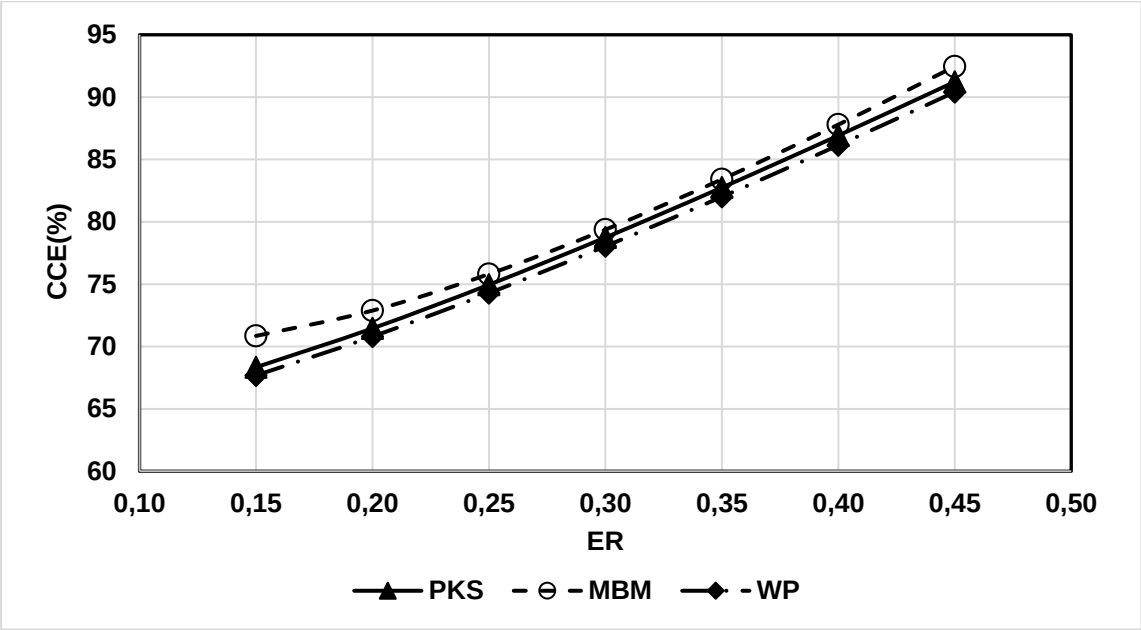

Figure 5-10: The carbon conversion efficiency as function of ER for PKS, MBM and WP gasification at T = 800 °C and P = 105 kPa.

MBM gasification has shown the highest CCE compared to other feedstock. The ratio of volatile matter to fixed carbon is greater for MBM than other feedstock. Campoy et al. (2014) reported a carbon conversion efficiency of MBM gasification, relatively at 99 %, whilst wood pellets varied between 90 and 96 %. Campoy and co-authors did not consider the amount of un-reacted carbon in their computation that exited with the syngas as volatiles in their study, which can increase their carbon conversion efficiency. In this study, ER between 0.2 and 0.4 resulted in a CCE from 72.8 to 87.8 % for MBM gasification. While WP gasification produced CCE from 70.8 to 86.4 % and PKS, gasification produced CCE from 71.46 to 86.92 %. A reduced CCE was produced since char was not completely converted by this gasification model. This indicates the presence of particulates in the syngas produced and it can also cause by the efficiency of cyclone which was at 85 % to simulate the plant conditions.

5.4 Sensitivity analysis on gasifier pressure

5.4.1 Influence of pressure on syngas composition for PKS, MBM and WP gasification.

The gasifier pressure was investigated to gain insight into its influence on the syngas composition and yield, lower heating value, and gasifier performance. The gasifier pressure was varied between 0.1 and 2 MPa while ER was kept at 0.3 and gasification temperature kept at 800 °C. Figure 5-11 shows the influence of gasifier pressure on the syngas composition of PKS, MBM and WP gasification using air.

An increase in gasifier pressure was found to increase the concentration of CO and CH_4 while decreases H_2 and CO_2.

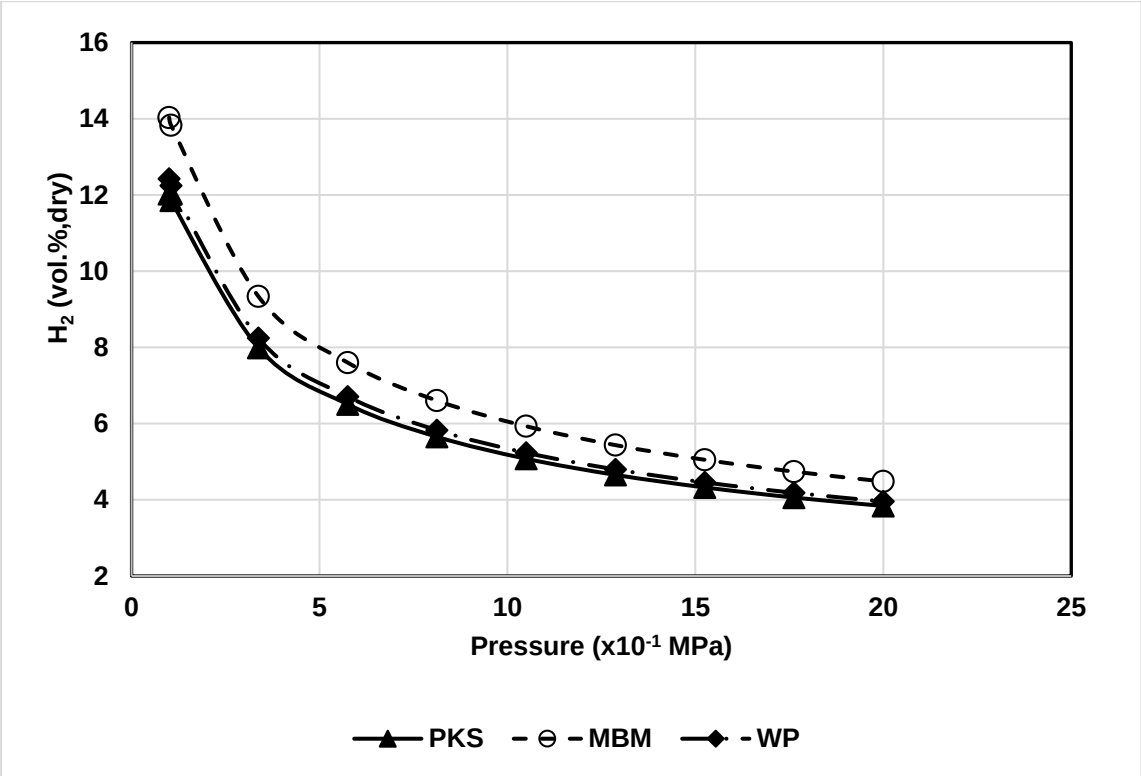

Figure 5-11 A: Hydrogen concentration as a function of gasifier pressure

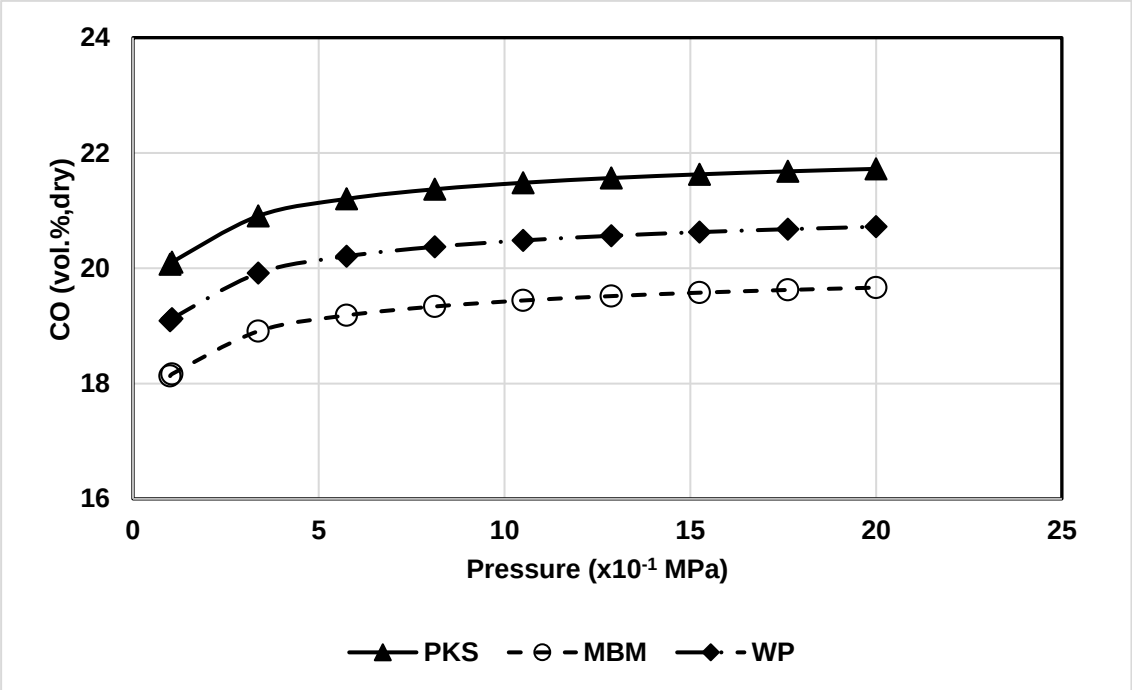

Figure 5-11 B: Carbon monoxide concentration as a function of gasifier pressure

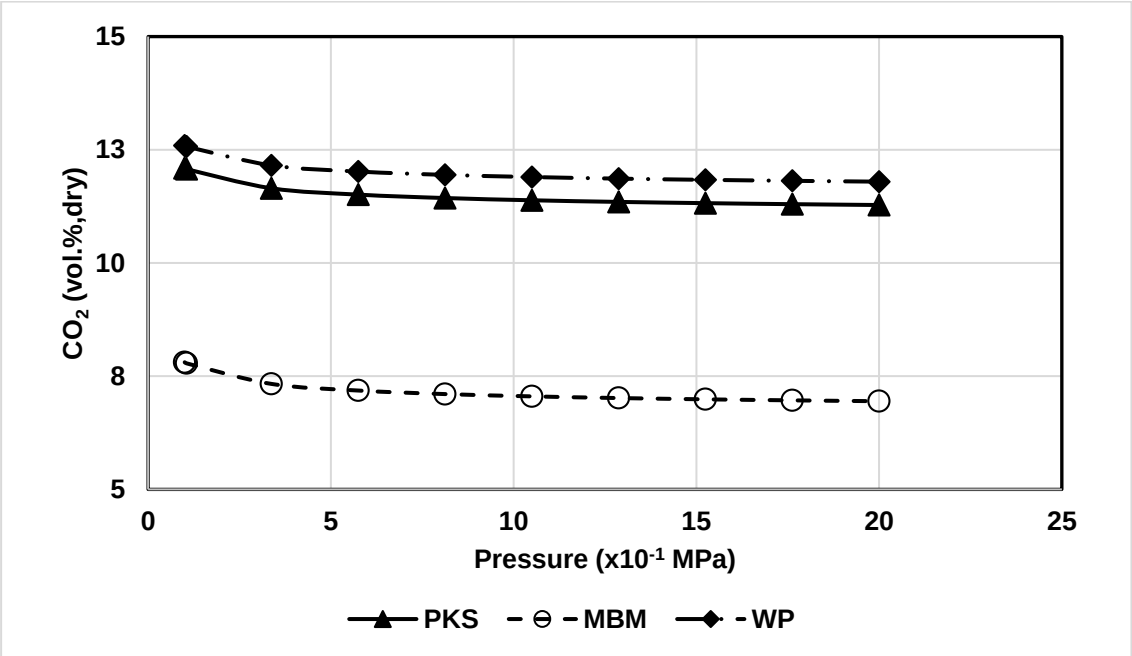

Figure 5-11 C: Carbon dioxide concentration as a function of gasifier pressure

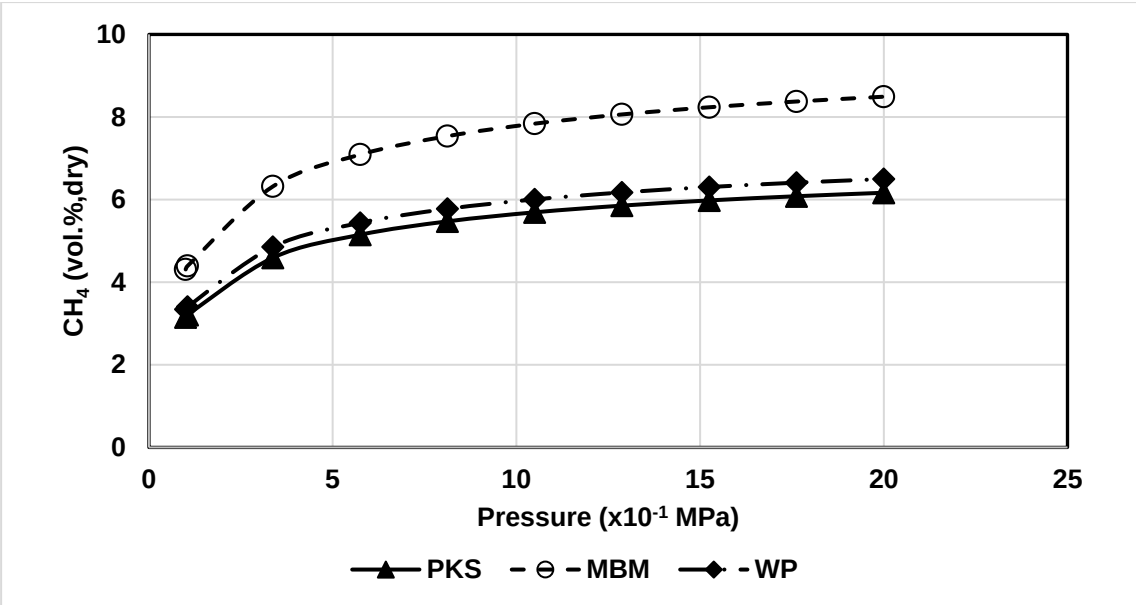

Figure 5-11: The syngas composition (H_2, CO, CO_2 and CH_4) as a function of a gasifier pressure for PKS, MBM and WP gasification using air at ER = 0.3 and T = 800 °C.

According to Le Chateliar's principle, an increase in pressure will shift the equilibrium to favour fewer gas moles in a chemical reaction. Based on gasification reactions used for the model, methane formation was expected to increase due to the activity of steam methane reforming (Equation 4.8) and methanation (equation 4.4) reactions. The hydrogen formation was expected to decrease with an increase in pressure as it has greater moles of gases in the oxidation of hydrogen reaction. However, an increase in CO concentration and decrease in CO_2 can be explained by a water-gas shift reaction (Equation 4.7) at low temperatures. MBM gasification produced greater H_2 and CH_4 concentration relative to other feedstock due to the high H/C ratio from its ultimate analysis (Basu, 2018). In contrast, WP and PKS gasification produced more CO and CO_2 due to these feedstock compositions' more significant O/C proportion.

Table 5-4: The H_2/CO ratio and char content of PKS, MBM and WP gasification at different gasifier pressures.

				H_2/CO				
Pressure (MPa)	**0.1**	**0.105**	**0.338**	**0.575**	**1.05**	**1.288**	**1.525**	**2.0**
PKS	0.79	0.78	0.54	0.44	0.34	0.32	0.29	0.26
MBM	1.01	1.00	0.69	0.56	0.44	0.32	0.38	0.34
WP	0.86	0.85	0.58	0.48	0.37	0.34	0.32	0.28
				Char content (g/Nm^3)				
Pressure (MPa)	**0.1**	**0.105**	**0.338**	**0.575**	**1.05**	**1.288**	**1.525**	**2.0**
PKS	28.36	28.42	28.72	28.34	27.73	27.51	27.32	27.04
MBM	31.98	31.93	29.37	27.68	25.70	25.06	24.54	23.75
WP	31.99	32.06	32.47	32.12	31.54	31.33	31.15	30.87

Table 5-4 shows the ratio of hydrogen to carbon monoxide and char content produced at different gasifier pressure. The H_2/CO ratio decreases with an increase in pressure which points out at higher pressure, syngas application is difficult for further processing. At atmospheric pressure a ratio close to 1.0 is achievable, which is suitable for ethanol production. On the other hand, char content is above the range from 1.43 to 14 g/Nm^3 which is the expected from circulating fluidized bed gasifier (Bermudez and Fidalgo, 2016, Basu, 2018). An increase in pressure had no significant in reduction of char content (less than 5%). However, this can be explained by an limitations in the gasification model.

5.4.2 Influence of gasifier pressure on syngas yield and lower heating value for PKS, MBM and WP gasification.

Figure 5-12 shows the effect of gasifier pressure on syngas yield (G_Y) for PKS, MBM and WP gasification. An increase in gasifier pressure has shown to produce low syngas yield than atmospheric (P = 101.3 kPa) operated gasifier. MBM gasification produced greater syngas yield when compared with PKS and WP gasification. Atmospheric pressure conditions are preferred over a pressurized gasifier in terms of syngas yield.

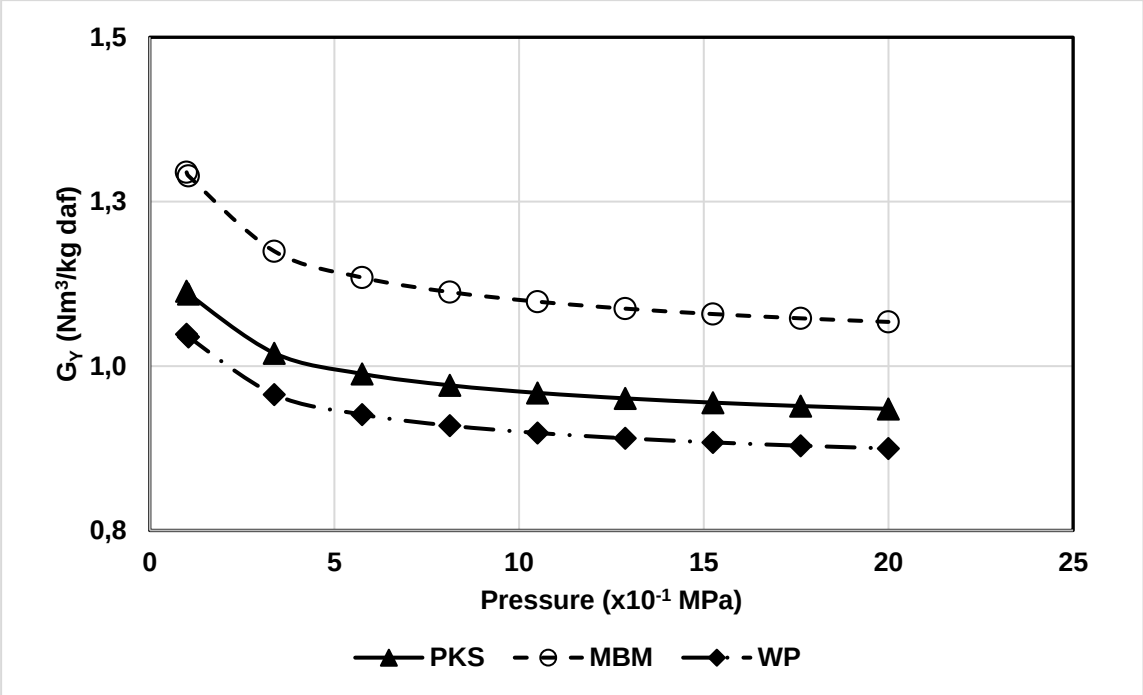

Figure 5-12: Syngas yield as a function of gasifier pressure for PKS, MBM and WP gasification using air at ER = 0.3 and T =800 °C.

The sensitivity analysis results pointed out that the gasifier pressure between 0.1 and 2.0 MPa produces a syngas yield from 1.07 to 1.29 Nm^3/kg for MBM, 0.93 to 1.11 Nm^3/kg for PKS and 0.87 to 1.05 Nm^3/kg for WP. Figure 5-13 shows syngas lower heating value as a function of gasifier pressure from PKS, MBM and WP gasification using air. An increase in gasifier pressure improves the syngas lower heating value due to an increase in combustible gases such as CO and CH_4.

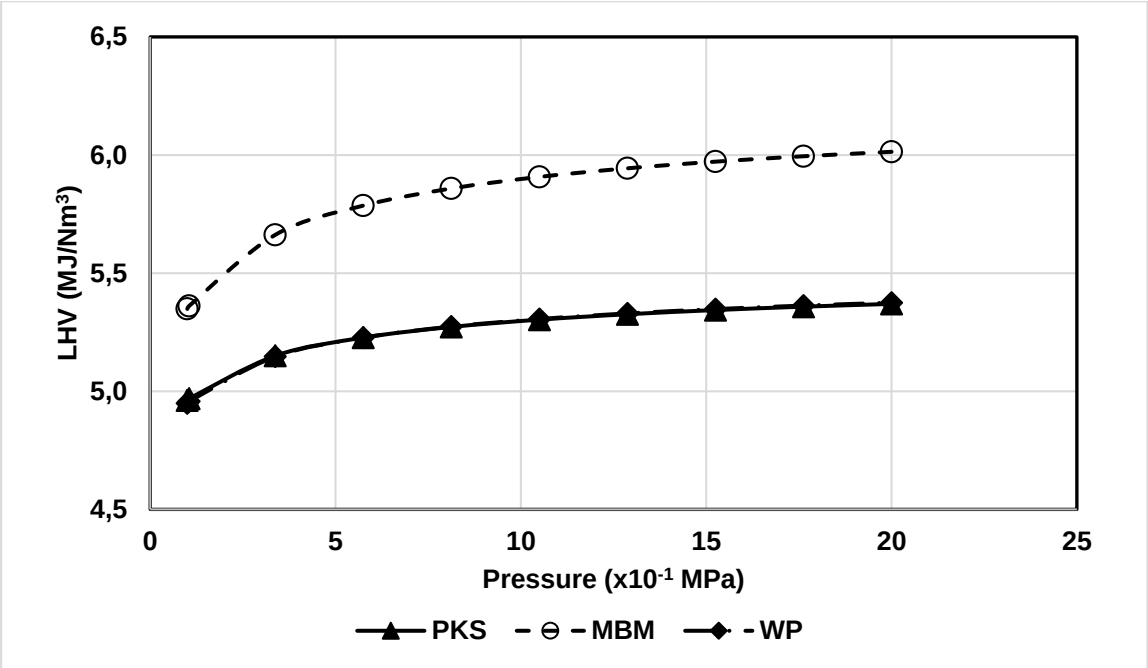

Figure 5-13: The syngas lower heating value as a function of gasifier pressure for PKS, MBM and WP gasification using air at ER = 0.3 and T = 800 °C.

The model predicted the syngas LHV between 4.5 and 6.5 MJ/Nm^3 has been reported for other air gasification studies (Basu, 2010, Brown, 2011). The H/C ratio is reason why the syngas lower heating value of MBM was higher while WP and PKS had relative equal syngas LHV. The higher syngas lower heating value is desirable since it indicates a high amount of syngas produced per low quantity of feedstock used. When gasifier pressure was varied between 0.1 and 2 MPa, the syngas LHV ranged from 5.35 to 6.01 MJ/Nm^3 of MBM, and 4.95 to 5.37 MJ/Nm^3 of WP and PKS was produced.

5.4.3 Influence of gasifier pressure on cold gas efficiency for PKS, MBM and WP gasification.

Figure 5-14 shows the effect of gasifier pressure on cold gas efficiency for PKS, MBM and WP gasification. An increase in gasifier pressure improves the cold gas efficiency of MBM by 2 %, while the other feedstock decreases slightly.

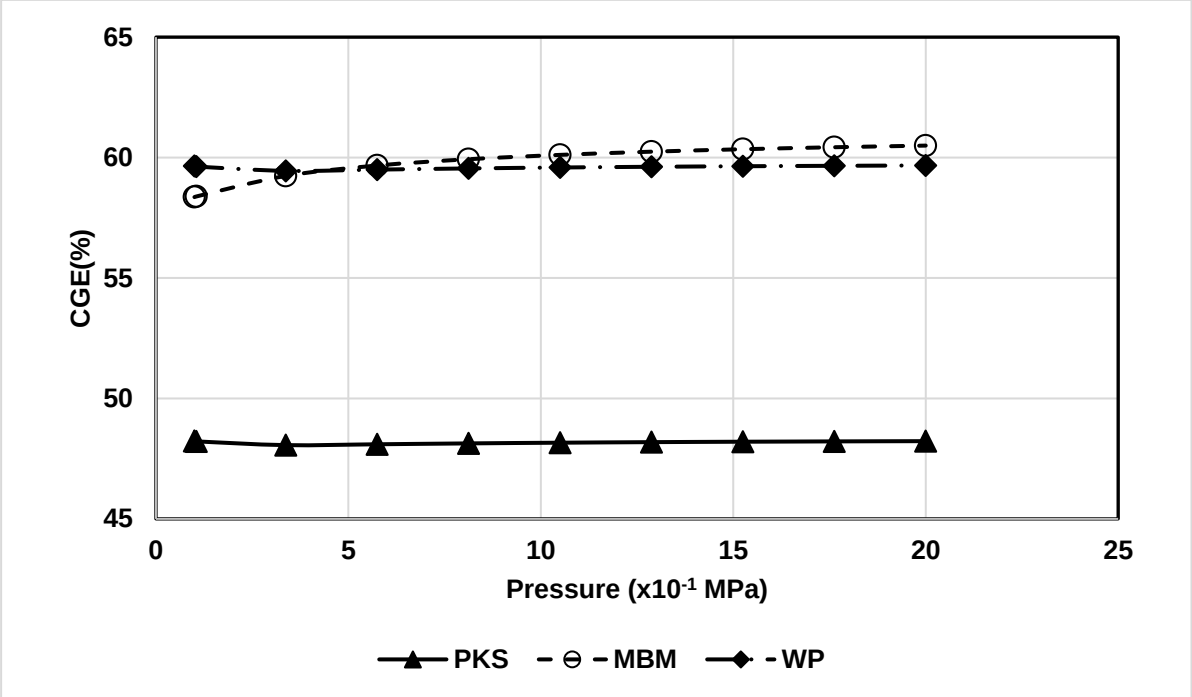

Figure 5-14: Cold gas efficiency as a function of gasifier pressure for PKS, MBM and WP gasification using air at ER = 0.3 and T = 800 °C.

The cold gas efficiency for MBM was higher when pressure was above 0.6 MPa. The cold gas efficiency was relatively constant since the variation of syngas lower heating value was minimal. Other scholars (De Andres et al., 2011, Rodrigues et al., 2017) have reported a cold gas efficiency ranges from 40 to 70 % in atmospheric pressure gasification systems. There is little variation in cold gas efficiency when the gasifier pressure is increased. For cost implications, the atmospheric conditions are favourable other than using compression which is high intensive cost application (Brown, 2011).

5.4.4 Influence of gasifier pressure on carbon conversion efficiency for PKS, MBM and WP gasification.

Carbon conversion efficiency as a function of gasifier pressure for the three feedstock is depicted in Figure 5-15. Carbon conversion is determined by dividing the amount of carbon converted to useful syngas by the carbon accessible from the feedstock. Carbon conversion efficiency increased for MBM and WP as gasifier pressure increased, while CCE decreased for PKS.

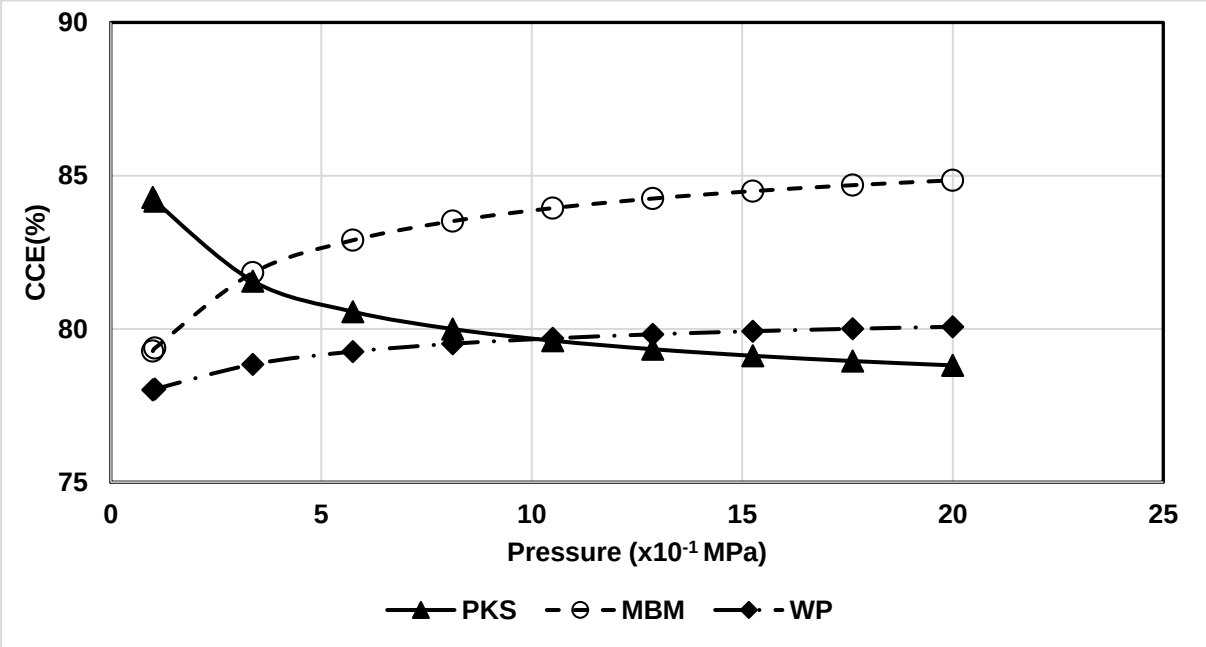

Figure 5-15: Carbon conversion efficiency as a function of gasifier pressure for PKS, MBM and WP gasification using air at ER = 0.3 and T = 800 °C.

An increase in CCE can be explained by the presence of char in the gasifier that is converted to syngas components such as CO, CO_2 and CH_4. Gasification of MBM produced high CCE due to the high relative ratio between fixed carbon and ash content compared to other feedstock (Campoy et al., 2014). The char reactivity of MBM is higher, and it is the possible reason for achieving higher CCE. MBM gasification shows higher carbon conversion efficiency, while the lowest occurs at PKS gasification. A decrease in CCE for PKS was not expected, and this can be caused by model limitations, as it does not consider the bed hydrodynamics and reaction kinetics.

CHAPTER 6 : CONCLUSIONS AND RECOMMENDATIONS

In the air-gasification process, three different feedstock were used: palm kernel shell (PKS), meat and bone meal (MBM), and wood pellets (WP). ASPEN Plus was used in the study to simulate gasification in a circulating fluidized bed reactor. Non-stoichiometric refers to an equilibrium model that does not require stoichiometry. To forecast the equilibrium concentrations, the model used Gibbs free energy minimization. It was chosen for its ability to forecast the impact of input conditions on gasifier performance parameters. For this study, the prevailing input conditions were equivalence ratio, gasification temperature, and gasifier pressure.

The non-stoichiometric model was validated against the experimental results from hemlock wood, and it agreed with them. The model was able to predict the gasification performance indicators. When compared to other feedstock, MBM gasification produced a higher syngas yield and a lower heating value. It was due to a lack of oxygen, which kept the gasifier temperature at higher levels. When compared to MBM and PKS, WP gasification produced higher cold gas efficiency and carbon conversion efficiency. The equivalence ratio and gasification temperature influenced the gasification process. However, the pressure reached the chemical equilibrium above atmospheric conditions, which had no significant effect on the process.

An increase in gasification temperature improved hydrogen (H_2) and carbon dioxide concentration while decreasing carbon monoxide (CO) and methane (CH_4) concentration. Le Chateliar's principle can be used to explain the rate of formation of the syngas composition. The combustible gases decreased with an increase in temperature as a result the syngas lower heating value also decreased. Syngas yield, cold gas efficiency and carbon conversion efficiency increases with an increase in gasification temperature. High temperature was favorable for high syngas yield; however, a proper temperature control is required to avoid ash agglomeration due to the presence of inorganic matter. Syngas lower heating value was higher at 600°C, however these temperature is not suitable for gasification process as more char was unreacted. The char content produced at temperature above 850°C, was less than 30 g/Nm^3 which can be used for various applications. The H_2/CO was above 1.0, when temperature is increased above 900°C making feedstock suitable for chemical production.

An increase in the equivalence ratio produced low production of combustible gases and they were consumed by oxygen in air. The lower heating value of syngas and cold gas efficiency decreased as the equivalence ratio increased. Conversely, as the equivalence ratio increases, so do the syngas yield and carbon conversion efficiency. However, PKS and WP comprised of higher quantity of fixed carbon does not volatize completely as it leaves residual char contributed to low carbon conversion. An optimal ER is between 0.20 and 0.40 achieved usable syngas lower heating value which is economical. A char

content is low less than 20g/Nm^3 is produced when ER is above 0.30, which can be used in water purification industries.

The feedstock properties determines the production of syngas composition. The following was concluded using the ultimate and proximate analysis. The hydrogen to carbon (H/C) atomic ratio from the feedstock showed to have an influence on production of CH_4 concentration since MBM gasification produced the highest. While the oxygen to carbon (O/C) determines the concentration of CO, and this was predicted to be higher for MBM. A low fixed carbon quantity indicated that high carbon conversion efficiency will be obtained, since less carbon residues would not volatize after the pyrolysis stage. The range of carbon conversion efficiency obtained from this model was between 70 and 85% when equivalence ratio was varied between 0.20 and 0.40. A high ash content of MBM (~19.1 wt.%) relative to other feedstock produced higher syngas yield. MBM gasification produced a high content of ash which can be used in cement industries due to their binding agent ability.

Atmospheric pressure conditions (P =101.3 kPa) was preferred over a pressurized gasifier in terms of syngas yield. It can result in reducing unnecessary cost related to high pressurized equipment. An increase in gasifier pressure from 0.1 to 2.0 MPa had no significant cold gas efficiency as it was relative constant for all feedstock. However, a 20% increase was found in syngas lower heating value to maximum of 6 MJ/Nm^3 for MBM gasification which may not significant for capital cost required for high pressure systems. CO and CH_4 concentration improved at high pressures except H_2 and CO_2.

The syngas lower heating value predicted by the model were between 3.8 and 8.2 MJ/Nm^3, which can be used for energy production. In addition, the steam produced can be used as supplementary feed to turbines. MBM gasification is the most feasible process to utilize syngas for chemical production since it produces a H_2/CO ratio close to 1.0 atmospheric conditions. The H_2/CO ratio can be improved by adopting the steam-methane reforming for applications to various industries.

The particle size of the feedstock, air pre-heating and fluidizing velocity are parameters that can improve the results of this study which further investigated. Other parameters, include the influence of bed hydrodynamics and reaction kinetics, were not studied, which can further elaborate on the design requirement for the gasifier. It will give a rigorous study on the fluidization medium and consider the residence time distribution inside the reactor. The tar content was not studied, which can be incorporated in furthering this investigation.

REFERENCES

ACEVEDO, J., POSSO, F., DURÁN, J. & ARENAS, E. 2018. Simulation of the gasification process of palm kernel shell using Aspen PLUS. *Journal of Physics: Conference Series.* IOP Publishing.

ADENIYI, A. G., IGHALO, J. O. & AMOSA, M. K. 2019. Modelling and simulation of banana (Musa spp.) waste pyrolysis for bio-oil production. *Biofuels***,** 1-5.

ALAUDDIN, Z. A. B. Z., LAHIJANI, P., MOHAMMADI, M. & MOHAMED, A. R. 2010. Gasification of lignocellulosic biomass in fluidized beds for renewable energy development: A review. *Renewable Sustainable Energy Reviews,* 14**,** 2852-2862.

ALTAFINI, C. R., WANDER, P. R. & BARRETO, R. M. 2003. Prediction of the working parameters of a wood waste gasifier through an equilibrium model. *Energy Conversion Management,* 44**,** 2763-2777.

ASPEN PLUS 2018. Aspen Plus V10 User Guide. Aspen Technology Inc. Bedford, MA, USA.

BAI, D. & KATO, K. 1999. Quantitative estimation of solids holdups at dense and dilute regions of circulating fluidized beds. *Powder Technology,* 101**,** 183-190.

BASU, P. 2010. *Biomass gasification and pyrolysis: practical design and theory*, Academic press.

BASU, P. 2018. *Biomass gasification, pyrolysis and torrefaction: practical design and theory*, Academic Press.

BEHESHTI, S., GHASSEMI, H. & SHAHSAVAN-MARKADEH, R. 2015. Process simulation of biomass gasification in a bubbling fluidized bed reactor. *Energy Conversion Management,* 94**,** 345-352.

BERMUDEZ, J. & FIDALGO, B. 2016. Production of bio-syngas and bio-hydrogen via gasification. *Handbook of Biofuels Production***,** 431-494.

BROWN, R. C. 2011. *Thermochemical processing of biomass: conversion into fuels, chemicals and power*, John Wiley & Sons.

CALIFANO, F., MONGIELLO, C. & FREDA, C. 2017. Combined heat and power production from meat and bone meal via gasification and gas turbine: technical and economic analysis. *Waste Biomass Valorization,* 8**,** 975-986.

CAMPOY, M., GÓMEZ-BAREA, A., OLLERO, P. & NILSSON, S. 2014. Gasification of wastes in a pilot fluidized bed gasifier. *Fuel Processing Technology,* 121**,** 63-69.

CHANG, A. C., CHANG, H.-F., LIN, F.-J., LIN, K.-H. & CHEN, C.-H. 2011. Biomass gasification for hydrogen production. *International Journal of Hydrogen Energy,* 36**,** 14252-14260.

CHANNIWALA, S. & PARIKH, P. 2002. A unified correlation for estimating HHV of solid, liquid and gaseous fuels. *Fuel,* 81**,** 1051-1063.

CHOI, Y. C., LI, X. Y., PARK, T. J., KIM, J. & LEE, J. 2001. Numerical study on the coal gasification characteristics in an entrained flow coal gasifier. *Fuel,* 80**,** 2193-2201.

CORELLA, J. & SANZ, A. 2005. Modeling circulating fluidized bed biomass gasifiers. A pseudo-rigorous model for stationary state. *Fuel Processing Technology,* 86**,** 1021-1053.

DE ANDRES, J. M., NARROS, A. & RODRÍGUEZ, M. E. 2011. Air-steam gasification of sewage sludge in a bubbling bed reactor: Effect of alumina as a primary catalyst. *Fuel Processing Technology,* 92**,** 433-440.

DE ANDRÉS, J. M., VEDRENNE, M., BRAMBILLA, M. & RODRÍGUEZ, E. 2019. Modeling and model performance evaluation of sewage sludge gasification in fluidized-bed gasifiers using Aspen Plus. *Journal of the Air Waste Management Association,* 69**,** 23-33.

DE CARVALHO MIRANDA, J. C., PONCE, G. H. S. F., ARELLANO-GARCIA, H., MACIEL FILHO, R. & MACIEL, M. R. W. 2020. Process design and evaluation of syngas-to-ethanol conversion plants. *Journal of Cleaner Production,* 269**,** 122078.

DEPARTMENT OF ENVIRONMENTAL AFFAIRS 2018. South Africa State of Waste. A report on the state of the environment.

DOHERTY, W., REYNOLDS, A. & KENNEDY, D. 2008. Simulation of a circulating fluidised bed biomass gasifier using ASPEN Plus: a performance analysis.

DOHERTY, W., REYNOLDS, A. & KENNEDY, D. 2009. The effect of air preheating in a biomass CFB gasifier using ASPEN Plus simulation. *Biomass and Bioenergy,* 33**,** 1158-1167.

ERAKHRUMEN, A. A. 2012. Biomass gasification: Documented information for adoption/adaptation and further improvements toward sustainable utilisation of renewable natural resources. *International Scholarly Research Notices,* 2012.

ESFAHANI, R. M., WAN AB KARIM GHANI, W. A., MOHD SALLEH, M. A. & ALI, S. 2012. Hydrogen-rich gas production from palm kernel shell by applying air gasification in fluidized bed reactor. *Energy Fuels,* 26**,** 1185-1191.

FOGLER, H. S. 2010. *Essentials of Chemical Reaction Engineering: Essenti Chemica Reactio Engi,* Pearson Education.

GÓMEZ-BAREA, A. & LECKNER, B. 2010. Modeling of biomass gasification in fluidized bed. *Progress in Energy Combustion Science,* 36**,** 444-509.

GONZÁLEZ-VÁZQUEZ, M. D. P., GARCÍA, R., GIL, M., PEVIDA, C. & RUBIERA, F. 2018. Comparison of the gasification performance of multiple biomass types in a bubbling fluidized bed. *Energy Conversion Management,* 176**,** 309-323.

GU, H., TANG, Y., YAO, J. & CHEN, F. 2019. Study on biomass gasification under various operating conditions. *Journal of the Energy Institute,* 92**,** 1329-1336.

HANNULA, I. 2009. Hydrogen production via thermal gasification of biomass in near-to-medium term. *Espoo: VTT Working papers.* Finland: VTT Technical Research Centre of Finland.

HERNÁNDEZ, S., FARKHONDEHFAL, M. A., SASTRE, F., MAKKEE, M., SARACCO, G. & RUSSO, N. 2017. Syngas production from electrochemical reduction of CO2: current status and prospective implementation. *Green Chemistry,* 19**,** 2326-2346.

HIGMAN, C. & VAN DER BURGT, M. 2008. Gasification processes. *Gasification.* Gulf Professional Publishing Burlington.

HUSSAIN, M., TUFA, L. D., YUSUP, S. & ZABIRI, H. 2018. A kinetic-based simulation model of palm kernel shell steam gasification in a circulating fluidized bed using Aspen Plus®: A case study. *Biofuels,* 9**,** 635-646.

INAYAT, A., AHMAD, M. M., YUSUP, S. & MUTALIB, M. I. A. 2010. Biomass steam gasification with in-situ CO2 capture for enriched hydrogen gas production: a reaction kinetics modelling approach. *Energies,* 3**,** 1472-1484.

JAHROMI, R., REZAEI, M., SAMADI, S. H. & JAHROMI, H. 2021. Biomass gasification in a downdraft fixed-bed gasifier: Optimization of operating conditions. *Chemical Engineering Science,* 231**,** 116249.

KATAKI, R., CHUTIA, R. S., MISHRA, M., BORDOLOI, N., SAIKIA, R. & BHASKAR, T. 2015. Feedstock suitability for thermochemical processes. *Recent Advances in Thermo-Chemical Conversion of Biomass.* Elsevier.

KIRKELS, A. F. & VERBONG, G. P. 2011. Biomass gasification: Still promising? A 30-year global overview. *Renewable Sustainable Energy Reviews,* 15**,** 471-481.

LA VILLETTA, M., COSTA, M. & MASSAROTTI, N. 2017. Modelling approaches to biomass gasification: A review with emphasis on the stoichiometric method. *Renewable Sustainable Energy Reviews,* 74**,** 71-88.

LEI, H. & HORIO, M. 1998. A comprehensive pressure balance model of circulating fluidized beds. *Journal of Chemical Engineering of Japan,* 31**,** 83-94.

LI, X., GRACE, J., LIM, C., WATKINSON, A., CHEN, H. & KIM, J. 2004. Biomass gasification in a circulating fluidized bed. *Biomass and Bioenergy,* 26**,** 171-193.

LI, X., GRACE, J., WATKINSON, A., LIM, C. & ERGÜDENLER, A. 2001. Equilibrium modeling of gasification: a free energy minimization approach and its application to a circulating fluidized bed coal gasifier. *Fuel,* 80**,** 195-207.

LIAN, Z., WANG, Y., ZHANG, X., YUSUF, A., FAMIYEH, L., MURINDABABISHA, D., JIN, H., LIU, Y., HE, J. & WANG, Y. 2021. Hydrogen Production by Fluidized Bed Reactors: A Quantitative Perspective Using the Supervised Machine Learning Approach. *Multidisciplinary Scientific Journal,* 4**,** 266-287.

LÜCKING, L. 2017. *Methanol Production from Syngas: Process modelling and design utilising biomass gasification and integrating hydrogen supply*. Master's Thesis Masters, Delft University of Technology.

LV, P., XIONG, Z., CHANG, J., WU, C., CHEN, Y. & ZHU, J. 2004. An experimental study on biomass air–steam gasification in a fluidized bed. *Bioresource technology,* 95**,** 95-101.

LV, P., YUAN, Z., MA, L., WU, C., CHEN, Y. & ZHU, J. 2007. Hydrogen-rich gas production from biomass air and oxygen/steam gasification in a downdraft gasifier. *Renewable Energy,* 32**,** 2173-2185.

MANSARAY, K., GHALY, A., AL-TAWEEL, A., HAMDULLAHPUR, F. & UGURSAL, V. 1999. Air gasification of rice husk in a dual distributor type fluidized bed gasifier. *Biomass Bioenergy,* 17**,** 315-332.

MARCANTONIO, V., DE FALCO, M., CAPOCELLI, M., BOCCI, E., COLANTONI, A. & VILLARINI, M. 2019. Process analysis of hydrogen production from biomass gasification in fluidized bed reactor with different separation systems. *International journal of hydrogen energy,* 44**,** 10350-10360.

MAVUKWANA, A., JALAMA, K., NTULI, F. & HARDING, K. Simulation of sugarcane bagasse gasification using aspen plus. International Conference on Chemical and Environmental Engineering (ICCEE), Johannesburg, South Africa, 2013. 70-74.

MAYERHOFER, M., MITSAKIS, P., MENG, X., DE JONG, W., SPLIETHOFF, H. & GADERER, M. 2012. Influence of pressure, temperature and steam on tar and gas in allothermal fluidized bed gasification. *Fuel,* 99**,** 204-209.

MCKENDRY, P. 2002. Energy production from biomass (part 3): gasification technologies. *Bioresource technology,* 83**,** 55-63.

MEEHAN, P. M. 2009. *Investigations into the fate and behavior of selected inorganic compounds during biomass gasification*, Iowa State University.

MOHAMMED, M., SALMIATON, A., AZLINA, W. W., AMRAN, M. M. & FAKHRU'L-RAZI, A. 2011. Air gasification of empty fruit bunch for hydrogen-rich gas production in a fluidized-bed reactor. *Energy Conversion Management,* 52**,** 1555-1561.

NAM, H., WANG, S., SANJEEV, K., SEO, M. W., ADHIKARI, S., SHAKYA, R., LEE, D. & SHANMUGAM, S. R. 2020. Enriched hydrogen production over air and air-steam fluidized bed gasification in a bubbling fluidized bed reactor with CaO: Effects of biomass and bed material catalyst. *Energy Conversion Management,* 225**,** 113408.

NAVEED, S., MALIK, A., RAMZAN, N. & AKRAM, M. 2009. A COMPARATIVE STUDY OF GASIFICATION OF FOOD WASTE (FW), POULTRY WASTE (PW), MUNICIPAL SOLID WASTE (MSW) AND USED TIRES (UT). *Nucleus,* 46**,** 77-81.

NIKOO, M. B. & MAHINPEY, N. 2008. Simulation of biomass gasification in fluidized bed reactor using ASPEN PLUS. *Biomass Bioenergy,* 32**,** 1245-1254.

PENG, B., FARAHANI, M. R. & GAO, W. 2017. Aspen Plus simulation of steam-gasification of different crude oils: A detailed comparison. *Petroleum Science Technology,* 35**,** 332-337.

PÉREZ-FORTES, M., BOJARSKI, A., FERRER-NADAL, S., KOPANOS, G. M., NOUGUÉS, J. M., VELO, E. & PUIGJANER, L. 2008. Enhanced modeling and integrated simulation of gasification and purification gas units targeted to clean power production. *Computer aided chemical engineering.* Elsevier.

PFEIFER, C., KOPPATZ, S. & HOFBAUER, H. 2011. Steam gasification of various feedstocks at a dual fluidised bed gasifier: Impacts of operation conditions and bed materials. *Biomass Conversion Biorefinery,* 1**,** 39-53.

PRADANA, Y. S. & BUDIMAN, A. 2015. Bio-syngas derived from Indonesian oil palm empty fruit bunch (EFB) using middle-scale gasification. *Journal of Engineering Science Technology,* 10**,** 1-8.

PRINS, M. J., PTASINSKI, K. J. & JANSSEN, F. J. 2007. From coal to biomass gasification: Comparison of thermodynamic efficiency. *Energy,* 32**,** 1248-1259.

PUIG-ARNAVAT, M., BRUNO, J. C. & CORONAS, A. 2010. Review and analysis of biomass gasification models. *Renewable sustainable energy reviews,* 14**,** 2841-2851.

RAGLAND, K., AERTS, D. & BAKER, A. 1991. Properties of wood for combustion analysis. *Bioresource technology,* 37**,** 161-168.

REZAIYAN, J. & CHEREMISINOFF, N. P. 2005. *Gasification technologies: a primer for engineers and scientists,* CRC press.

ROBINSON, T., BRONSON, B., GOGOLEK, P. & MEHRANI, P. 2016. Comparison of the air-blown bubbling fluidized bed gasification of wood and wood–PET pellets. *Fuel,* 178**,** 263-271.

RODRIGUES, S., ALMEIDA, A., RIBEIRO, A., NETO, P., RAMALHO, E. & PILÃO, R. 2017. Influence of temperature on the gasification of cork wastes. *Energy Procedia,* 136**,** 127-132.

RUIZ, J. A., JUÁREZ, M., MORALES, M., MUÑOZ, P. & MENDÍVIL, M. 2013. Biomass gasification for electricity generation: Review of current technology barriers. *Renewable Sustainable Energy Reviews,* 18**,** 174-183.

RUPESH, S., MURALEEDHARAN, C. & ARUN, P. 2016. ASPEN plus modelling of air–steam gasification of biomass with sorbent enabled CO2 capture. *Resource-efficient technologies,* 2**,** 94-103.

SEO, Y.-C., ALAM, M. T. & YANG, W.-S. 2018. Gasification of municipal solid waste. *Gasif. Low-Grade Feedstock.*

SHAHBAZ, M., YUSUP, S., INAYAT, A., AMMAR, M., PATRICK, D. O., PRATAMA, A. & NAQVI, S. R. 2017. Syngas production from steam gasification of palm kernel shell with subsequent CO2 capture using CaO sorbent: an aspen plus modeling. *Energy Fuels,* 31**,** 12350-12357.

SIKARWAR, V. S., ZHAO, M., CLOUGH, P., YAO, J., ZHONG, X., MEMON, M. Z., SHAH, N., ANTHONY, E. J. & FENNELL, P. S. 2016. An overview of advances in biomass gasification. *Energy & Environmental Science,* 9**,** 2939-2977.

SKOULOU, V., SWIDERSKI, A., YANG, W. & ZABANIOTOU, A. 2009. Process characteristics and products of olive kernel high temperature steam gasification (HTSG). *Bioresource technology,* 100**,** 2444-2451.

SKOULOU, V., ZABANIOTOU, A., STAVROPOULOS, G. & SAKELAROPOULOS, G. 2008. Syngas production from olive tree cuttings and olive kernels in a downdraft fixed-bed gasifier. *International journal of hydrogen energy,* 33**,** 1185-1194.

SONI, C. G., WANG, Z., DALAI, A. K., PUGSLEY, T. & FONSTAD, T. Syngas/Hydrogen Production Via Gasification of Meat and Bone Meal. The 2008 Spring National Meeting, 2008.

SREEJITH, C., MURALEEDHARAN, C. & ARUN, P. 2014. Performance prediction of steam gasification of wood using an ASPEN PLUS thermodynamic equilibrium model. *International journal of sustainable energy,* 33**,** 416-434.

THE PEEPAL LEAF. 2019. *Activated carbon* [Online]. Available: https://www.the-peepal-leaf.com/products/activated-carbon/ [Accessed 12/05 2021].

TINAUT, F. V., MELGAR, A., PEREZ, J. F. & HORRILLO, A. 2008. Effect of biomass particle size and air superficial velocity on the gasification process in a downdraft fixed bed gasifier. An experimental and modelling study. *Fuel processing technology,* 89**,** 1076-1089.

VAN DER DRIFT, A., VAN DOORN, J. & VERMEULEN, J. 2001. Ten residual biomass fuels for circulating fluidized-bed gasification. *Biomass Bioenergy,* 20**,** 45-56.

WAN AB KARIM GHANI, W., MOGHADAM, R. A., SALLEH, M. & ALIAS, A. 2009. Air gasification of agricultural waste in a fluidized bed gasifier: hydrogen production performance. *Energies,* 2**,** 258-268.

WANG, L., WELLER, C. L., JONES, D. D. & HANNA, M. A. J. 2008. Contemporary issues in thermal gasification of biomass and its application to electricity and fuel production. *Biomass Bioenergy,* 32**,** 573-581.

WORLEY, M. & YALE, J. 2012. Biomass gasification technology assessment. *Harris Group Inc, National Renewable Energy Laboratory, Atlanta.*

XIAO, G., NI, M.-J., CHI, Y., JIN, B.-S., XIAO, R., ZHONG, Z.-P. & HUANG, Y.-J. 2009. Gasification characteristics of MSW and an ANN prediction model. *Waste Management,* 29**,** 240-244.

YANG, X., HAMIDZADEH, A., ILKHANI, M., FOROUGHI, A., ESFAHANI, M. J. & MOTAHARI-NEZHAD, M. 2016. Aspen plus simulation of heavy oil gasification in a fluidized bed gasifier. *Petroleum Science Technology,* 34**,** 1530-1533.

YAO, X., ZHAO, Z., CHEN, S., ZHOU, H. & XU, K. 2020. Migration and transformation behaviours of ash residues from a typical fixed-bed gasification station for biomass syngas production in China. *Energy,* 201**,** 117646.

ZHANG, J. & ZHANG, X. 2019. The thermochemical conversion of biomass into biofuels. *Biomass, Biopolymer-Based Materials, and Bioenergy.* Elsevier.

APPENDICES

APPENDIX A : Calculator blocks

ASPEN Plus calculator blocks and FORTRAN code

ULTANAL and PROXANAL represent the non-conventional components in ASPEN Plus, which stands for ultimate and proximate analysis. The component attributes in the proximate analysis are defined by elements, where the first one is WATER. It represents the moisture content value of the feedstock FDSTOCK stream. The variable name ULT is a vector used for assessing the ultimate analysis of the feedstock.

Table A-1: The definition of feedstock moisture content and ultimate analysis used in BRKDWN calculator block.

Variable Name	Type	Stream	Substream	Component	Attribute	Elements
WATER	Compattr-Vec	BIOMASS	NC	FDSTOCK	PROXANAL	1
ULT	Compattr-Vec	BIOMASS	NC	FDSTOCK	ULTANAL	

Using mass-yield estimation, the DECOMP block decomposed the ultimate and proximate analysis to different components listed as ID1, where ID2 represents the component classification based on different phases.

Table A-2: The definition of variables for pyrolysis of feedstock in DECOMP reactor block using BRKDWN calculator block.

Variable Name	Type	Block	Variable	ID1	ID2
WATER	Block-Var	DECOMP	MASS-YIELD	H2O	MIXED
ASH	Block-Var	DECOMP	MASS-YIELD	ASH	NC
CARB	Block-Var	DECOMP	MASS-YIELD	C	CISOLID
N2	Block-Var	DECOMP	MASS-YIELD	N2	MIXED
H2	Block-Var	DECOMP	MASS-YIELD	H2	MIXED
O2	Block-Var	DECOMP	MASS-YIELD	O2	MIXED
SULF	Block-Var	DECOMP	MASS-YIELD	S	MIXED
CL2	Block-Var	DECOMP	MASS-YIELD	CL2	MIXED

The feedstock needs to be computed on a wet basis; hence, the FACT converts the ultimate analysis to a wet base. The BRKDWN calculator block was calculated before the DECOMP block.

FORTRAN code for BRKDWN calculator block

```
FACT = (100 – WATER)/100

H2O = WATER / 100

ASH = ULT(1) / 100 * FACT

CARB = ULT(2) / 100 * FACT

H2 = ULT(3) / 100 * FACT

N2 = ULT(4) / 100 * FACT

CL2 = ULT(5) / 100 * FACT

SULF = ULT(6) / 100 * FACT

O2 = ULT(7) / 100 * FACT
```

APPENDIX B : Sample calculations

Equivalence ratio calculation

Ultimate analysis of the palm kernel shell on a moisture-ash-free basis:

$C = 51.63\, wt.\%$ $H = 5.52\, wt.\%$ $S = 0.5\, wt.\%$ $N = 1.89\, wt.\%$ and

$O = 40.91\, wt.\%$; $Ash = 8.97\, wt.\%$

$Molecular\ weights\ (MW): C = 12, H = 1, S = 32, N = 14\ and\ O = 16$

$Air\ flowrates = 55.74\, kg/h\ (O_2 = 23.3\, wt.\%\ and\ N_2 = 77.7\, wt.\%)$

$M_{fuel} = 33.626\, kg/h$

$Mass\ feed\ rate\ of\ oxygen = 0.233 \times 55.74 = 12.99\, kg/h$

The molar feed rate of oxygen and carbon is determined using the procedure below:

To calculate the number of moles of substances, use the formula below:

$$n_C = \frac{m}{MW} = \frac{0.6163 \times 33.626}{12} = 1.45\, kmol/hr$$

$$n_O = \frac{0.4091 \times 33.626}{16 \times 2} = 0.406\, kmol/hr$$

$$O/C\ \ molar\ ratio = \frac{0.406}{1.456} = 0.28$$

To determine the stoichiometric oxygen required, the oxygen required to oxidize carbon to carbon dioxide, hydrogen to water, and sulphur to sulphur dioxide has to be computed.

12 g of carbon reacts with 32 g of oxygen (1 mole) to produce 44 g of carbon dioxide (1 mole)

$$C + O_2 \leftrightarrow CO_2$$

32 g of sulfur reacts with 32 g of oxygen (1 mole) to produce 64 g of sulfur dioxide (1 mole)

$$S + O_2 \leftrightarrow SO_2$$

4 g of hydrogen reacts with 32 g of oxygen (1 mole) to produce 36 g of water (2 mole)

$$2H_2 + O_2 \leftrightarrow 2H_2O$$

Stoichiometric oxygen required for the above reactions:

$$Stoich.O_2 = \frac{32}{12} \times C + \frac{36}{4} \times H + \frac{32}{32} \times - O$$

$$Stoich.O_2 = \frac{32}{12} \times 0.5163 + \frac{36}{4} \times 0.0552 + \frac{32}{32} \times 0.005 - 0.4091 = 1.41\ kg\ O2\ per\ kg\ of\ fuel$$

$$Total\ O_2\ required = 33.626 \times (1 - 0.0897) \times 1.41 = 43.29\ kg\ O_2\ /hr$$

$$mass\ of\ O_2\ supplied = n_{O_2} \times MW = 0.406 \times 32 = 12.99\ kg\ O_2\ /hr$$

$Calculation\ of\ equivalence\ ratio$

$$ER = \frac{Stoichiometric\ O_2\ required}{Actual\ O_2\ supplied} = \frac{12.99}{43.29} = 0.3$$

The product gas composition on dry basis of PKS gasification at ER= 0.3, gasifier pressure of 1.05 bar and gasification temperature of 850°C.

$$N_2 = 50.77\ vol.\%\ ;\ H_2 = 15.02\ vol.\%\ ; CO = 19.35\ vol.\%\ ;\ CO_2 = 12.60\ vol.\%$$

$$and\ \ CH_4 = 2.26\ vol.\%\ \ \frac{H_2}{CO}\ ratio = \frac{15.02}{19.35} = 0.78$$

$$Q_{syngas} = 68.18\ Nm^3/hr\ dry\ N_2\ free\ basis$$

Calculation of the syngas yield

$$GY = \frac{Q_{syngas}(1 - y_{N_2})}{M_{fuel} \times (1 - MC - w_{Ash})}$$

$$GY = \frac{68.18 \times (1 - 0.5077)}{33.616 \times (1 - 0.0796 - 0.0897)}$$

$$GY = 1.20 \frac{Nm^3}{kg}\ dry\ N_2\ /daf\ basis$$

Calculation of the syngas lower heating value

$$LHV_{gas} = 10.78\ y_{H_2} + 12.63\ y_{CO} + 35.88\ y_{CH_4}$$

$LHV_{gas} = 10.78 \times 0.1502 + 12.63 \times 0.1935 + 35.88 \times 0.0226$

$LHV_{gas} = 4.87\ MJ/Nm^3$

Calculation of cold gas efficiency

$$\eta_{CGE}\ (\%) = \frac{M_{gas} \times LHV_{gas}}{M_{fuel} \times LHV_{fuel}} \times 100$$

$$\eta_{CGE}\ (\%) = \frac{68.18 \times 4.87}{33.626 \times 21.845 \times (1 - 0.0796)} \times 100$$

$\eta_{CGE}\ (\%) = 49.16\%$

Calculation of carbon conversion efficiency

$M_{CO} = 16.495\ kg/h$; $M_{CO_2} = 16.8776\ kg/h\ and\ M_{CH_4} = 1.1048\ kg/h$

$$\eta_{CCE}(\%) = \frac{Q_{syngas} \times \sum_{j=1}^{n} x_{j,c}}{M_{fuel} \times y_c} \times 100 = \frac{Amount\ of\ C\ in\ syngas}{Amount\ of\ C\ in\ fuel} \times 100$$

$$\eta_{CCE}(\%) = \frac{(\frac{12}{28} \times 16.495 + \frac{12}{44} \times 16.8776 + \frac{12}{16} \times 1.1048\ )}{33.626 \times 0.5163 \times (1 - 0.0897)} \times 100$$

$\eta_{CCE} = 79.10\ \%$

APPENDIX C : Supplementary information

Table C- 1: Mass and energy balances over the simulation of gasification of palm kernel shell.

Stream Name	Units	BIOMASS	ELEM	CCONV	VOLAT	OXIDANT	GASF1OUT	GASF2OUT	RAWGAS	SYNGAS	RESIDUES	ASHPROD
Stream Class		MIXCINC	MIXCINC	MIXCINC	MIXCINC	MIXCINC	MIXCINC	MIXCINC	MIXCINC	MIXCINC	MIXCINC	MIXCINC
Total Stream												
Temperature	C	25.00	550.00	550.00	550.00	450.00	1340.88	800.00	798.99	798.99	798.99	1250.33
Pressure	bar	1.05	1.05	1.00	1.00	1.05	1.05	1.05	1.05	1.05	1.05	1.05
Mass Vapor Fraction		0.00	0.49	0.00	0.50	1.00	0.93	0.87	0.98	0.97	1.00	0.00
Mass Solid Fraction		1.00	0.51	1.00	0.50	0.00	0.07	0.13	0.02	0.03	0.00	1.00
Mass Enthalpy	kJ/kg	-995.30	-135.42	746.93	-155.09	442.96	57.56	-2066.81	-2486.16	-1662.70	-11777.73	767.54
Mass Density	kg/m^3	1361.44	0.39	2250.02	0.37	0.50	0.19	0.34	0.31	0.32	0.21	3337.73
Enthalpy Flow	MJ/hr	-33.48	-4.54	0.54	-5.11	24.696	5.616	-200.736	-215.28	-132.264	-76.098	2.124
Mass Flows	kg/hr	**33.63**	**33.63**	**0.73**	**32.89**	**55.74**	**99.68**	**97.13**	**86.59**	**79.54**	**7.05**	**2.77**
FDSTOCK	kg/hr	33.63	0.00	0.00	0.00	0.00	0.00	0.00	0.00	0.00	0.00	0.00
ASH	kg/hr	0.00	2.55	0.00	2.55	0.00	2.55	0.00	0.00	0.00	0.00	2.55
C	kg/hr	0.00	14.66	0.73	13.93	0.00	4.73	12.53	1.99	1.99	0.00	0.23
H2	kg/hr	0.00	1.57	0.00	1.57	0.00	1.86	0.70	0.70	0.70	0.00	0.00
O2	kg/hr	0.00	11.62	0.00	11.62	12.98	0.00	0.00	0.00	0.00	0.00	0.00
N2	kg/hr	0.00	0.54	0.00	0.54	42.76	43.29	43.29	43.29	43.29	0.00	0.00
H2O	kg/hr	0.00	2.68	0.00	2.68	0.00	0.01	7.03	7.03	0.00	7.03	0.00
CO	kg/hr	0.00	0.00	0.00	0.00	0.00	47.21	16.49	16.49	16.49	0.00	0.00
CO2	kg/hr	0.00	0.00	0.00	0.00	0.00	0.01	15.56	15.56	15.56	0.00	0.00
CH4	kg/hr	0.00	0.00	0.00	0.00	0.00	0.00	1.51	1.51	1.51	0.00	0.00
S	kg/hr	0.00	0.01	0.00	0.01	0.00	0.00	0.00	0.00	0.00	0.00	0.00
H2S	kg/hr	0.00	0.00	0.00	0.00	0.00	0.02	0.02	0.02	0.00	0.02	0.00
CL2	kg/hr	0.00	0.00	0.00	0.00	0.00	0.00	0.00	0.00	0.00	0.00	0.00
HCL	kg/hr	0.00	0.00	0.00	0.00	0.00	0.00	0.00	0.00	0.00	0.00	0.00
NH3	kg/hr	0.00	0.00	0.00	0.00	0.00	0.00	0.01	0.01	0.00	0.01	0.00
Volume Flow	Nm^3/hr	0.02	85.35	0.00	89.61	110.67	531.40	282.19	281.92	248.73	33.18	0.00
Mole Flow	kmol/hr	0.00	1.31		1.31	1.93	4.16	3.32	3.32	2.93	0.39	0.00

Table C- 2: Mass and energy balances over the simulation of gasification of meat and bone meal.

	Units	BIOMASS	ELEM	CCONV	VOLAT	OXIDANT	GASF1OUT	GASF2OUT	RAWGAS	SYNGAS	RESIDUES	ASHPROD
Stream Class		MIXCINC	MIXCINC	MIXCINC	MIXCINC	MIXCINC	MIXCINC	MIXCINC	MIXCINC	MIXCINC	MIXCINC	MIXCINC
Total Stream												
Temperature	C	25.00	550.00	550.00	550.00	450.00	953.49	800.00	799.11	799.11	799.11	937.01
Pressure	bar	1.05	1.05	1.00	1.00	1.05	1.05	1.05	1.05	1.05	1.05	1.05
Mass Vapor Fraction		0.00	0.42	0.00	0.43	1.00	0.87	0.86	0.97	0.97	1.00	0.00
Mass Solid Fraction		1.00	0.58	1.00	0.57	0.00	0.13	0.14	0.03	0.03	0.00	1.00
Mass Enthalpy	MJ/kg	-2.05	0.09	0.75	0.08	0.44	-0.22	-1.52	-1.91	-1.06	-11.45	0.22
Mass Density	kg/cum	1298.18	0.35	2250.02	0.33	0.50	0.25	0.33	0.29	0.30	0.22	3394.61
Enthalpy Flow	MJ/hr	-68.86	3.04	0.54	2.50	27.90	-24.04	-157.88	-174.87	-88.61	-86.27	1.17
Mass Flows	kg/hr	**33.63**	**33.63**	**0.72**	**32.91**	**62.99**	**108.69**	**103.67**	**91.33**	**83.79**	**7.53**	**5.28**
FDSTOCK	kg/hr	33.63	0.00	0.00	0.00	0.00	0.00	0.00	0.00	0.00	0.00	0.00
ASH	kg/hr	0.00	5.02	0.00	5.02	0.00	5.02	0.00	0.00	0.00	0.00	5.02
C	kg/hr	0.00	14.38	0.72	13.66	0.00	8.61	14.65	2.30	2.30	0.00	0.26
H2	kg/hr	0.00	2.05	0.00	2.05	0.00	2.27	0.90	0.90	0.90	0.00	0.00
O2	kg/hr	0.00	7.26	0.00	7.26	14.67	0.00	0.00	0.00	0.00	0.00	0.00
N2	kg/hr	0.00	2.39	0.00	2.39	48.32	50.71	50.70	50.70	50.70	0.00	0.00
H2O	kg/hr	0.00	2.32	0.00	2.32	0.00	0.16	7.31	7.31	0.00	7.31	0.00
CO	kg/hr	0.00	0.00	0.00	0.00	0.00	41.32	16.49	16.49	16.49	0.00	0.00
CO2	kg/hr	0.00	0.00	0.00	0.00	0.00	0.34	11.11	11.11	11.11	0.00	0.00
CH4	kg/hr	0.00	0.00	0.00	0.00	0.00	0.05	2.28	2.28	2.28	0.00	0.00
S	kg/hr	0.00	0.21	0.00	0.21	0.00	0.00	0.00	0.00	0.00	0.00	0.00
H2S	kg/hr	0.00	0.00	0.00	0.00	0.00	0.22	0.22	0.22	0.00	0.22	0.00
CL2	kg/hr	0.00	0.00	0.00	0.00	0.00	0.00	0.00	0.00	0.00	0.00	0.00
HCL	kg/hr	0.00	0.00	0.00	0.00	0.00	0.00	0.00	0.00	0.00	0.00	0.00
NH3	kg/hr	0.00	0.00	0.00	0.00	0.00	0.00	0.01	0.01	0.00	0.01	0.00
Volume Flow	Nm^3/hr	0.03	95.49	0.00	100.26	125.06	430.92	310.63	310.36	275.33	35.02	0.00
Mole Flows	kmol/hr	0.00	1.46	0.00	1.46	2.18	4.44	3.65	3.65	3.24	0.41	0.00

Table C- 3 : Mass and energy balances over the simulation of gasification of wood pellets.

Stream Name	Units	BIOMASS	ELEM	CCONV	VOLAT	OXIDANT	GASF1OUT	GASF2OUT	RAWGAS	SYNGAS	RESIDUES	ASHPROD
Stream Class		**MIXCINC**	**MIXCINC**	**MIXCINC**	**MIXCINC**	**MIXCINC**	**MIXCINC**	**MIXCINC**	**MIXCINC**	**MIXCINC**	**MIXCINC**	**MIXCINC**
Total Stream												
Temperature	C	25.00	550.00	550.00	550.00	450.00	742.10	800.00	799.02	799.02	799.02	784.17
Pressure	bar	1.05	1.05	1.00	1.00	1.05	1.05	1.05	1.05	1.05	1.05	1.05
Mass Vapor Fraction		0.00	0.53	0.00	0.54	1.00	0.91	0.86	0.97	0.97	1.00	0.00
Mass Solid Fraction		1.00	0.47	1.00	0.46	0.00	0.09	0.14	0.03	0.03	0.00	1.00
Mass Enthalpy	MJ/kg	-5.47	0.20	0.75	0.18	0.44	-1.35	-2.07	-2.55	-1.69	-11.77	0.70
Mass Density	kg/m^3	1283.44	0.35	2250.02	0.33	0.50	0.31	0.35	0.31	0.32	0.21	2678.59
Enthalpy Flow	MJ/hr	-183.96	6.63	0.58	6.04	25.87	-140.84	-215.96	-233.26	-141.52	-91.74	0.34
Mass Flows	kg/hr	**33.63**	**33.63**	**0.78**	**32.85**	**58.40**	**104.32**	**104.10**	**91.54**	**83.75**	**7.79**	**0.49**
FDSTOCK	kg/hr	33.63	0.00	0.00	0.00	0.00	0.00	0.00	0.00	0.00	0.00	0.00
ASH	kg/hr	0.00	0.22	0.00	0.22	0.00	0.22	0.00	0.00	0.00	0.00	0.22
C	kg/hr	0.00	15.60	0.78	14.82	0.00	9.68	14.92	2.35	2.35	0.00	0.27
H2	kg/hr	0.00	1.82	0.00	1.82	0.00	1.80	0.76	0.76	0.76	0.00	0.00
O2	kg/hr	0.00	13.22	0.00	13.22	13.60	0.00	0.00	0.00	0.00	0.00	0.00
N2	kg/hr	0.00	0.63	0.00	0.63	44.80	45.42	45.42	45.42	45.42	0.00	0.00
H2O	kg/hr	0.00	2.12	0.00	2.12	0.00	1.75	7.77	7.77	0.00	7.77	0.00
CO	kg/hr	0.00	0.00	0.00	0.00	0.00	36.62	16.49	16.49	16.49	0.00	0.00
CO2	kg/hr	0.00	0.00	0.00	0.00	0.00	8.57	17.04	17.04	17.04	0.00	0.00
CH4	kg/hr	0.00	0.00	0.00	0.00	0.00	0.24	1.68	1.68	1.68	0.00	0.00
S	kg/hr	0.00	0.02	0.00	0.02	0.00	0.00	0.00	0.00	0.00	0.00	0.00
H2S	kg/hr	0.00	0.00	0.00	0.00	0.00	0.02	0.02	0.02	0.00	0.02	0.00
CL2	kg/hr	0.00	0.00	0.00	0.00	0.00	0.00	0.00	0.00	0.00	0.00	0.00
HCL	kg/hr	0.00	0.00	0.00	0.00	0.00	0.00	0.00	0.00	0.00	0.00	0.00
NH3	kg/hr	0.00	0.00	0.00	0.00	0.00	0.00	0.01	0.01	0.00	0.01	0.00
Volume Flow	Nm^3/hr	0.03	94.88	0.00	99.62	115.95	331.89	298.46	298.18	261.49	36.68	0.00
Mole Flows	kmol/hr	0.00	1.46	0.00	1.46	2.02	4.13	3.51	3.51	3.08	0.43	0.00

Table C- 4: The syngas composition of PKS, MBM and WP gasification at different equivalence ratios and temperature when pressure was kept at 105kPa.

Temp (°C)	ER	Syngas composition of PKS (vol.%)					Syngas composition of MBM (vol.%)					Syngas composition of WP (vol.%)				
		N_2	H_2	CO	CO_2	CH_4	N_2	H_2	CO	CO_2	CH_4	N_2	H_2	CO	CO_2	CH_4
600	0.15	45.07	2.31	33.94	6.55	12.13	47.59	2.72	29.58	2.11	18.00	45.34	2.37	32.49	7.22	12.59
	0.2	51.60	2.01	29.32	7.81	9.26	54.50	2.40	25.99	3.26	13.85	51.82	2.06	28.04	8.41	9.67
	0.25	56.35	1.76	25.71	8.93	7.25	59.57	2.13	23.04	4.43	10.83	56.54	1.82	24.58	9.46	7.60
	0.3	59.91	1.57	22.83	9.91	5.79	63.34	1.90	20.61	5.55	8.61	60.08	1.62	21.82	10.38	6.10
	0.35	62.63	1.41	20.49	10.76	4.71	66.17	1.70	18.58	6.60	6.95	62.79	1.45	19.58	11.19	4.99
	0.4	64.76	1.27	18.56	11.51	3.90	68.33	1.54	16.87	7.57	5.70	64.91	1.32	17.74	11.89	4.14
	0.45	66.45	1.16	16.95	12.17	3.27	70.00	1.40	15.43	8.44	4.73	66.60	1.20	16.20	12.51	3.49
650	0.15	43.81	4.56	32.99	7.19	11.45	46.56	5.35	28.94	2.48	16.68	44.00	4.68	31.53	7.88	11.90
	0.2	50.22	3.99	28.53	8.44	8.83	53.26	4.73	25.40	3.73	12.88	50.36	4.10	27.25	9.06	9.23
	0.25	54.92	3.52	25.05	9.52	6.98	58.19	4.20	22.51	4.96	10.14	55.05	3.63	23.93	10.07	7.33
	0.3	58.48	3.15	22.28	10.46	5.63	61.88	3.76	20.13	6.10	8.13	58.59	3.25	21.28	10.95	5.94
	0.35	61.23	2.84	20.03	11.27	4.63	64.68	3.39	18.16	7.15	6.62	61.33	2.93	19.13	11.71	4.90
	0.4	63.40	2.58	18.18	11.98	3.86	66.84	3.07	16.51	8.10	5.48	63.50	2.67	17.36	12.37	4.10
	0.45	65.15	2.36	16.62	12.60	3.26	68.55	2.81	15.11	8.95	4.59	65.25	2.45	15.87	12.96	3.48
700	0.15	42.30	7.91	31.85	7.79	10.16	45.19	9.26	28.09	2.86	14.61	42.41	8.12	30.39	8.50	10.58
	0.2	48.57	6.93	27.59	9.03	7.87	51.68	8.18	24.65	4.20	11.29	48.65	7.13	26.32	9.66	8.24
	0.25	53.23	6.15	24.28	10.09	6.26	56.48	7.27	21.85	5.48	8.92	53.28	6.33	23.16	10.65	6.58
	0.3	56.78	5.51	21.64	10.99	5.08	60.10	6.52	19.56	6.65	7.18	56.82	5.69	20.64	11.49	5.36
	0.35	59.56	4.99	19.49	11.77	4.20	62.88	5.89	17.66	7.69	5.88	59.59	5.15	18.59	12.22	4.45
	0.4	61.77	4.55	17.71	12.45	3.52	65.06	5.36	16.07	8.62	4.89	61.81	4.71	16.89	12.85	3.74
	0.45	63.58	4.18	16.22	13.04	2.99	66.80	4.91	14.72	9.45	4.12	63.61	4.33	15.47	13.40	3.19

Temp (°C)	ER	Syngas composition of PKS (vol.%)					Syngas composition of MBM (vol.%)					Syngas composition of WP (vol.%)				
		N_2	H_2	CO	CO_2	CH_4	N_2	H_2	CO	CO_2	CH_4	N_2	H_2	CO	CO_2	CH_4
750	0.15	40.54	12.18	30.53	8.39	8.36	43.51	14.26	27.04	3.27	11.91	40.57	12.51	29.08	9.11	8.72
	0.2	46.68	10.69	26.52	9.62	6.49	49.79	12.57	23.74	4.71	9.19	46.68	11.00	25.26	10.26	6.81
	0.25	51.28	9.50	23.39	10.66	5.18	54.47	11.17	21.07	6.02	7.26	51.26	9.79	22.28	11.22	5.46
	0.3	54.83	8.53	20.89	11.53	4.21	58.04	10.02	18.88	7.20	5.86	54.80	8.81	19.90	12.03	4.46
	0.35	57.63	7.74	18.86	12.28	3.49	60.81	9.06	17.07	8.24	4.81	57.60	8.00	17.97	12.73	3.71
	0.4	59.89	7.07	17.17	12.93	2.94	63.01	8.26	15.56	9.16	4.01	59.86	7.32	16.36	13.33	3.13
	0.45	61.75	6.51	15.75	13.49	2.51	64.78	7.58	14.28	9.97	3.39	61.72	6.74	15.01	13.85	2.68
800	0.15	38.66	16.88	29.11	9.01	6.34	41.66	19.75	25.89	3.74	8.96	38.61	17.35	27.67	9.73	6.64
	0.2	44.66	14.82	25.37	10.22	4.93	47.74	17.36	22.76	5.25	6.89	44.58	15.26	24.12	10.85	5.19
	0.25	49.21	13.18	22.45	11.23	3.94	52.31	15.42	20.23	6.60	5.44	49.11	13.60	21.35	11.79	4.16
	0.3	52.76	11.85	20.11	12.07	3.21	55.83	13.83	18.16	7.78	4.39	52.65	12.25	19.12	12.57	3.40
	0.35	55.59	10.76	18.19	12.79	2.66	58.60	12.52	16.45	8.81	3.61	55.48	11.13	17.31	13.24	2.84
	0.4	57.90	9.85	16.60	13.41	2.25	60.83	11.42	15.02	9.71	3.02	57.79	10.20	15.80	13.81	2.40
	0.45	59.81	9.07	15.26	13.94	1.92	62.65	10.49	13.81	10.50	2.56	59.71	9.41	14.52	14.31	2.05
850	0.15	36.84	21.34	27.74	9.63	4.46	39.83	24.93	24.75	4.26	6.23	36.71	21.95	26.31	10.35	4.69
	0.2	42.71	18.74	24.27	10.81	3.47	45.72	21.86	21.80	5.83	4.79	42.55	19.32	23.03	11.44	3.66
	0.25	47.22	16.69	21.54	11.79	2.77	50.20	19.41	19.42	7.19	3.78	47.04	17.23	20.45	12.34	2.94
	0.3	50.77	15.02	19.35	12.60	2.26	53.69	17.42	17.47	8.37	3.05	50.59	15.54	18.37	13.10	2.41
	0.35	53.63	13.66	17.55	13.28	1.88	56.48	15.77	15.86	9.38	2.51	53.45	14.14	16.67	13.73	2.01
	0.4	55.98	12.51	16.05	13.87	1.59	58.74	14.40	14.50	10.25	2.10	55.81	12.97	15.25	14.28	1.70
	0.45	58.03	11.53	14.80	14.33	1.30	60.60	13.24	13.35	11.01	1.79	57.78	11.97	14.05	14.75	1.45

Table C- 5: The syngas composition of PKS, MBM and WP gasification at different equivalence ratios and temperature when pressure was kept at 105kPa.

Temp (°C)	ER	Syngas composition of PKS (vol.%)					Syngas composition of MBM (vol.%)					Syngas composition of WP (vol.%)				
		N_2	H_2	CO	CO_2	CH_4	N_2	H_2	CO	CO_2	CH_4	N_2	H_2	CO	CO_2	CH_4
900	0.15	35.23	25.06	26.53	10.22	2.96	38.21	29.16	23.75	4.80	4.07	36.71	21.95	26.31	10.35	4.69
	0.2	41.00	22.03	23.29	11.37	2.30	43.95	25.56	20.96	6.40	3.13	42.55	19.32	23.03	11.44	3.66
	0.25	45.47	19.64	20.74	12.31	1.84	48.36	22.70	18.70	7.76	2.47	47.04	17.23	20.45	12.34	2.94
	0.3	49.02	17.71	18.68	13.08	1.50	51.83	20.39	16.86	8.92	2.00	50.59	15.54	18.37	13.10	2.41
	0.35	51.91	16.11	16.99	13.74	1.25	54.62	18.49	15.34	9.91	1.65	53.45	14.14	16.67	13.73	2.01
	0.4	54.31	14.77	15.57	14.29	1.06	56.91	16.90	14.05	10.75	1.38	55.81	12.97	15.25	14.28	1.70
	0.45	56.73	13.52	14.47	14.57	0.71	58.82	15.56	12.96	11.48	1.18	57.78	11.97	14.05	14.75	1.45
950	0.15	33.93	27.88	25.54	10.76	1.89	36.90	32.28	22.93	5.32	2.57	33.67	28.72	24.13	11.48	2.00
	0.2	39.61	24.55	22.50	11.86	1.47	42.51	28.31	20.27	6.93	1.97	39.32	25.34	21.28	12.50	1.56
	0.25	44.05	21.92	20.09	12.76	1.18	46.86	25.17	18.13	8.28	1.56	43.75	22.66	19.01	13.32	1.26
	0.3	47.61	19.78	18.14	13.50	0.97	50.32	22.64	16.37	9.41	1.27	47.30	20.48	17.18	14.00	1.03
	0.35	50.52	18.02	16.53	14.13	0.81	53.12	20.55	14.91	10.36	1.05	50.21	18.68	15.66	14.58	0.86
	0.4	52.94	16.55	15.18	14.65	0.68	55.43	18.81	13.69	11.18	0.88	52.64	17.17	14.39	15.07	0.73
	0.45	55.87	14.84	14.25	14.73	0.32	57.38	17.34	12.64	11.89	0.75	54.97	15.77	13.37	15.36	0.52
1000	0.15	32.92	29.89	24.78	11.21	1.19	35.90	34.42	22.31	5.78	1.59	32.62	30.80	23.37	11.94	1.26
	0.2	38.53	26.36	21.89	12.28	0.93	41.41	30.23	19.74	7.38	1.23	38.20	27.22	20.67	12.91	0.99
	0.25	42.95	23.57	19.59	13.14	0.75	45.71	26.92	17.68	8.71	0.98	42.60	24.38	18.52	13.70	0.80
	0.3	46.51	21.30	17.72	13.85	0.61	49.16	24.25	15.99	9.81	0.80	46.16	22.07	16.77	14.35	0.66
	0.35	49.44	19.43	16.18	14.44	0.51	51.97	22.05	14.59	10.74	0.66	49.09	20.15	15.31	14.90	0.55
	0.4	51.88	17.86	14.87	14.95	0.43	54.30	20.21	13.41	11.53	0.56	51.55	18.54	14.09	15.36	0.47
	0.45	55.43	15.51	14.14	14.81	0.12	56.35	18.62	12.42	12.17	0.44	54.34	16.74	13.22	15.47	0.23

Table C- 6: Syngas flow, yield and LHV, CGE, CCE for different feedstock at different temperatures and equivalence ratios when P = 105 kPa.

Temp (°C)	ER	Syngas flow (Nm^3/h)			Syngas Yield (Nm^3/kg)			LHV (MJ/Nm^3)			CGE (%)			CCE (%)		
		PKS	MBM	WP	PKS	MBM	WP	PKS	MBM	WP	PKS	MBM	WP	PKS	MBM	WP
600	0.15	38.87	44.60	40.60	0.76	0.94	0.71	8.89	10.49	8.88	51.10	70.14	62.85	69.39	79.87	68.47
	0.2	45.00	50.76	47.05	0.78	0.93	0.72	7.24	8.51	7.23	48.21	64.78	59.34	70.82	78.84	69.96
	0.25	51.31	57.25	53.67	0.80	0.93	0.75	6.04	7.02	6.03	45.82	60.31	56.42	72.90	79.01	72.06
	0.3	57.78	64.01	60.45	0.83	0.94	0.77	5.13	5.89	5.12	43.84	56.59	53.98	75.51	80.19	74.66
	0.35	64.37	71.00	67.35	0.86	0.97	0.80	4.43	5.02	4.42	42.19	53.49	51.92	78.53	82.20	77.65
	0.4	71.05	78.18	74.35	0.90	1.00	0.83	3.88	4.34	3.87	40.79	50.89	50.17	81.87	84.89	80.95
	0.45	77.82	85.51	81.43	0.93	1.03	0.87	3.44	3.80	3.43	39.60	48.70	48.67	85.48	88.11	84.52
650	0.15	39.99	45.59	41.83	0.80	0.98	0.75	8.77	10.22	8.76	51.86	69.84	63.90	70.04	79.01	69.22
	0.2	46.24	51.94	48.40	0.82	0.98	0.77	7.20	8.34	7.20	49.25	64.96	60.73	71.84	78.64	71.07
	0.25	52.65	58.60	55.13	0.85	0.98	0.79	6.05	6.93	6.04	47.10	60.95	58.09	74.21	79.42	73.45
	0.3	59.19	65.52	61.99	0.88	1.00	0.82	5.17	5.86	5.17	45.30	57.63	55.87	77.05	81.13	76.27
	0.35	65.84	72.64	68.95	0.91	1.03	0.85	4.50	5.04	4.49	43.79	54.85	53.99	80.24	83.58	79.44
	0.4	72.57	79.92	76.00	0.95	1.06	0.89	3.96	4.38	3.95	42.50	52.52	52.37	83.73	86.62	82.88
	0.45	79.37	87.32	83.11	0.99	1.10	0.92	3.53	3.86	3.52	41.39	50.54	50.97	87.44	90.12	86.55
700	0.15	41.42	46.96	43.40	0.86	1.03	0.80	8.52	9.79	8.51	52.19	68.93	64.40	69.97	77.10	69.23
	0.2	47.80	53.52	50.11	0.88	1.04	0.82	7.06	8.05	7.05	49.90	64.58	61.61	72.16	77.42	71.45
	0.25	54.33	60.37	56.96	0.91	1.06	0.85	5.97	6.74	5.97	48.01	61.05	59.29	74.87	78.85	74.16
	0.3	60.96	67.45	63.92	0.94	1.08	0.88	5.15	5.75	5.14	46.43	58.15	57.34	77.98	81.13	77.25
	0.35	67.69	74.71	70.96	0.98	1.11	0.92	4.50	4.97	4.50	45.10	55.74	55.68	81.41	84.06	80.65
	0.4	74.48	82.10	78.08	1.02	1.15	0.95	3.99	4.36	3.98	43.96	53.71	54.25	85.08	87.50	84.28
	0.45	81.34	89.61	85.25	1.06	1.20	0.99	3.57	3.87	3.57	42.98	51.98	53.00	88.96	91.35	88.11

Temp (°C)	ER	Syngas flow (Nm^3/h)			Syngas Yield (Nm^3/kg)			LHV (MJ/Nm^3)			CGE (%)			CCE (%)		
		PKS	MBM	WP	PKS	MBM	WP	PKS	MBM	WP	PKS	MBM	WP	PKS	MBM	WP
750	0.15	43.21	48.78	45.37	0.92	1.11	0.86	8.17	9.23	8.15	52.21	67.50	64.49	69.30	74.23	68.62
	0.2	49.74	55.55	52.23	0.95	1.12	0.89	6.83	7.65	6.82	50.26	63.74	62.12	71.94	75.35	71.27
	0.25	56.39	62.60	59.20	0.98	1.15	0.92	5.84	6.47	5.83	48.67	60.75	60.16	75.03	77.50	74.35
	0.3	63.13	69.85	66.27	1.02	1.18	0.96	5.07	5.57	5.06	47.35	58.31	58.52	78.46	80.39	77.75
	0.35	69.95	77.26	73.42	1.06	1.22	1.00	4.47	4.86	4.46	46.24	56.30	57.13	82.16	83.86	81.42
	0.4	76.82	84.78	80.62	1.10	1.26	1.03	3.99	4.30	3.98	45.29	54.61	55.93	86.07	87.76	85.29
	0.45	83.74	92.40	87.86	1.15	1.31	1.08	3.59	3.84	3.58	44.47	53.18	54.89	90.15	92.00	89.33
800	0.15	45.32	50.95	47.67	1.00	1.19	0.94	7.77	8.61	7.75	52.09	65.83	64.41	68.34	70.85	67.69
	0.2	51.99	57.95	54.68	1.03	1.22	0.97	6.57	7.22	6.55	50.53	62.74	62.49	71.46	72.88	70.80
	0.25	58.76	65.20	61.79	1.07	1.25	1.01	5.67	6.17	5.65	49.26	60.33	60.93	74.96	75.81	74.28
	0.3	65.61	72.62	68.97	1.11	1.29	1.04	4.97	5.36	4.96	48.22	58.39	59.63	78.74	79.38	78.04
	0.35	72.52	80.17	76.21	1.15	1.33	1.08	4.41	4.72	4.40	47.34	56.79	58.53	82.75	83.41	82.01
	0.4	79.47	87.82	83.50	1.20	1.38	1.13	3.96	4.21	3.95	46.59	55.47	57.59	86.92	87.80	86.14
	0.45	86.45	95.55	90.82	1.24	1.43	1.17	3.59	3.79	3.58	45.95	54.34	56.77	91.23	92.46	90.41
850	0.15	47.56	53.29	50.14	1.08	1.29	1.01	7.40	8.05	7.37	52.09	64.34	64.44	67.47	67.67	66.82
	0.2	54.36	60.50	57.29	1.11	1.32	1.05	6.33	6.83	6.30	50.90	61.95	62.99	71.07	70.65	70.41
	0.25	61.24	67.93	64.51	1.16	1.36	1.09	5.51	5.90	5.49	49.94	60.10	61.80	74.97	74.36	74.30
	0.3	68.18	75.50	71.79	1.20	1.41	1.13	4.87	5.18	4.86	49.16	58.64	60.83	79.10	78.57	78.39
	0.35	75.17	83.19	79.12	1.25	1.46	1.18	4.36	4.60	4.35	48.51	57.45	60.01	83.39	83.15	82.65
	0.4	82.19	90.95	86.47	1.30	1.51	1.22	3.95	4.14	3.93	47.96	56.46	59.32	87.82	88.00	87.04
	0.45	89.10	98.77	93.86	1.34	1.56	1.27	3.58	3.76	3.59	47.18	55.62	58.72	91.96	93.05	91.53

Temp (°C)	ER	Syngas flow (Nm^3/h)			Syngas Yield (Nm^3/kg)			LHV (MJ/Nm^3)			CGE (%)			CCE (%)		
		PKS	MBM	WP	PKS	MBM	WP	PKS	MBM	WP	PKS	MBM	WP	PKS	MBM	WP
900	0.15	49.73	55.55	50.14	1.15	1.38	1.01	7.11	7.61	7.37	52.32	63.35	64.44	66.96	65.28	64.52
	0.2	56.63	62.94	57.29	1.20	1.42	1.05	6.14	6.52	6.30	51.46	61.59	62.99	70.99	69.12	68.34
	0.25	63.60	70.52	64.51	1.24	1.46	1.09	5.40	5.70	5.49	50.77	60.25	61.80	75.25	73.52	72.42
	0.3	70.61	78.22	71.79	1.29	1.51	1.13	4.81	5.05	4.86	50.22	59.19	60.83	79.67	78.28	76.67
	0.35	77.66	86.01	79.12	1.34	1.57	1.18	4.33	4.52	4.35	49.75	58.33	60.01	84.21	83.31	81.06
	0.4	84.73	93.87	86.47	1.39	1.63	1.22	3.94	4.09	3.93	49.36	57.62	59.32	88.84	88.54	85.57
	0.45	91.16	101.77	93.86	1.41	1.68	1.27	3.54	3.74	3.59	47.74	57.02	58.72	91.96	93.91	90.15
950	0.15	51.64	57.52	54.67	1.22	1.46	1.16	6.91	7.30	6.86	52.78	62.94	65.40	66.89	63.86	66.27
	0.2	58.62	65.07	62.00	1.27	1.50	1.20	6.02	6.32	5.98	52.18	61.68	64.66	71.25	68.38	70.61
	0.25	65.65	72.77	69.37	1.32	1.55	1.25	5.32	5.56	5.30	51.70	60.72	64.06	75.78	73.30	75.11
	0.3	72.71	80.58	76.78	1.36	1.61	1.29	4.77	4.96	4.75	51.31	59.97	63.58	80.41	78.49	79.72
	0.35	79.80	88.45	84.22	1.41	1.67	1.34	4.32	4.48	4.30	50.99	59.36	63.18	85.14	83.86	84.42
	0.4	86.91	96.37	91.67	1.46	1.73	1.39	3.95	4.07	3.93	50.72	58.87	62.84	89.93	89.37	89.18
	0.45	92.56	104.33	98.64	1.46	1.79	1.42	3.51	3.74	3.58	48.11	58.45	61.52	91.96	94.99	93.00
1000	0.15	53.22	59.13	56.43	1.28	1.52	1.22	6.78	7.10	6.73	53.38	62.96	66.18	67.12	63.23	66.52
	0.2	60.26	66.81	63.82	1.33	1.57	1.26	5.94	6.19	5.90	52.95	62.06	65.67	71.73	68.24	71.11
	0.25	67.33	74.60	71.24	1.38	1.63	1.31	5.28	5.49	5.25	52.62	61.38	65.26	76.44	73.53	75.80
	0.3	74.43	82.48	78.68	1.43	1.69	1.35	4.76	4.92	4.73	52.35	60.84	64.92	81.23	79.01	80.57
	0.35	81.55	90.41	86.15	1.48	1.75	1.40	4.32	4.46	4.30	52.13	60.42	64.65	86.09	84.62	85.40
	0.4	88.68	98.38	93.63	1.53	1.81	1.45	3.96	4.07	3.95	51.94	60.06	64.41	90.99	90.33	90.27
	0.45	93.30	106.24	99.79	1.49	1.86	1.46	3.50	3.73	3.56	48.31	59.50	61.89	91.96	95.78	93.00

Table C- 7: The syngas composition from PKS, MBM and WP gasification at different gasification temperatures and pressure, ER = 0.3.

Temp (°C)	ER = 0.3	Syngas composition of PKS (vol.%)					Syngas composition of MBM (vol.%)					Syngas composition of WP (vol.%)				
	Pressure ($x10^{-1}$MPa)	N_2	H_2	CO	CO_2	CH_4	N_2	H_2	CO	CO_2	CH_4	N_2	H_2	CO	CO_2	CH_4
600	1.00	59.89	1.60	22.82	9.91	5.78	63.31	1.94	20.60	5.56	8.59	60.06	1.66	21.81	10.39	6.09
	1.05	59.91	1.57	22.83	9.91	5.79	63.34	1.90	20.61	5.55	8.61	60.08	1.62	21.82	10.38	6.10
	3.38	60.27	0.89	22.97	9.83	6.03	63.73	1.08	20.74	5.49	8.97	60.45	0.92	21.96	10.31	6.36
	5.75	60.39	0.69	23.01	9.81	6.10	63.85	0.83	20.78	5.47	9.08	60.57	0.71	22.00	10.29	6.43
	8.13	60.45	0.58	23.04	9.79	6.14	63.91	0.70	20.80	5.45	9.13	60.64	0.60	22.03	10.27	6.46
	10.50	60.49	0.51	23.05	9.78	6.16	63.96	0.62	20.81	5.44	9.16	60.68	0.53	22.04	10.26	6.49
	12.88	60.52	0.46	23.07	9.78	6.17	63.99	0.56	20.82	5.44	9.19	60.71	0.48	22.05	10.25	6.50
	15.25	60.55	0.43	23.08	9.77	6.18	64.02	0.52	20.83	5.43	9.20	60.74	0.44	22.06	10.25	6.51
	17.63	60.57	0.40	23.08	9.76	6.19	64.04	0.48	20.84	5.42	9.22	60.76	0.41	22.07	10.24	6.52
	20.00	60.59	0.37	23.09	9.76	6.19	64.06	0.45	20.85	5.42	9.23	60.78	0.38	22.08	10.23	6.52
650	1.00	58.44	3.22	22.27	10.47	5.60	61.84	3.84	20.12	6.11	8.09	58.55	3.32	21.27	10.95	5.91
	1.05	58.48	3.15	22.28	10.46	5.63	61.88	3.76	20.13	6.10	8.13	58.59	3.25	21.28	10.95	5.94
	3.38	59.17	1.84	22.55	10.33	6.11	62.62	2.19	20.38	5.98	8.83	59.30	1.89	21.54	10.82	6.44
	5.75	59.39	1.43	22.63	10.29	6.27	62.85	1.70	20.45	5.94	9.05	59.53	1.47	21.62	10.78	6.60
	8.13	59.51	1.21	22.68	10.27	6.34	62.98	1.44	20.49	5.92	9.17	59.65	1.24	21.67	10.76	6.68
	10.50	59.58	1.07	22.71	10.25	6.39	63.06	1.27	20.52	5.91	9.24	59.73	1.10	21.70	10.74	6.73
	12.88	59.64	0.97	22.73	10.24	6.43	63.12	1.15	20.54	5.90	9.29	59.79	1.00	21.72	10.73	6.77
	15.25	59.68	0.89	22.75	10.23	6.45	63.17	1.06	20.56	5.89	9.33	59.83	0.92	21.73	10.72	6.79
	17.63	59.72	0.83	22.76	10.22	6.47	63.20	0.99	20.57	5.88	9.36	59.87	0.85	21.75	10.71	6.81
	20.00	59.75	0.78	22.77	10.21	6.49	63.24	0.93	20.58	5.87	9.38	59.90	0.80	21.76	10.71	6.83

Temp (°C)	ER = 0.3	Syngas composition of PKS (vol.%)					Syngas composition of MBM (vol.%)					Syngas composition of WP (vol.%)				
	Pressure ($x10^{-1}$MPa)	N_2	H_2	CO	CO_2	CH_4	N_2	H_2	CO	CO_2	CH_4	N_2	H_2	CO	CO_2	CH_4
700	1.00	56.72	5.62	21.61	11.01	5.04	60.04	6.65	19.53	6.66	7.12	56.76	5.80	20.62	11.50	5.32
	1.05	56.78	5.51	21.64	10.99	5.08	60.10	6.52	19.56	6.65	7.18	56.82	5.69	20.64	11.49	5.36
	3.38	57.92	3.33	22.07	10.78	5.89	61.33	3.94	19.96	6.44	8.33	58.00	3.43	21.07	11.29	6.21
	5.75	58.29	2.61	22.22	10.72	6.16	61.73	3.09	20.09	6.37	8.72	58.39	2.69	21.21	11.22	6.49
	8.13	58.49	2.22	22.29	10.68	6.31	61.95	2.63	20.16	6.34	8.92	58.59	2.29	21.28	11.19	6.64
	10.50	58.63	1.97	22.34	10.66	6.40	62.09	2.33	20.21	6.32	9.06	58.73	2.03	21.33	11.16	6.74
	12.88	58.72	1.79	22.38	10.64	6.47	62.19	2.12	20.24	6.30	9.15	58.83	1.85	21.37	11.15	6.81
	15.25	58.79	1.65	22.41	10.63	6.52	62.27	1.95	20.27	6.29	9.22	58.91	1.70	21.40	11.13	6.86
	17.63	58.85	1.54	22.43	10.62	6.56	62.34	1.82	20.29	6.28	9.28	58.97	1.59	21.42	11.12	6.90
	20.00	58.90	1.45	22.45	10.61	6.59	62.39	1.72	20.30	6.27	9.33	59.02	1.50	21.44	11.11	6.94
717.85	1.00	56.04	6.66	21.35	11.20	4.75	59.32	7.85	19.30	6.86	6.67	56.05	6.87	20.36	11.70	5.02
	1.05	56.11	6.53	21.38	11.19	4.80	59.39	7.70	19.32	6.84	6.74	56.12	6.74	20.38	11.68	5.07
	3.38	57.43	4.01	21.89	10.94	5.74	60.82	4.72	19.79	6.60	8.07	57.49	4.13	20.88	11.44	6.05
	5.75	57.87	3.16	22.05	10.86	6.06	61.29	3.72	19.95	6.52	8.52	57.94	3.26	21.05	11.37	6.38
	8.13	58.10	2.70	22.15	10.82	6.23	61.55	3.18	20.03	6.48	8.76	58.19	2.78	21.14	11.33	6.56
	10.50	58.26	2.40	22.20	10.80	6.34	61.72	2.82	20.08	6.45	8.92	58.35	2.47	21.20	11.30	6.68
	12.88	58.37	2.18	22.25	10.78	6.42	61.84	2.57	20.12	6.43	9.04	58.47	2.24	21.24	11.28	6.77
	15.25	58.46	2.01	22.28	10.76	6.49	61.93	2.37	20.16	6.42	9.12	58.56	2.07	21.27	11.27	6.83
	17.63	58.53	1.88	22.31	10.75	6.53	62.01	2.21	20.18	6.41	9.19	58.63	1.94	21.30	11.25	6.88
	20.00	58.59	1.77	22.33	10.74	6.57	62.07	2.09	20.20	6.40	9.25	58.69	1.82	21.32	11.24	6.92

Temp (°C)	ER = 0.3	Syngas composition of PKS (vol.%)					Syngas composition of MBM (vol.%)					Syngas composition of WP (vol.%)				
	Pressure ($x10^{-1}$MPa)	N_2	H_2	CO	CO_2	CH_4	N_2	H_2	CO	CO_2	CH_4	N_2	H_2	CO	CO_2	CH_4
750	1.00	54.74	8.68	20.86	11.55	4.16	57.95	10.20	18.85	7.22	5.78	54.71	8.96	19.87	12.05	4.40
	1.05	54.83	8.53	20.89	11.53	4.21	58.04	10.02	18.88	7.20	5.86	54.80	8.81	19.90	12.03	4.46
	3.38	56.48	5.41	21.52	11.22	5.36	59.82	6.36	19.47	6.88	7.47	56.51	5.58	20.53	11.73	5.66
	5.75	57.04	4.31	21.74	11.12	5.78	60.44	5.06	19.67	6.78	8.05	57.09	4.45	20.74	11.63	6.10
	8.13	57.36	3.71	21.86	11.07	6.01	60.77	4.35	19.78	6.73	8.37	57.41	3.82	20.86	11.58	6.34
	10.50	57.56	3.30	21.94	11.03	6.16	60.99	3.88	19.85	6.69	8.59	57.62	3.40	20.93	11.54	6.50
	12.88	57.71	3.01	22.00	11.01	6.27	61.15	3.53	19.90	6.67	8.74	57.78	3.10	20.99	11.52	6.61
	15.25	57.83	2.79	22.04	10.99	6.36	61.28	3.27	19.94	6.65	8.86	57.90	2.87	21.03	11.50	6.70
	17.63	57.92	2.61	22.08	10.97	6.43	61.38	3.06	19.98	6.63	8.95	57.99	2.69	21.07	11.48	6.77
	20.00	58.00	2.46	22.11	10.96	6.48	61.46	2.89	20.00	6.62	9.03	58.07	2.53	21.10	11.47	6.83
800	1.00	52.66	12.03	20.07	12.09	3.15	55.72	14.03	18.13	7.81	4.31	52.55	12.43	19.09	12.59	3.34
	1.05	52.76	11.85	20.11	12.07	3.21	55.83	13.83	18.16	7.78	4.39	52.65	12.25	19.12	12.57	3.40
	3.38	54.86	7.99	20.91	11.65	4.59	58.11	9.34	18.91	7.33	6.32	54.83	8.25	19.92	12.16	4.86
	5.75	55.63	6.51	21.20	11.51	5.15	58.94	7.60	19.18	7.18	7.09	55.63	6.71	20.21	12.02	5.44
	8.13	56.07	5.65	21.37	11.43	5.47	59.42	6.60	19.34	7.10	7.54	56.08	5.83	20.37	11.95	5.78
	10.50	56.36	5.08	21.48	11.38	5.69	59.74	5.93	19.44	7.05	7.84	56.38	5.23	20.48	11.90	6.01
	12.88	56.58	4.65	21.57	11.35	5.85	59.97	5.44	19.52	7.02	8.06	56.60	4.80	20.56	11.86	6.17
	15.25	56.74	4.33	21.63	11.32	5.98	60.15	5.05	19.58	6.99	8.24	56.78	4.46	20.63	11.84	6.30
	17.63	56.88	4.06	21.68	11.30	6.08	60.29	4.74	19.62	6.97	8.38	56.91	4.18	20.68	11.81	6.41
	20.00	56.99	3.84	21.72	11.28	6.17	60.42	4.48	19.66	6.95	8.49	57.03	3.96	20.72	11.80	6.50

Temp (°C)	ER = 0.3 Pressure ($x10^{-1}$MPa)	Syngas composition of PKS (vol.%)					Syngas composition of MBM (vol.%)					Syngas composition of WP (vol.%)				
		N_2	H_2	CO	CO_2	CH_4	N_2	H_2	CO	CO_2	CH_4	N_2	H_2	CO	CO_2	CH_4
850	1.00	50.66	15.20	19.31	12.62	2.21	53.58	17.61	17.43	8.40	2.97	50.48	15.71	18.34	13.12	2.35
	1.05	50.77	15.02	19.35	12.60	2.26	53.69	17.42	17.47	8.37	3.05	50.59	15.54	18.37	13.10	2.41
	3.38	53.14	10.84	20.25	12.08	3.69	56.27	12.61	18.31	7.79	5.03	53.04	11.19	19.27	12.58	3.91
	5.75	54.09	9.05	20.62	11.89	4.35	57.30	10.53	18.65	7.59	5.93	54.03	9.34	19.63	12.40	4.60
	8.13	54.65	7.98	20.83	11.79	4.75	57.91	9.28	18.85	7.48	6.48	54.61	8.23	19.84	12.30	5.02
	10.50	55.04	7.23	20.98	11.73	5.03	58.33	8.42	18.98	7.41	6.86	55.01	7.46	19.98	12.24	5.31
	12.88	55.32	6.68	21.09	11.68	5.24	58.64	7.77	19.08	7.36	7.15	55.30	6.88	20.09	12.19	5.53
	15.25	55.54	6.24	21.17	11.64	5.41	58.88	7.26	19.16	7.32	7.38	55.53	6.43	20.17	12.16	5.71
	17.63	55.72	5.88	21.24	11.61	5.55	59.07	6.84	19.23	7.29	7.57	55.72	6.06	20.24	12.13	5.85
	20.00	55.88	5.58	21.30	11.58	5.66	59.24	6.49	19.28	7.26	7.73	55.87	5.75	20.30	12.10	5.97
900	1.00	48.93	17.86	18.64	13.11	1.46	51.72	20.56	16.83	8.95	1.94	48.67	18.48	17.68	13.61	1.56
	1.05	49.02	17.71	18.68	13.08	1.50	51.83	20.39	16.86	8.92	2.00	48.78	18.32	17.72	13.58	1.60
	3.38	51.44	13.66	19.60	12.50	2.80	54.44	15.82	17.71	8.25	3.78	51.28	14.11	18.63	13.00	2.98
	5.75	52.51	11.72	20.01	12.27	3.48	55.60	13.59	18.09	8.00	4.71	52.39	12.10	19.03	12.78	3.69
	8.13	53.16	10.50	20.26	12.15	3.92	56.32	12.18	18.33	7.86	5.31	53.07	10.84	19.28	12.66	4.16
	10.50	53.62	9.63	20.44	12.06	4.25	56.81	11.17	18.49	7.77	5.75	53.54	9.94	19.45	12.57	4.49
	12.88	53.97	8.96	20.57	12.00	4.50	57.19	10.40	18.61	7.70	6.09	53.90	9.25	19.58	12.51	4.75
	15.25	54.25	8.43	20.68	11.95	4.70	57.49	9.78	18.71	7.65	6.37	54.19	8.69	19.69	12.47	4.97
	17.63	54.47	7.99	20.76	11.91	4.86	57.74	9.26	18.79	7.61	6.59	54.42	8.24	19.77	12.43	5.14
	20.00	54.66	7.61	20.84	11.88	5.01	57.95	8.83	18.86	7.57	6.79	54.62	7.85	19.85	12.40	5.29

Temp (°C)	ER = 0.3	Syngas composition of PKS (vol.%)					Syngas composition of MBM (vol.%)					Syngas composition of WP (vol.%)				
	Pressure ($x10^{-1}$MPa)	N_2	H_2	CO	CO_2	CH_4	N_2	H_2	CO	CO_2	CH_4	N_2	H_2	CO	CO_2	CH_4
950	1.00	47.52	19.91	18.11	13.53	0.93	50.23	22.77	16.34	9.44	1.22	47.21	20.61	17.15	14.03	1.00
	1.05	47.61	19.78	18.14	13.50	0.97	50.32	22.64	16.37	9.41	1.27	47.30	20.48	17.18	14.00	1.03
	3.38	49.88	16.19	19.01	12.90	2.03	52.76	18.66	17.17	8.71	2.70	49.66	16.74	18.04	13.40	2.16
	5.75	50.98	14.28	19.43	12.65	2.66	53.96	16.50	17.56	8.42	3.56	50.81	14.76	18.46	13.15	2.83
	8.13	51.69	13.02	19.70	12.50	3.10	54.72	15.05	17.81	8.25	4.16	51.54	13.45	18.72	13.00	3.29
	10.50	52.20	12.08	19.89	12.39	3.43	55.28	13.98	17.99	8.13	4.62	52.07	12.48	18.91	12.90	3.64
	12.88	52.59	11.35	20.04	12.32	3.70	55.71	13.13	18.13	8.05	4.98	52.47	11.72	19.06	12.83	3.92
	15.25	52.91	10.75	20.17	12.26	3.92	56.05	12.44	18.24	7.98	5.28	52.80	11.09	19.18	12.77	4.15
	17.63	53.17	10.25	20.27	12.21	4.11	56.34	11.86	18.34	7.93	5.53	53.07	10.57	19.28	12.72	4.35
	20.00	53.40	9.81	20.35	12.17	4.27	56.59	11.36	18.42	7.89	5.75	53.31	10.13	19.37	12.68	4.52
1000	1.00	46.44	21.40	17.70	13.87	0.59	49.08	24.35	15.97	9.84	0.76	46.08	22.17	16.74	14.38	0.63
	1.05	46.51	21.30	17.72	13.85	0.61	49.16	24.25	15.99	9.81	0.80	46.16	22.07	16.77	14.35	0.66
	3.38	48.53	18.29	18.49	13.27	1.42	51.31	20.99	16.70	9.13	1.87	48.26	18.93	17.53	13.77	1.51
	5.75	49.59	16.55	18.90	13.00	1.96	52.46	19.05	17.07	8.82	2.60	49.36	17.12	17.93	13.50	2.08
	8.13	50.30	15.34	19.17	12.83	2.36	53.23	17.68	17.32	8.63	3.14	50.10	15.86	18.20	13.34	2.51
	10.50	50.83	14.41	19.37	12.72	2.67	53.80	16.62	17.51	8.50	3.57	50.65	14.89	18.40	13.22	2.84
	12.88	51.24	13.66	19.53	12.63	2.93	54.26	15.76	17.66	8.40	3.92	51.08	14.11	18.56	13.14	3.11
	15.25	51.59	13.04	19.66	12.56	3.15	54.63	15.05	17.78	8.32	4.22	51.43	13.46	18.69	13.07	3.35
	17.63	51.87	12.50	19.77	12.50	3.34	54.94	14.44	17.88	8.26	4.48	51.73	12.91	18.79	13.01	3.55
	20.00	52.12	12.04	19.87	12.46	3.51	55.21	13.91	17.97	8.20	4.71	51.99	12.43	18.89	12.97	3.72

Table C- 8: Syngas flow, yield and LHV, CGE and CCE for PKS, MBM and WP gasification at different temperatures and pressures when ER = 0.3.

	ER = 0.3	Syngas flow (Nm^3/h)			Syngas Yield (Nm^3/kg)			LHV (MJ/Nm^3)			CGE (%)			CCE (%)		
Temp (°C)	**Pressure ($x10^{-1}MPa$)**	**PKS**	**MBM**	**WP**	**PKS**	**MBM**	**WP**	**PKS**	**MBM**	**WP**	**PKS**	**MBM**	**WP**	**PKS**	**MBM**	**WP**
600	1,00	57.80	64.03	60.47	0.83	0.94	0.77	5.13	5.89	5.12	43.84	56.58	53.98	79.66	80.17	74.65
	1,05	57.78	64.01	60.45	0.83	0.94	0.77	5.13	5.89	5.12	43.84	56.59	53.98	79.64	80.19	74.66
	3,38	57.43	63.62	60.07	0.82	0.93	0.76	5.16	5.95	5.15	43.84	56.80	53.98	79.25	80.68	74.80
	5,75	57.32	63.49	59.95	0.81	0.92	0.76	5.17	5.97	5.16	43.83	56.85	53.97	79.14	80.81	74.84
	8,13	57.26	63.43	59.89	0.81	0.92	0.75	5.17	5.98	5.17	43.82	56.87	53.95	79.09	80.87	74.84
	10,50	57.22	63.38	59.85	0.81	0.92	0.75	5.18	5.98	5.17	43.81	56.88	53.94	79.06	80.90	74.84
	12,88	57.19	63.35	59.81	0.81	0.92	0.75	5.18	5.99	5.17	43.79	56.88	53.92	79.04	80.92	74.83
	15,25	57.16	63.32	59.79	0.81	0.92	0.75	5.18	5.99	5.17	43.78	56.87	53.90	79.02	80.93	74.82
	17,63	57.14	63.30	59.76	0.81	0.91	0.75	5.18	5.99	5.17	43.76	56.87	53.88	79.01	80.93	74.81
	20,00	57.13	63.28	59.74	0.81	0.91	0.75	5.18	5.99	5.17	43.75	56.86	53.86	79.01	80.93	74.80
650	1,00	59.23	65.56	62.03	0.88	1.01	0.82	5.17	5.86	5.17	45.30	57.60	55.87	79.88	81.08	76.26
	1,05	59.19	65.52	61.99	0.88	1.00	0.82	5.17	5.86	5.17	45.30	57.63	55.87	79.84	81.13	76.27
	3,38	58.50	64.74	61.24	0.86	0.97	0.80	5.24	5.98	5.24	45.34	58.05	55.92	79.04	82.09	76.61
	5,75	58.28	64.50	61.01	0.85	0.96	0.79	5.26	6.01	5.26	45.34	58.17	55.93	78.80	82.38	76.71
	8,13	58.17	64.37	60.88	0.84	0.96	0.79	5.27	6.03	5.27	45.34	58.23	55.93	78.68	82.53	76.76
	10,50	58.09	64.28	60.80	0.84	0.95	0.78	5.28	6.04	5.27	45.34	58.27	55.92	78.60	82.62	76.78
	12,88	58.03	64.22	60.74	0.84	0.95	0.78	5.28	6.05	5.28	45.33	58.29	55.91	78.54	82.68	76.79
	15,25	57.99	64.17	60.69	0.84	0.95	0.78	5.28	6.06	5.28	45.32	58.30	55.90	78.51	82.72	76.80
	17,63	57.95	64.13	60.65	0.84	0.95	0.78	5.29	6.06	5.28	45.31	58.31	55.89	78.48	82.75	76.80
	20,00	57.92	64.10	60.62	0.83	0.95	0.78	5.29	6.07	5.29	45.30	58.31	55.87	78.45	82.77	76.80
		Syngas flow (Nm^3/h)			**Syngas Yield (Nm^3/kg)**			**LHV (MJ/Nm^3)**			**CGE (%)**			**CCE (%)**		
Temp (°C)	**Pressure ($x10^{-1}MPa$)**	**PKS**	**MBM**	**WP**	**PKS**	**MBM**	**WP**	**PKS**	**MBM**	**WP**	**PKS**	**MBM**	**WP**	**PKS**	**MBM**	**WP**

700	1.00	61.03	67.53	63.98	0.95	1.08	0.88	5.14	5.74	5.14	46.43	58.12	57.34	80.81	81.05	77.23
	1.05	60.96	67.45	63.92	0.94	1.08	0.88	5.15	5.75	5.14	46.43	58.15	57.34	80.74	81.13	77.25
	3.38	59.76	66.09	62.61	0.90	1.03	0.84	5.26	5.94	5.26	46.50	58.83	57.43	79.35	82.71	77.84
	5.75	59.37	65.66	62.20	0.89	1.01	0.83	5.30	6.00	5.30	46.53	59.06	57.47	78.91	83.24	78.04
	8.13	59.17	65.43	61.97	0.88	1.00	0.82	5.32	6.03	5.32	46.54	59.18	57.48	78.67	83.52	78.15
	10.50	59.04	65.28	61.83	0.87	0.99	0.82	5.33	6.05	5.33	46.55	59.25	57.49	78.52	83.70	78.22
	12.88	58.94	65.17	61.72	0.87	0.99	0.81	5.34	6.07	5.34	46.55	59.30	57.49	78.41	83.82	78.26
	15.25	58.86	65.09	61.64	0.87	0.99	0.81	5.35	6.08	5.35	46.55	59.34	57.49	78.33	83.91	78.29
	17.63	58.80	65.02	61.58	0.87	0.98	0.81	5.35	6.09	5.35	46.54	59.37	57.49	78.27	83.98	78.31
	20.00	58.75	64.97	61.52	0.86	0.98	0.81	5.36	6.10	5.36	46.54	59.39	57.48	78.22	84.04	78.32
717,85	1.00	61.77	68.34	64.79	0.97	1.12	0.91	5.12	5.68	5.11	46.78	58.20	57.78	90.69	79.71	81.45
	1.05	61.70	68.26	64.71	0.97	1.11	0.91	5.13	5.69	5.12	46.78	58.24	57.78	90.64	79.66	81.39
	3.38	60.27	66.65	63.16	0.92	1.05	0.86	5.25	5.90	5.25	46.84	59.00	57.87	89.11	78.90	80.11
	5.75	59.81	66.13	62.67	0.90	1.03	0.84	5.30	5.98	5.30	46.88	59.27	57.92	88.08	79.01	79.78
	8.13	59.57	65.86	62.40	0.89	1.02	0.83	5.32	6.02	5.32	46.90	59.42	57.95	87.31	79.29	79.70
	10.50	59.41	65.68	62.23	0.89	1.01	0.83	5.34	6.04	5.34	46.91	59.51	57.96	86.70	79.59	79.70
	12.88	59.29	65.55	62.11	0.88	1.01	0.82	5.35	6.06	5.35	46.91	59.57	57.97	86.18	79.90	79.74
	15.25	59.20	65.45	62.01	0.88	1.00	0.82	5.36	6.07	5.36	46.92	59.62	57.97	85.75	80.18	79.80
	17.63	59.13	65.37	61.93	0.88	1.00	0.82	5.36	6.09	5.37	46.92	59.66	57.97	85.37	80.45	79.87
	20.00	59.07	65.30	61.87	0.88	1.00	0.82	5.37	6.09	5.37	46.91	59.68	57.97	85.04	80.71	79.94

Temp (°C)	Pressure ($x10^{-1}$MPa)	Syngas flow (Nm^3/h)			Syngas Yield (Nm^3/kg)			LHV (MJ/Nm^3)			CGE (%)			CCE (%)		
		PKS	MBM	WP	PKS	MBM	WP	PKS	MBM	WP	PKS	MBM	WP	PKS	MBM	WP
750	1,00	63,23	69,96	66,38	1,02	1,18	0,96	5,06	5,55	5,06	47,36	58,27	58,53	82,36	80,29	77,72
	1,05	63,13	69,85	66,27	1,02	1,18	0,96	5,07	5,57	5,06	47,35	58,31	58,52	82,26	80,39	77,75
	3,38	61,28	67,76	64,27	0,95	1,09	0,89	5,23	5,82	5,23	47,38	59,19	58,56	80,21	82,57	78,55
	5,75	60,67	67,07	63,61	0,93	1,07	0,87	5,28	5,92	5,29	47,42	59,53	58,63	79,50	83,38	78,87
	8,13	60,34	66,70	63,25	0,92	1,05	0,86	5,32	5,97	5,32	47,45	59,73	58,67	79,11	83,83	79,05
	10,50	60,12	66,45	63,01	0,91	1,04	0,85	5,34	6,01	5,34	47,47	59,85	58,69	78,86	84,12	79,17
	12,88	59,97	66,28	62,84	0,91	1,03	0,85	5,35	6,03	5,36	47,49	59,94	58,71	78,67	84,33	79,26
	15,25	59,85	66,14	62,71	0,90	1,03	0,84	5,37	6,05	5,37	47,50	60,01	58,72	78,53	84,49	79,32
	17,63	59,75	66,03	62,61	0,90	1,02	0,84	5,37	6,07	5,38	47,50	60,06	58,73	78,42	84,62	79,37
	20,00	59,67	65,94	62,52	0,90	1,02	0,84	5,38	6,08	5,39	47,50	60,11	58,73	78,33	84,72	79,40
800	1,00	65,73	72,76	69,11	1,11	1,29	1,05	4,96	5,35	4,95	48,24	58,36	59,65	84,29	79,28	78,02
	1,05	65,61	72,62	68,97	1,11	1,29	1,04	4,97	5,36	4,96	48,22	58,39	59,63	84,17	79,38	78,04
	3,38	63,09	69,76	66,23	1,02	1,17	0,96	5,15	5,66	5,15	48,06	59,24	59,45	81,56	81,83	78,85
	5,75	62,21	68,77	65,28	0,99	1,13	0,93	5,23	5,79	5,23	48,10	59,67	59,50	80,57	82,90	79,26
	8,13	61,73	68,22	64,75	0,97	1,11	0,91	5,27	5,86	5,27	48,13	59,93	59,55	80,00	83,52	79,52
	10,50	61,40	67,85	64,40	0,96	1,10	0,90	5,30	5,91	5,31	48,16	60,11	59,59	79,62	83,94	79,70
	12,88	61,17	67,59	64,15	0,95	1,09	0,89	5,33	5,94	5,33	48,19	60,24	59,62	79,34	84,26	79,83
	15,25	60,99	67,38	63,95	0,94	1,08	0,88	5,34	5,97	5,35	48,20	60,35	59,64	79,13	84,50	79,93
	17,63	60,84	67,22	63,79	0,94	1,07	0,88	5,36	5,99	5,36	48,22	60,43	59,66	78,95	84,69	80,01
	20,00	60,72	67,08	63,66	0,93	1,07	0,87	5,37	6,01	5,37	48,23	60,50	59,67	78,81	84,85	80,07

Temp (°C)	Pressure ($x10^{-1}$MPa)	Syngas flow (Nm^3/h)			Syngas Yield (Nm^3/kg)			LHV (MJ/Nm^3)			CGE (%)			CCE (%)		
		PKS	MBM	WP	PKS	MBM	WP	PKS	MBM	WP	PKS	MBM	WP	PKS	MBM	WP
850	1.00	68.32	75.66	71.94	1.21	1.41	1.14	4.87	5.17	4.85	49.20	58.64	60.88	86.24	78.51	78.39
	1.05	68.18	75.50	71.79	1.20	1.41	1.13	4.87	5.18	4.86	49.16	58.64	60.83	86.12	78.57	78.39
	3.38	65.14	72.05	68.46	1.09	1.27	1.03	5.05	5.48	5.04	48.67	59.16	60.22	83.24	80.79	78.93
	5.75	63.98	70.74	67.20	1.05	1.21	0.99	5.14	5.62	5.14	48.64	59.59	60.19	82.01	81.98	79.36
	8.13	63.33	69.99	66.49	1.03	1.18	0.97	5.19	5.71	5.19	48.65	59.89	60.22	81.27	82.73	79.65
	10.50	62.88	69.49	66.01	1.01	1.16	0.95	5.23	5.77	5.23	48.68	60.10	60.25	80.76	83.27	79.87
	12.88	62.56	69.12	65.66	1.00	1.15	0.94	5.26	5.81	5.27	48.70	60.27	60.28	80.39	83.67	80.04
	15.25	62.30	68.84	65.38	0.99	1.14	0.93	5.29	5.85	5.29	48.72	60.40	60.31	80.09	84.00	80.18
	17.63	62.10	68.60	65.16	0.98	1.13	0.92	5.31	5.88	5.31	48.74	60.51	60.34	79.85	84.26	80.29
	20.00	61.93	68.41	64.98	0.98	1.12	0.92	5.32	5.91	5.33	48.76	60.61	60.36	79.65	84.48	80.39
900	1.00	70.75	78.38	74.61	1.29	1.52	1.22	4.80	5.04	4.78	50.27	59.21	62.25	87.91	78.26	78.98
	1.05	70.61	78.22	74.46	1.29	1.51	1.22	4.81	5.05	4.79	50.22	59.19	62.18	87.80	78.28	78.96
	3.38	67.29	74.46	70.81	1.17	1.36	1.10	4.95	5.30	4.94	49.30	59.15	61.03	85.01	79.79	78.99
	5.75	65.91	72.90	69.31	1.12	1.30	1.06	5.04	5.44	5.03	49.14	59.46	60.83	83.65	80.90	79.32
	8.13	65.10	71.98	68.42	1.09	1.26	1.03	5.10	5.53	5.09	49.10	59.73	60.79	82.80	81.69	79.60
	10.50	64.54	71.34	67.81	1.07	1.24	1.01	5.14	5.60	5.14	49.10	59.95	60.79	82.19	82.28	79.83
	12.88	64.12	70.86	67.36	1.06	1.22	0.99	5.18	5.66	5.18	49.10	60.12	60.80	81.73	82.75	80.02
	15.25	63.79	70.49	67.00	1.04	1.20	0.98	5.21	5.70	5.21	49.12	60.27	60.82	81.36	83.13	80.17
	17.63	63.53	70.19	66.71	1.04	1.19	0.97	5.23	5.74	5.23	49.13	60.40	60.84	81.05	83.44	80.31
	20.00	63.30	69.94	66.47	1.03	1.18	0.96	5.25	5.77	5.25	49.14	60.51	60.86	80.79	83.71	80.42

Temp (°C)	Pressure ($x10^{-1}$MPa)	Syngas flow (Nm^3/h)			Syngas Yield (Nm^3/kg)			LHV (MJ/Nm^3)			CGE (%)			CCE (%)		
		PKS	MBM	WP	PKS	MBM	WP	PKS	MBM	WP	PKS	MBM	WP	PKS	MBM	WP
950	1.00	72.85	80.72	76.93	1.37	1.61	1.30	4.77	4.96	4.75	51.38	60.02	63.67	89.18	78.50	79.77
	1.05	72.71	80.58	76.78	1.36	1.61	1.29	4.77	4.96	4.75	51.31	59.97	63.58	89.10	78.49	79.72
	3.38	69.40	76.83	73.12	1.25	1.46	1.18	4.87	5.15	4.86	50.02	59.34	61.94	86.65	79.09	79.19
	5.75	67.89	75.13	71.47	1.19	1.39	1.12	4.95	5.28	4.94	49.69	59.43	61.52	85.32	79.94	79.33
	8.13	66.96	74.07	70.46	1.16	1.35	1.09	5.00	5.37	4.99	49.56	59.60	61.36	84.42	80.64	79.52
	10.50	66.30	73.32	69.74	1.13	1.32	1.07	5.05	5.44	5.04	49.50	59.77	61.30	83.75	81.21	79.71
	12.88	65.81	72.76	69.20	1.12	1.30	1.05	5.08	5.49	5.08	49.47	59.93	61.27	83.23	81.68	79.88
	15.25	65.41	72.30	68.76	1.10	1.28	1.04	5.11	5.54	5.11	49.46	60.06	61.25	82.81	82.07	80.03
	17.63	65.08	71.93	68.41	1.09	1.26	1.03	5.14	5.58	5.13	49.46	60.19	61.25	82.45	82.42	80.16
	20.00	64.81	71.62	68.11	1.08	1.25	1.02	5.16	5.61	5.16	49.46	60.30	61.26	82.15	82.71	80.28
1000	1.00	74.55	82.61	78.81	1.43	1.69	1.36	4.75	4.92	4.73	52.42	60.91	65.02	90.08	79.05	80.63
	1.05	74.43	82.48	78.68	1.43	1.69	1.35	4.76	4.92	4.73	52.35	60.84	64.92	90.02	79.01	80.57
	3.38	71.33	79.00	75.25	1.31	1.55	1.24	4.82	5.04	4.80	50.82	59.75	62.95	88.03	78.82	79.58
	5.75	69.79	77.27	73.56	1.26	1.48	1.19	4.87	5.14	4.86	50.31	59.59	62.32	86.82	79.30	79.47
	8.13	68.81	76.15	72.48	1.22	1.43	1.16	4.92	5.22	4.91	50.07	59.61	62.02	85.96	79.80	79.53
	10.50	68.09	75.33	71.69	1.20	1.40	1.13	4.96	5.28	4.95	49.94	59.69	61.86	85.30	80.27	79.64
	12.88	67.53	74.70	71.08	1.18	1.37	1.11	4.99	5.34	4.98	49.86	59.79	61.76	84.76	80.68	79.76
	15.25	67.09	74.19	70.59	1.16	1.35	1.10	5.02	5.38	5.01	49.81	59.89	61.70	84.32	81.04	79.87
	17.63	66.71	73.76	70.18	1.15	1.34	1.08	5.05	5.42	5.04	49.78	59.99	61.67	83.94	81.36	79.99
	20.00	66.39	73.40	69.84	1.14	1.32	1.07	5.07	5.46	5.06	49.76	60.08	61.64	83.60	81.66	80.09

Table C- 9: The H_2/CO ratio and char content obtainable from various gasification temperature and equivalence ratio at atmospheric pressure.

Temp (°C)	ER	H2/CO [-]			Char content (g/Nm3)		
		PKS	MBM	WP	PKS	MBM	WP
600	0.15	0.07	0.09	0.07	85.42	50.33	93.31
	0.2	0.07	0.09	0.07	69.27	46.92	75.78
	0.25	0.07	0.09	0.07	54.97	41.18	60.55
	0.3	0.07	0.09	0.07	42.40	34.34	47.34
	0.35	0.07	0.09	0.07	31.40	27.16	35.85
	0.4	0.07	0.09	0.07	21.75	20.07	25.83
	0.45	0.07	0.09	0.07	13.27	13.30	17.04
650	0.15	0.14	0.18	0.15	80.72	51.74	87.86
	0.2	0.14	0.19	0.15	64.29	46.36	70.24
	0.25	0.14	0.19	0.15	50.04	39.28	55.18
	0.3	0.14	0.19	0.15	37.70	31.63	42.27
	0.35	0.14	0.19	0.15	26.99	24.02	31.14
	0.4	0.14	0.19	0.15	17.67	16.74	21.48
	0.45	0.14	0.19	0.15	9.50	9.95	13.04
700	0.15	0.25	0.33	0.27	78.16	55.65	84.65
	0.2	0.25	0.33	0.27	61.21	48.00	66.68
	0.25	0.25	0.33	0.27	46.77	39.38	51.54
	0.3	0.25	0.33	0.28	34.42	30.73	38.70
	0.35	0.26	0.33	0.28	23.81	22.49	27.71
	0.4	0.26	0.33	0.28	14.63	14.85	18.22
	0.45	0.26	0.33	0.28	6.62	7.86	9.97
750	0.15	0.40	0.53	0.43	77.10	61.44	82.99
	0.2	0.40	0.53	0.44	59.45	51.22	64.50
	0.25	0.41	0.53	0.44	44.66	40.86	49.12
	0.3	0.41	0.53	0.44	32.15	31.06	36.19
	0.35	0.41	0.53	0.45	21.50	22.08	25.20
	0.4	0.41	0.53	0.45	12.34	13.96	15.77
	0.45	0.41	0.53	0.45	4.40	6.67	7.60
800	0.15	0.58	0.76	0.63	76.53	67.65	81.88
	0.2	0.58	0.76	0.63	58.18	54.77	62.86
	0.25	0.59	0.76	0.64	43.01	42.67	47.20
	0.3	0.59	0.76	0.64	30.32	31.74	34.14
	0.35	0.59	0.76	0.64	19.58	22.02	23.11
	0.4	0.59	0.76	0.65	10.41	13.41	13.70
	0.45	0.59	0.76	0.65	2.49	5.80	5.57

Temp (deg C)	ER	H_2/CO			Char content (g/Nm3)		
		PKS	MBM	WP	PKS	MBM	WP
850	0.15	0.77	1.01	0.83	75.50	72.62	80.40
	0.2	0.77	1.00	0.84	56.64	57.37	60.99
	0.25	0.77	1.00	0.84	41.22	43.79	45.17
	0.3	0.78	1.00	0.85	28.42	31.93	32.06
	0.35	0.78	0.99	0.85	17.66	21.62	21.04
	0.4	0.78	0.99	0.85	8.51	12.65	11.67
	0.45	0.78	0.99	0.85	1.23	4.81	3.60
900	0.15	0.94	1.23	0.83	73.63	75.40	80.40
	0.2	0.95	1.22	0.84	54.54	58.38	60.99
	0.25	0.95	1.21	0.84	39.06	43.77	45.17
	0.3	0.95	1.21	0.85	26.30	31.31	32.06
	0.35	0.95	1.21	0.85	15.60	20.65	21.04
	0.4	0.95	1.20	0.85	6.53	11.47	11.67
	0.45	0.93	1.20	0.85	1.21	3.52	3.60
950	0.15	1.09	1.41	1.19	71.10	76.11	75.24
	0.2	1.09	1.40	1.19	52.06	57.98	55.86
	0.25	1.09	1.39	1.19	36.70	42.80	40.23
	0.3	1.09	1.38	1.19	24.07	30.05	27.36
	0.35	1.09	1.38	1.19	13.52	19.25	16.61
	0.4	1.09	1.37	1.19	4.58	10.01	7.50
	0.45	1.04	1.37	1.18	1.19	2.05	1.19
1000	0.15	1.21	1.54	1.32	68.35	75.46	72.20
	0.2	1.20	1.53	1.32	49.52	56.76	53.10
	0.25	1.20	1.52	1.32	34.37	41.33	37.73
	0.3	1.20	1.52	1.32	21.94	28.50	25.09
	0.35	1.20	1.51	1.32	11.57	17.70	14.54
	0.4	1.20	1.51	1.32	2.80	8.50	5.60
	0.45	1.10	1.50	1.27	1.18	1.02	1.17

Table C- 10: The H_2/CO ratio and char content obtainable from gasification of PKS, MBM and WP at various temperature and equivalence ratio when atmospheric pressure was kept constant.

	ER = 0,3	H_2/CO			Char content (g/Nm3)		
Temp (°C)	**Pressure (bar)**	**PKS**	**MBM**	**WP**	**PKS**	**MBM**	**WP**
600	1.00	0.07	0.09	0.08	42.39	34.39	47.32
	1.05	0.07	0.09	0.07	42.40	34.34	47.34
	3.38	0.04	0.05	0.04	42.32	33.55	47.28
	5.75	0.03	0.04	0.03	42.32	33.33	47.29
	8.13	0.03	0.03	0.03	42.36	33.24	47.34
	10.50	0.02	0.03	0.02	42.39	33.19	47.38
	12.88	0.02	0.03	0.02	42.42	33.18	47.41
	15.25	0.02	0.02	0.02	42.44	33.19	47.46
	17.63	0.02	0.02	0.02	42.50	33.18	47.51
	20.00	0.02	0.02	0.02	42.55	33.19	47.56
650	1.00	0.14	0.19	0.16	37.71	31.71	42.28
	1.05	0.14	0.19	0.15	37.70	31.63	42.27
	3.38	0.08	0.11	0.09	37.36	30.04	41.97
	5.75	0.06	0.08	0.07	37.26	29.55	41.89
	8.13	0.05	0.07	0.06	37.23	29.30	41.86
	10.50	0.05	0.06	0.05	37.22	29.15	41.86
	12.88	0.04	0.06	0.05	37.22	29.06	41.87
	15.25	0.04	0.05	0.04	37.25	28.99	41.90
	17.63	0.04	0.05	0.04	37.27	28.95	41.93
	20.00	0.03	0.05	0.04	37.28	28.92	41.95
700	1.00	0.26	0.34	0.28	34.45	30.85	38.72
	1.05	0.25	0.33	0.28	34.42	30.73	38.70
	3.38	0.15	0.20	0.16	33.78	28.16	38.11
	5.75	0.12	0.15	0.13	33.53	27.28	37.88
	8.13	0.10	0.13	0.11	33.41	26.81	37.76
	10.50	0.09	0.12	0.10	33.33	26.51	37.70
	12.88	0.08	0.10	0.09	33.28	26.30	37.66
	15.25	0.07	0.10	0.08	33.26	26.14	37.63
	17.63	0.07	0.09	0.07	33.24	26.03	37.62
	20.00	0.06	0.08	0.07	33.23	25.94	37.62

Temp (°C)	ER = 0,3	H_2/CO			Char content (g/Nm3)		
	Pressure (bar)	**PKS**	**MBM**	**WP**	**PKS**	**MBM**	**WP**
750	1.00	0.42	0.54	0.45	32.17	31.20	36.20
	1.05	0.41	0.53	0.44	32.15	31.06	36.19
	3.38	0.25	0.33	0.27	31.38	27.74	35.48
	5.75	0.20	0.26	0.21	30.98	26.42	35.10
	8.13	0.17	0.22	0.18	30.74	25.67	34.87
	10.50	0.15	0.20	0.16	30.58	25.18	34.72
	12.88	0.14	0.18	0.15	30.47	24.82	34.61
	15.25	0.13	0.16	0.14	30.38	24.55	34.54
	17.63	0.12	0.15	0.13	30.32	24.33	34.48
	20.00	0.11	0.14	0.12	30.27	24.16	34.44
800	1.00	0.60	0.77	0.65	30.31	31.85	34.13
	1.05	0.59	0.76	0.64	30.32	31.74	34.14
	3.38	0.38	0.49	0.41	29.84	28.35	33.75
	5.75	0.31	0.40	0.33	29.36	26.70	33.29
	8.13	0.26	0.34	0.29	29.03	25.70	32.98
	10.50	0.24	0.31	0.26	28.79	25.00	32.75
	12.88	0.22	0.28	0.23	28.61	24.49	32.58
	15.25	0.20	0.26	0.22	28.47	24.08	32.44
	17.63	0.19	0.24	0.20	28.36	23.76	32.33
	20.00	0.18	0.23	0.19	28.26	23.49	32.24
850	1.00	0.79	1.01	0.86	28.36	31.98	31.99
	1.05	0.78	1.00	0.85	28.42	31.93	32.06
	3.38	0.54	0.69	0.58	28.72	29.37	32.47
	5.75	0.44	0.56	0.48	28.34	27.68	32.12
	8.13	0.38	0.49	0.41	28.00	26.54	31.80
	10.50	0.34	0.44	0.37	27.73	25.70	31.54
	12.88	0.32	0.41	0.34	27.51	25.06	31.33
	15.25	0.29	0.38	0.32	27.32	24.54	31.15
	17.63	0.28	0.36	0.30	27.17	24.11	31.00
	20.00	0.26	0.34	0.28	27.04	23.75	30.87

Temp (°C)	ER = 0,3	H2/CO			Char content (g/Nm3)		
	Pressure (bar)	**PKS**	**MBM**	**WP**	**PKS**	**MBM**	**WP**
900	1.00	0.96	1.22	1.05	26.19	31.29	29.65
	1.05	0.95	1.21	1.03	26.30	31.31	29.76
	3.38	0.70	0.89	0.76	27.63	30.21	31.25
	5.75	0.59	0.75	0.64	27.56	28.82	31.21
	8.13	0.52	0.66	0.56	27.33	27.74	31.01
	10.50	0.47	0.60	0.51	27.10	26.88	30.79
	12.88	0.44	0.56	0.47	26.89	26.18	30.59
	15.25	0.41	0.52	0.44	26.70	25.60	30.40
	17.63	0.38	0.49	0.42	26.53	25.11	30.24
	20.00	0.37	0.47	0.40	26.38	24.69	30.09
950	1.00	1.10	1.39	1.20	23.94	29.97	27.22
	1.05	1.09	1.38	1.19	24.07	30.05	27.36
	3.38	0.85	1.09	0.93	26.35	30.47	29.84
	5.75	0.74	0.94	0.80	26.71	29.66	30.25
	8.13	0.66	0.85	0.72	26.71	28.83	30.28
	10.50	0.61	0.78	0.66	26.60	28.10	30.19
	12.88	0.57	0.72	0.61	26.46	27.46	30.06
	15.25	0.53	0.68	0.58	26.32	26.90	29.93
	17.63	0.51	0.65	0.55	26.18	26.40	29.79
	20.00	0.48	0.62	0.52	26.04	25.97	29.66
1000	1.00	1.21	1.53	1.32	21.80	28.39	24.94
	1.05	1.20	1.52	1.32	21.95	28.50	25.09
	3.38	0.99	1.26	1.08	24.86	30.10	28.22
	5.75	0.88	1.12	0.95	25.65	29.95	29.09
	8.13	0.80	1.02	0.87	25.93	29.51	29.40
	10.50	0.74	0.95	0.81	26.01	29.01	29.50
	12.88	0.70	0.89	0.76	26.00	28.52	29.51
	15.25	0.66	0.85	0.72	25.95	28.07	29.47
	17.63	0.63	0.81	0.69	25.88	27.64	29.41
	20.00	0.61	0.77	0.66	25.79	27.25	29.33